

Toward Two Loops Five Massless Partons Scattering Amplitudes from Kinematic Limits

Mathieu Giroux, Department of Physics

McGill University, Montreal

March, 2021

*A thesis submitted to McGill University in partial fulfillment of the
requirements of the degree of*

MASTER OF SCIENCE

©Mathieu Giroux, 2021

*“The world was to me a secret,
which I desired to devine.”*

– Mary Shelley (1797-1851), FRANKENSTEIN

Declaration of Authorship

THE MAIN PROJECT discussed in this thesis is an idea proposed to me by my supervisor, Prof. Simon Caron-Huot, and was done in collaboration with him. They are some of the many ideas that were suggested during general discussions and that lead to further investigation. Unless specified otherwise, I worked out myself all the results that I present, even those that originated initially from other people. In this spirit, ideas coming from the research literature are referred as much as possible in the text. I therefore agree to deposit this thesis in the University's open access institutional repository or allow the library to do so on my behalf, subject to Canada's Copyright Legislation and McGill University Library conditions of use and acknowledgement.

— M.G., April 2021.

Abstract

THE COMPUTATION of massless 5-point 2-loop scattering amplitudes requires the analytical expressions for about 32400 master integrals. In this thesis, we present a method to evaluate all these integrals from a much smaller set corresponding to a fix ordering of the external particles. The integration constants for different leg orderings are determined by using multiple scaling limits of the associated (canonical) differential equations' alphabet letters. The choice of scaling limits is constrained by the requirement the paths they describe in the kinematic space are generated *only* by harmonic polylogarithms (HPLs). Such constraint ensures using scaling limits makes the *analytic* evaluation of the solutions fast and simple. Our method is suitable to show the existence of a “web of computational highways” in the kinematic space relating *all* evaluated master integrals.

Abrégé

LE CALCUL à 2-boucle d'amplitudes de diffusion pour un processus impliquant 5-parton à hautes énergies requiert l'évaluation d'une base de 32400 intégrales de Feynman en quatre dimensions (*master integrals*). Dans cette thèse, nous présentons une méthode pour évaluer toutes ces intégrales à partir d'un ensemble d'intégrales beaucoup plus petit correspondant à une configuration fixée des particules extérieures. Les constantes d'intégrations pour différentes configurations des états initiaux et finaux sont déterminées en utilisant de multiples mises à l'échelle (limites cinématiques) des lettres apparaissant dans les équations différentielles associées. Le choix de ces limites est soumis à la contrainte que les chemins qu'elles décrivent dans l'espace de cinématique soient générés par des polylogarithmes harmoniques (HPLs) uniquement. Une telle contrainte assure que l'utilisation de limite rend le calcul *analytique* des solutions rapide et simple. Notre méthode est celle qui est privilégiée pour montrer l'existence d'un réseau dans l'espace de cinématique reliant *toutes* les constantes d'intégrations.

Acknowledgements

I FIRST WISH to thank my supervisor, Pr. Simon Caron-Huot, for his constant attention paid to me during the degree despite the unusual circumstances of 2020-2021. His contagious passion for physics is really inspiring and I am convinced that everyone working with him is lucky to benefit from his unique way of seeing things. I hope this collaboration will continue on for a long time.

I thank my friends in the McGill high-energy theory group and especially Andrzej for stimulating physics discussions and for helping me in my beginnings with MATHEMATICA; our many confrontations have always been an important occasion to reflect.

I thank my parents, Lynda and Paul, and my brother Jeff for the immense opportunity they gave me to achieve this goal; their advice, confidence, material and moral support have allowed me to keep on going. I thank my friends since day one, Gaël, Ludovick, Étienne, and Dany for everything your friendships provided to me since we were little. No friendship is an accident. I also want to greet with affection my grandparents as well as my friend and mentor Philippe for their support and for their valuable contribution in my growth.

Special thanks are dedicated to the best girlfriend I could ever have, Audrey, with whom I shared every moment of my experience in grad school so far: her sympathy, love and spontaneity were been a huge source of motivation. I am also grateful to her family for their hospitality. Lastly, I am grateful to the examiners, especially Charles Gale, for their feedback on the manuscript.

“Physics isn’t the most important thing. Love is.”

– Richard P. Feynman (1918-1988)

Table of Contents

| | |
|---|-------------|
| Abstract | iii |
| Abrégé | iv |
| Acknowledgements | v |
| List of Figures | viii |
| List of Figures | ix |
| 1 Introduction | 1 |
| 2 Scattering Amplitudes in Gauge Theory | 8 |
| 2.1 Review of Fundamental Concepts | 8 |
| 2.1.1 Conventions | 8 |
| 2.1.2 Perturbative QCD | 9 |
| 2.1.3 A Word on Renormalization and Running Couplings | 13 |
| 2.1.4 Color Stripped Amplitudes | 16 |
| 2.1.5 Spinor-Helicity Formalism | 20 |
| 2.2 Loop-Integral Methods | 27 |
| 2.2.1 d -Dimensional Feynman Integrals | 27 |
| 2.2.2 From Tensorial to Scalar Feynman Integrals | 28 |
| 2.2.3 Regularizing Feynman Integrals from Dimensions | 29 |
| 2.2.4 The Landau Equations | 32 |
| 2.2.5 Algebraic Relations Between Feynman Integrals | 34 |
| 2.2.6 Example: IPBs for the Massless Box | 37 |
| 2.2.7 Recycling Tree Amplitudes: Unitary Cuts | 39 |
| 2.2.8 Generalized Unitarity | 40 |

| | | |
|----------|---|-----------|
| 2.2.9 | Leading Singularities and $d \log$ Forms | 42 |
| 2.2.10 | Example: The Leading Singularities of the Massless Box | 43 |
| 2.3 | On the Evaluation of Master Integrals | 46 |
| 2.3.1 | The (Canonical) Differential Equations | 48 |
| 2.3.2 | Determining a Boundary Constant from Physical Consistency | 54 |
| 2.3.3 | Example: Differential Equations for the Massless Box | 55 |
| 3 | Scattering Of 5-Gluon at 2-Loop | 60 |
| 3.1 | Setup and Preliminaries | 60 |
| 3.1.1 | The Kinematic Space of $2 \rightarrow 3$ Scatterings | 60 |
| 3.1.2 | Massless 5-particle 2-loop Topologies and their IBPs | 62 |
| 3.1.3 | Function Space and the Pentagon Alphabet | 64 |
| 3.2 | Kinematic Sectors | 66 |
| 3.2.1 | The Multi-Regge Kinematics | 67 |
| 3.2.2 | Collinear Kinematics | 70 |
| 3.3 | Pure Master Integrals in a MRK-background | 71 |
| 3.4 | A Numerical Method for Crosschecks | 74 |
| 4 | Original Contributions | 78 |
| 4.1 | θ -parameterization: A Bridge Between Limits | 79 |
| 4.2 | Moving Between Regions: An Example | 81 |
| 4.3 | Permuting Spacelike Separated Gluons: A Word on Analytic Continuation | 85 |
| 5 | Summary and Conclusion | 89 |
| A | The Massless Box IBPs | 91 |
| B | Computation of M_2 and M_3 | 93 |
| C | Kinematic Limits and Their Geometries | 95 |
| | References | 99 |

List of Figures

| | | |
|-----|---|----|
| 1.1 | Tree-level versus loop-level Feynman diagrams. | 2 |
| 1.2 | Electrons repel because they exchange photons. | 3 |
| 1.3 | Left: Tri-jet event within the CMS detector, as seen in looking down the beam-pipe (z -axis) in the event-plane (xy -plane). The three protrusions of rectangles together with the solid and dotted purple lines in the middle circle represent the three jets of partons. The black lines represent the corresponding hadronized jets. Right: ATLAS and CMS data for top quark and anti-quark pair production rate $\sigma_{\text{tot}}(\text{pb})$ (vertical axis) as a function of the center of mass energy \sqrt{s} (horizontal axis) [1]. The measurements are the colored points, with bars indicating their experimental uncertainties. The theoretical predictions are given by the colored bands – the blue for the tree-level prediction (LO), the red after the first virtual correction (NLO) and grey for the second virtual correction (NNLO). Their widths indicate the uncertainty of the predictions. | 5 |
| 2.1 | QCD Feynman rules (ghost fields excluded). | 12 |
| 2.2 | s -, t - and u -channel exchanges for a 4-point process. | 18 |
| 2.3 | Feynman diagram for $e^+e^- \rightarrow qg\bar{q}$, in which the quark q is shown as radiating a gluon g . Time flows horizontally. | 27 |
| 2.4 | Wick rotation. ℓ_0^\pm -poles in Feynman propagators are shown. Integrating over the real axis is then equivalent to integrating over the pole-free imaginary one. | 30 |
| 2.5 | Basis obtained from integral reduction for 1-loop integrals. | 38 |
| 2.6 | Visualization of 1-loop unitary cut. External particles are all outgoing. . . . | 39 |

| | | |
|-----|--|----|
| 2.7 | The sum of all Feynman diagrams localized on the cut where the propagators $(\ell)^{-2}$ and $(\ell - p_1 - p_2)^{-2}$ go on-shell (left) is equal to the product of two tree-amplitudes (right). | 40 |
| 3.1 | A 5-gluon process. | 61 |
| 3.2 | All the 8-propagator families. | 63 |
| 3.3 | Massless 4-point process singularity structure. | 64 |
| 3.4 | 2-loop massless 5-point (pentagon) alphabet. | 64 |
| 3.5 | Color plot of $-\text{Li}_2(1 - Z)$ | 66 |
| 3.6 | Visualization of the 5-point multi-Regge kinematics. Each particle has its own light-cone frame. | 67 |
| 3.7 | Collider geometry for 5-point processes at high energies. | 68 |
| 3.8 | Visualization of the 5-point collinear limit. | 70 |
| 4.1 | Blowing up the path connecting $(0, 0)$ and $(1, 1)$ with a small corner around $(1, 0)$ | 79 |
| 4.2 | At leading order, the MRK and $(4 5)$ parameterizations won't overlap. Without leading order truncation, the MRK alphabet is not practical for computation and cannot be used to transport points (black dots) from truncated MRK to truncated collinear regions. | 80 |
| 4.3 | Connecting asymptotics. | 80 |
| 4.4 | $(4 5)$ approach within a MRK background. | 82 |
| 4.5 | The schematic web of HPLs to follow in order to permute 4 and 5 analytically. | 82 |
| 4.6 | Scale orderings for the first row of Fig. 4.5. | 82 |
| 4.7 | Putting gluon 4 into the past. | 87 |
| 4.8 | Complex section of \mathcal{K}_5 along the $s_{14} + s_{24} + s_{34} + s_{45} = 0$ hyperplane, in the limit where $s_{14}, s_{45} \rightarrow 0$ in a controlled manner. We sketch the (minimal) paths needed for the flipping. | 88 |
| C.1 | The geometry: The i^{th} edge vector is the momentum p_i^μ of particle i | 96 |

Chapter 1

Introduction

AS OF YET, our best description of all combined experimental data fits into the picture of both elementary particles and their local interactions. The former are viewed as excitations of the underlying quantum fields filling up our Universe. The formal framework to formulate the latter quantitatively is *Quantum Field Theory* (QFT). In particular, it offers a solid ground to an early quantum observation¹: To scrutinize the most elementary structures, one needs to observe the properties of very high-energetic particle interactions. Analyzing phenomena happening at short, or *quantum*, length scales requires high energy backgrounds, hence justifying the *classical* nature of our daily experience of the world.

A powerful theoretical tool we can sometimes use in QFT is *perturbation theory*, which makes computations of scattering amplitudes doable. The scattering amplitudes are essentially numbers representing the probabilities a certain set of particles turn into certain other particles after colliding. In the late 40's, Richard Feynman noticed that this could be done with pictures representing the different ways particles can shuffle during an interaction. Broadly speaking, the contributions to the scattering amplitudes may be labelled by Feynman diagrams. There are two types of contributions to the scattering amplitudes: Classical *tree-level* graphs and quantum *loop-level* graphs (see Fig. 1.1). To understand the difference

¹Recall that in primeval quantum mechanics, energy is related to frequency via Planck's relationship, $E = hf$, and frequency is related to wavelength via the speed of light, $f = c/\lambda$. Therefore, the higher the energy, the smaller is the associated wavelength representing the "resolution" with which one makes an observation.



Figure 1.1: Tree-level versus loop-level Feynman diagrams.

between “classical” and “quantum” labels, we must recall that, upon quantization, we have one more dimensional constant of Nature: The *Planck constant*, \hbar . Because Hamilton’s action, \mathcal{S} , for classical systems has units J·s, and because the Boltzmann factor in the Feynman path integral must have dimensionless argument, dimensional analysis requires the quantum action to be \mathcal{S}/\hbar . Consequently, the connection between the number of loops, L , and the powers of \hbar for a diagram involving *any* number of external legs is $\sim \hbar^{L-1}$ [2, §6.2.1-6.2.2]; the classical limit, $\hbar \rightarrow 0$, is therefore identified with the leading order (LO) diagrams in \hbar – i.e., with $L = 0$.

From the path integral, to each Feynman diagram is associated a mathematical quantity we can evaluate to a number. On one hand, the tree-level diagrams are generically rational functions of the kinematic variables. This makes them relatively easy to evaluate in practice. On the other hand, the higher order corrections are associated with one integral by loop order. These integrals are called *Feynman integrals* (FI). Often, these are highly non-trivial integrals, making the complexity of perturbative calculations grow with the number of parameters present – e.g., loop momenta, number of external legs and masses. Furthermore, they in general diverge in our four-dimensional spacetime. In order to match the finite results from physical experiments, a regularization procedure is needed to systematically subtract them. This can be rigorously done via *renormalization* protocols.

On many facets, the *Standard Model of particle physics* (SM) is the most successful QFT to date. It is a particular type of QFT known as a *gauge theory*. Broadly speaking, a theory is gauged if it explains the action of forces by imposing *local* symmetries on the equation of motions. For example, imposing a local U(1)-invariance on our equations of motion² led to

²Meaning they stay the same under phase rescalings in the fields – e.g., $\psi(x) \rightarrow \exp(i\alpha(x))\psi(x)$, for some real function $\alpha : \mathbb{R}^{1,3} \rightarrow \mathbb{R}$.

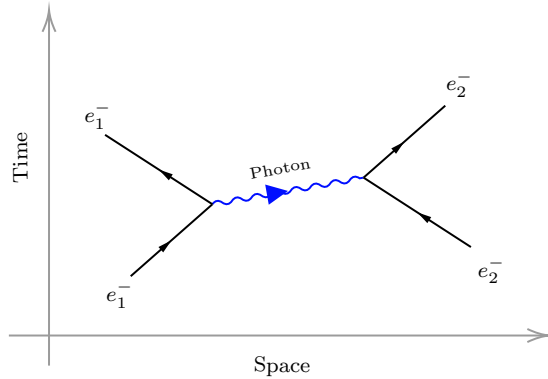


Figure 1.2: Electrons repel because they exchange photons.

something very real and physical: *Electromagnetism*. Here, $U(1)$ is called the *gauge group* of the theory. The locality requirement entails the coupling of matter fields to force carrying gauge fields. The gauge theory framework therefore provides a nice explanation to Newton’s mysterious concept of “forces” [3]. In electromagnetism, for example, electrons repel because they exchange virtual³ photons (see Fig. 1.2)!

The SM is the gauge theory imposing a local $SU(3)_C \otimes SU(2)_W \otimes U(1)_Y$ -symmetry on its equations of motion. The $SU(2)_W \otimes U(1)_Y$ -sector is linked to the theory of *electroweak interaction* (EW) also known as the *Glashow-Weinberg-Salam theory* [5–7]. This sector has $3 + 1$ degrees of freedom corresponding to four massless force carriers. At low collision energies ($E \lesssim 100\text{GeV}$), the electroweak symmetry is spontaneously broken via the *Higgs mechanism* [8–11], in which the symmetry group of the vacuum state is a subgroup of the full gauge group. This leaves a massless $U(1)$ photon field and a *massive* (broken) $SU(2)$ field that gives the weak sector W^\pm - and Z -boson force carriers. Finally, the $SU(3)_C$ -sector describes the *strong interactions* of *partons* (quarks and gluons), where the force mediating particles are *gluons*. It will be much more discussed in Section 2.1.2.

The SM has been carefully analyzed experimentally in the last decades – e.g., [12, 13]. Its last missing piece required to check its consistency, namely the Higgs particle, has been

³According to the uncertainty principle, if we want to measure the energy of a quantum system with accuracy ΔE , we need a time greater or equal than $\hbar/(2\Delta E)$. *Virtual* particles are, heuristically, those we “don’t have the time to measure” – i.e., those with propagating time satisfying $\Delta t \leq \hbar/(2\Delta E)$. For *massive* particles, $\Delta E \sim mc^2$, and so massive virtual particles tend to have very short lives (rare events). See [4] for more details.

observed in 2012 by the most powerful laboratory for studying high-energy collisions to date, the *Large Hadron Collider* (LHC) at CERN. On one hand, this is the very first model which can be extrapolated to the energy scales many orders of magnitude higher than any of its characteristic scales. On the other hand, it is also clear that the SM is not yet a complete theory. It fails to address a wide variety of theoretical concerns. For example, it does not consistently include gravity. Moreover, it lacks giving an explanation of some astrophysical observations such as the dominance of matter over antimatter in the observable Universe and the apparent existence of dark matter.

Consequently, the SM should be understood as a low-energy approximation of a more fundamental, perhaps *unknown*, theory. It is, therefore, of central importance to exactly determine the domain of its validity and establish harsh constraints on potential *Beyond-the-Standard-Model* (BSM) extensions.

A key ingredient in this quest is the ability to interpret measurements performed in collider experiments as precisely as possible. These have to be compared to precise predictions of the SM and possibly, new physics models. However, in the absence of such predictions from theory, new physics may remain undetected, or the SM backgrounds may be falsely identified as such. The discovery potential of hadron colliders is limited by both experimental and theoretical uncertainties. Naturally, one⁴ of the main source of theoretical uncertainties is the truncation of the couplings perturbation series at some fixed order. The systematic way to reduce this uncertainty is to include the higher orders.

It is a well-known fact that, at the characteristic energy scales μ of the high-energy scattering at the LHC, the effective strong coupling constant $\alpha_s(\mu)$ is in the perturbative domain (e.g., see [16, Fig. 9.3]), but still is relatively large compared to the electroweak couplings. Thus, the most important corrections are generally expected from higher-order terms in $\alpha_s(\mu)$. In this thesis we are interested in high-energy scatterings and we shall, therefore, focus on the strongly coupled sector of the SM. Given the standard “textbook” techniques

⁴We could also think about *parton distribution functions* (PDFs) errors, reflecting a possibly limited understating of proton structure, as the PDFs encode, by design, information about the proton’s deep structure (see [14, 15]).

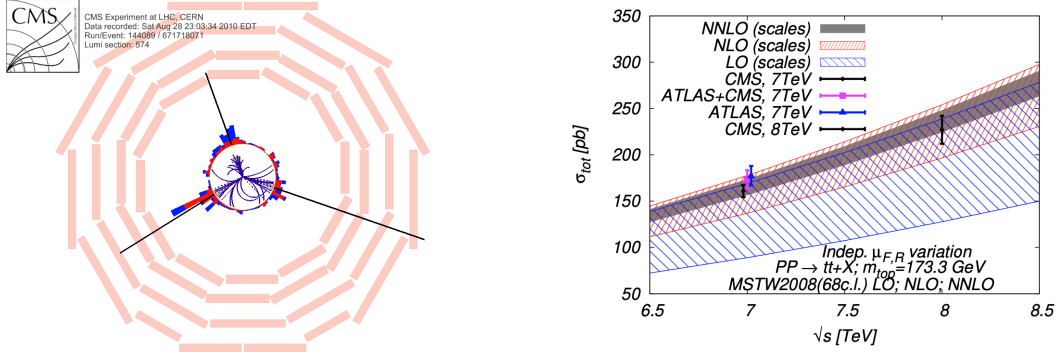


Figure 1.3: **Left:** Tri-jet event within the CMS detector, as seen in looking down the beam-pipe (z -axis) in the event-plane (xy -plane). The three protrusions of rectangles together with the solid and dotted purple lines in the middle circle represent the three jets of partons. The black lines represent the corresponding hadronized jets. **Right:** ATLAS and CMS data for top quark and anti-quark pair production rate σ_{tot} (pb) (vertical axis) as a function of the center of mass energy \sqrt{s} (horizontal axis) [1]. The measurements are the colored points, with bars indicating their experimental uncertainties. The theoretical predictions are given by the colored bands – the blue for the tree-level prediction (LO), the red after the first virtual correction (NLO) and grey for the second virtual correction (NNLO). Their widths indicate the uncertainty of the predictions.

for evaluating multi-loop amplitudes require too many computational resources, we will use state-of-the-art theoretical methods to study beyond 1-loop processes. In particular, we will be most interested in 2-loop (next-to-next-to-leading-order (NNLO)) non-planar 5-parton scatterings at high energies.

This choice of process is directly motivated from collider experiments. For example, in the case of quark/anti-quark production [1], we observe that the scale dependence of the first precision order for the predicted cross-section, σ_{tot} , is at NNLO – see Fig. 1.3. In the high-energy limit, where the quark masses can be effectively dropped, computations of 2-loop 5-gluon amplitudes are the starting point toward a full understanding of color multi-jet production at the LHC.

To evaluate NNLO scattering amplitudes, we first decompose the integrals in terms of an integral basis, called *master integrals* (MI), and evaluate them with cutting-edge tech-

niques. The word “decomposition” makes even more sense when one realizes that the space of Feynman integrals for a diagram topology is, in fact, a vector space – e.g., [17]. Therefore, as a vector can be decomposed along independent directions, scattering amplitudes can be decomposed in terms of independent integrals. Consequently, exactly as one decomposes a vector given a *choice* of basis and a way to *project* onto the basis (to extract the coefficients of the linear combination), so does scattering amplitudes. For a generic multi-loop amplitude, the basis is not known, *a priori*. By acting with the projector, we should then not only be able to determine the coefficients, but also the MIs. For any given scattering process the set of MI’s is also not unique, and, in practice, their choice is rather arbitrary. Usually MI’s are identified after applying the Laporta’s reduction algorithm [18], based on a Gaussian-type elimination on a system of equations obtained through *integration-by-part identities* (IBP) [19, 20]. The IBP relations imply that the MIs obey a linear system of first order differential equations in the 2-particle kinematics invariants: The generalized *Mandelstam invariants* $s_{ij} := (p_i + p_j)^2$. Therefore, evaluating Feynman integrals boils down to solving differential equations [21, 22]. Obviously, a proper choice of MI’s can simplify tremendously the form of the systems of differential equations and so their solution. Nevertheless, no general criteria for determining such optimal sets are, to this date, available. Although there are some known examples where this is not possible [23–28], we generically search for a basis of MIs that puts the system of differential equations into a *canonical form*, where the dependence on the ’t Hooft parameter, $\varepsilon = (4 - d)/2$, factors out of the kinematic linearly [29]. This factorization yields tremendous simplifications of the solution space, now spanned only by *Goncharov polylogarithms* [30, 31]. Thus, the integration is done in a similar way Wilson lines/loops are computed in familiar non-abelian gauge theories. Finally, we stress that along a path lying purely in the physical sector, *harmonic polylogarithms* (HPL) [32] are functions naturally appearing in the solutions of the system of the differential equations. For 2-loop 5-point scattering amplitudes, a canonical basis of MIs was recently made available (see Section 3.1.2), allowing us to study these processes further. The ultimate goal of our study

is to reveal a network in the kinematic space of invariants relating, via HPLs only, all the evaluated MI's for any leg configuration of 2-loop 5-gluon scatterings.

The Structure of the Thesis

In Chapter 2, we provide notations and some theoretical preliminaries required for the remaining content of the thesis. We review the strong coupling sector of the SM as a QFT, namely QCD. While focussing on 1-loop, the rest of the chapter aims to give a brief overview and many examples of standard computational methods for the evaluation of multi-loop integrals in gauge theory.

In Chapter 3, we discuss various details about the scattering of 5-gluon at 2-loop, such as the IBPs, the function space and the kinematics in different limits.

In Chapter 4, we present, through examples, the original contributions of the thesis: a method to find the analytic form of the integration constants contributing to the 5-point massless amplitudes in QCD at the NNLO approximation.

Chapter 2

Scattering Amplitudes in Gauge Theory

IN THIS CHAPTER, we give a brief, but condensed, overview of the theoretical framework for the work presented in this thesis, as well as the basic notions that we will operate with in the following chapters. For any details regarding the content of this chapter we refer to many excellent “textbooks”, such as [33, 34].

2.1 Review of Fundamental Concepts

2.1.1 Conventions

THROUGHOUT THIS THESIS, we will work in 4-spacetime dimensions and our metric convention is in the mostly-plus (Est Coast) one – i.e., $\eta_{\mu\nu} = \text{diag}(-1, 1, 1, 1)$, which we extend with further $+$ -signs when working in d -dimensions, and we will follow the spinor and Clifford algebra conventions of [35]. In the following, Greek indices are associated with spacetime, while Roman indices describe the structure in gauge group space. We will also need to introduce the 4-component Pauli matrices $\sigma_{\alpha\dot{\beta}}^{\mu} := (\sigma^0, \sigma^i)_{\alpha\dot{\beta}}$, for $1 \leq i \leq 3$, defined via

$$\sigma^0 = \begin{pmatrix} 1 & 0 \\ 0 & 1 \end{pmatrix}, \quad \sigma^1 = \begin{pmatrix} 0 & 1 \\ 1 & 0 \end{pmatrix}, \quad \sigma^2 = \begin{pmatrix} 0 & -i \\ i & 0 \end{pmatrix}, \quad \sigma^3 = \begin{pmatrix} 1 & 0 \\ 0 & -1 \end{pmatrix}. \quad (2.1)$$

The last three matrices form *a* fundamental representation for the three generators of $\text{SU}(2)$. Unitary symmetries and their representations are extensively reviewed in [36–38].

2.1.2 Perturbative QCD

QUANTUM CHROMODYNAMICS (QCD), the theory of the strong interactions within the SM, describes the building blocks of strongly interacting particles, like protons (p^+) and neutrons (n^0), and the forces acting *within* and *between* them.

The fundamental building blocks of these particles are the fermionic spin-1/2 *quarks* q , which come in three generations, simply arraying states according to increasing mass: The three lightest up, down and strange ($u_{+2/3}$, $d_{-1/3}$ and $s_{-1/3}$) quark flavors weigh only a small fraction of the proton mass, the charm ($c_{+2/3}$) quark flavor just about the proton mass, while the two heavy bottom and top ($b_{-1/3}$ and $t_{+2/3}$) quark flavors weigh more than 5 and 180 times the proton mass, respectively [16]. The lower indices label their respective electric charge, relating, together with the masses, the quark flavors together under exchanges (either decay or production) of charged W -bosons. *Baryons* are bound states composed of three quarks $q_i q_j q_k$ – e.g., $p^+ = uud$ and $n^0 = udd$ –, while *mesons* are bound states of quark-antiquark pairs $q_i \bar{q}_j$ – e.g., $\pi^+ = u\bar{d}$ ¹. A *residual* strong nuclear force is created between nucleons by the exchange of mesons; if a proton or neutron can get closer than about the proton size ($\sim 0.8\text{fm}$ [16]) to another nucleon, the exchange of mesons can occur, making possible for the particles to stick to each other. If they can't get that close, the strong force is too weak to make them stick together (see Section 2.1.3), and other competing forces (usually the electromagnetic force) can influence the particles to move apart.

Rather than start with the mathematical definition of the theory, let's consider, first, what our knowledge of Nature is; upon which we will base the theory. We know that the matter we believe to be composed of quarks have to be strong-force neutral – i.e., the baryonic wave function is observed to be symmetric under the permutations of quark states [39]. However, quarks being fermions, this violates the Pauli exclusion principle, or more generally the *spin-statistics theorem* [40]. The only way out of this problem is to ask the quarks to be labelled by (minimally) three new quantum numbers (or charge signs), called the *colors*: **Red**, **green** and **blue**.

¹Our discussion is excluding bound states with a higher number excitations – e.g., the pentaquarks $qqqq\bar{q}$.

Now, let's dive into the realm of theory: We are looking for an internal symmetry having a 3-dimensional representation which can give rise to a neutral combination of three particles (otherwise no color-neutral baryons). The simplest such statement is that a linear combination of each type of charge **red**, **green** and **blue** must be neutral, and, following a minimalist point of view, the simplest theory describing all the facts must be the correct one. We now postulate that the particles carrying this force, called gluons, must occur in color/anti-color units – i.e., $3^2 = 9$ of them. However, as '**red** + **green** + **blue**' is neutral, or "white", the linear combination '**red**/anti-**red** + **green**/anti-**green** + **blue**/anti-**blue**' must be non-interacting, since otherwise the colorless baryons would be able to emit these gluons and interact with each other via the strong force contrary to the evidence. This constraint says that a hypothetical particle that can't interact with anything can't be detected, and so doesn't exist, reducing the number of gluons to eight. The simplest theory describing the above is a $SU(3)$ *Yang-Mills theory*.

As for any other theory, to make predictions out of QCD, one starts by writing a classical Lagrangian and then quantize it by defining the *Feynman path integral* [35, 41, 42]. For a non-abelian gauge theory like QCD, the classical theory is well-described by the $SU(N_c)$ Yang-Mills Lagrangian

$$\mathcal{L} = -\frac{1}{4}F_{\mu\nu}F^{a\mu\nu} + \bar{\psi}(i\not{D}-m)\psi - gf^{abc}(\partial_\mu A_\nu^a)A^{b\mu}A^{c\nu} - \frac{g^2}{4}(f^{eab}A_\mu^a A_\nu^b)(f^{ecd}A^{c\mu}A^{d\nu}) + gA_\mu^a \bar{\psi}\gamma^\mu T^a \psi, \quad (2.2)$$

invariant under $\psi \rightarrow \mathbf{U}\psi$, $A^a T^a \rightarrow \mathbf{U}A^a T^a \mathbf{U}^{-1} - ig^{-1}(\partial_\mu \mathbf{U})\mathbf{U}^{-1}$, for $\mathbf{U} \in SU(N_c)$, and where

$$F_{\mu\nu}^a = \partial_\mu A_\nu^a - \partial_\nu A_\mu^a + gf^{abc}A_\mu^b A_\nu^c, \quad (2.3)$$

is the field strength tensor, where A is a boson gauge field (a gluon), ψ is a fermion field (a quark) and g is the *strong coupling*. The other symbols in (2.2) will be discussed later (see sections 2.1.3 and 2.1.4). The Feynman rules are constructed in the usual way. Although this construction from the path integral is somewhat technical to do formally, it is easy to see what these interactions will be from a heuristic point of view. The first two constituents of (2.2) will give the gauge and fermion propagators respectively. The third one involves three

A 's and represents a 3-gauge boson vertex, while, similarly, the fourth one gives a 4-boson vertex. Finally, the last term involves one A and two ψ and thus represents a vertex where two fermions interact with a gauge boson.

Gluons are taken massless, which is consistent with the absence of spinless fields in (2.2); we can't trigger a spontaneous symmetry-breaking similar to the Higgs mechanism in the EW-sector, giving the mass to the W^\pm - and Z -force-carriers in the process. We also see from (2.2) that gluons self-couple because they carry color charges. This has profound consequences for the QCD coupling, which will be discussed in Section 2.1.3.

As photons do in QED, our mathematical representation of gluons mathematically comes with two spurious degrees of freedom². This makes the quantization procedure complicated since only field configurations non-equivalent under gauge symmetry should be included in the path integral [43]. Otherwise, we would overcount. This means that the naive integration with the classical action is ill-defined. To eliminate the gauge-equivalent configurations, a (non-propagating) gauge-fixing term is added

$$\mathcal{L} \rightarrow \mathcal{L} - \frac{1}{2\xi}(\partial^\mu A_\mu^a)(\partial^\nu A_\nu^a), \quad (2.4)$$

where ξ is an arbitrary parameter. We can think of this auxiliary field as a Lagrange multiplier enforcing gauge fixing. Indeed, the ξ -equations of motion are just $\partial_\mu A_\mu^a = 0$, which is the Lorenz gauge constraint. This particular choice of gauge fixing has the advantage of being explicitly covariant. However, it keeps one spurious degree of freedom, which is compensated by adding “ghost” scalar fields, ω^a and $\bar{\omega}^a$, as

$$\mathcal{L} \rightarrow \mathcal{L} - \frac{1}{2\xi}(\partial^\mu A_\mu^a)(\partial^\nu A_\nu^a) - \partial^\mu \bar{\omega}^a \partial_\mu \omega^a + g f^{abc}(\partial^\mu \bar{\omega}^a)\omega^b A_\mu^c. \quad (2.5)$$

They are not physical because they violate spin-statistics theorem: They are scalar fields under any $SO(1,3)$ -transformation, but behave like fermions, as they anti-commute in the path integral. As it will be discussed below, in this thesis we will employ unitarity-based

²More generally, independently of the spin, massive particles have two *transverse* polarization states, but also a third state which is *longitudinal* (direction in which the particle travels). Massless particles cannot oscillate in their direction of motion because they must move at exactly the speed of light in that direction. If they oscillated, then their speed would vary; sometimes it would be slower than light and sometimes faster. This cannot happen. Massive particles can, a priori, move at any speed, as long as it is slower than light, allowing them to have longitudinal oscillations.

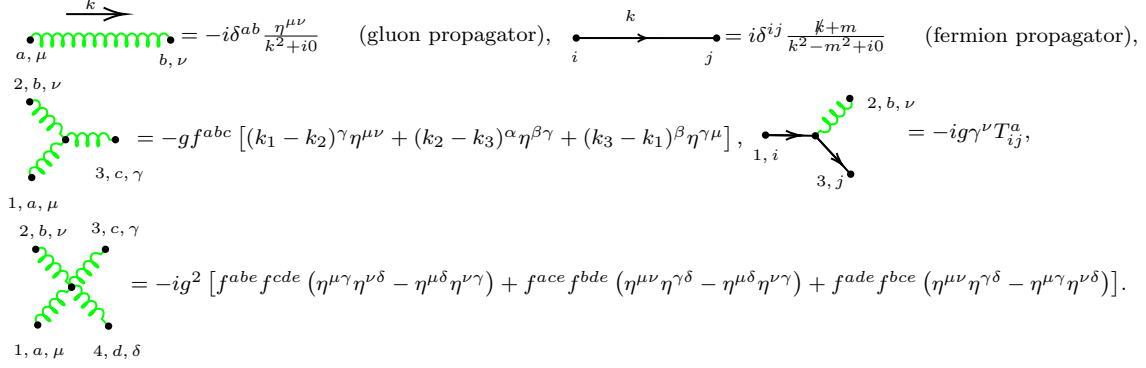


Figure 2.1: QCD Feynman rules (ghost fields excluded).

computational methods, which are formulated in terms of *gauge-invariant* building blocks. This allows us to discard ghost contributions explicitly.

Working in the Feynman gauge³, we set $\xi = 1$ in the general A -propagator

$$\frac{-i}{p^2 - i0} \left(\eta_{\mu\nu} - (1 - \xi) \frac{p_\mu p_\nu}{p^2} \right) \delta_{ab}, \quad (2.6)$$

where the “ $-i0$ ” enforces time ordering on 2-point functions in a simple way – i.e., it forbids information to propagate backward in time, as it is equivalent to adding various $\Theta(t)$ -factors [42, §6.2]. The Feynman rules for a $SU(N_c)$ gauge theory are given in Fig. 2.1.

Classical results are obtained from diagrams without any closed loops while quantum corrections involve an increasing number of loops. Even though gauge theories present many technical challenges, the way to proceed (at least perturbatively) is in principle well understood. In practice, however, the computational complexity grows rapidly with the number of external particles and the number of loops. Even at tree-level, where there is no loop to consider, the number of Feynman diagrams describing n -particle scattering of external gluons in QCD grows faster than factorially with n . For instance, from the QCD

³Note, however, that the choice of ξ is invisible in the correlation functions by BRST symmetry [44].

Feynman rules for gluons, one can check the following numbers

$$\left\{ \begin{array}{l} 2\text{-gluon} \rightarrow 2\text{-gluon} \Rightarrow 4 \text{ diagrams,} \\ 2\text{-gluon} \rightarrow 3\text{-gluon} \Rightarrow 25 \text{ diagrams,} \\ 2\text{-gluon} \rightarrow 4\text{-gluon} \Rightarrow 220 \text{ diagrams,} \\ 2\text{-gluon} \rightarrow 5\text{-gluon} \Rightarrow 2485 \text{ diagrams,} \\ 2\text{-gluon} \rightarrow 6\text{-gluon} \Rightarrow 34300 \text{ diagrams,} \\ 2\text{-gluon} \rightarrow 7\text{-gluon} \Rightarrow 559405 \text{ diagrams,} \\ 2\text{-gluon} \rightarrow 8\text{-gluon} \Rightarrow 10525900 \text{ diagrams.} \end{array} \right.$$

2.1.3 A Word on Renormalization and Running Couplings

IN THE PREVIOUS SECTION, we introduced a number of parameters in the QCD Lagrangian (2.2) – e.g., the coupling constant g and the fermion mass m . In any interacting QFT, these bare parameters of the Lagrangian may not directly correspond to any observable quantities. In fact, in the context of perturbation theory, most of these parameters contain explicit divergences associated to the high-energy or ultraviolet (UV) limit of the theory. An idea is to simply “reparametrized” the bare parameters in terms of measurable quantities, even if no divergences are encountered. This ‘ad hoc’ procedure is known as *renormalization* [35, 41, 42]. In fact, it is only after the renormalization is carried out that the theory can be predictive for experiments.

Broadly speaking, there are two options for how the renormalization of each bare parameter can be performed. First, in some cases it might be possible to connect the bare parameter to an observable quantity by simply multiplying it by a factor, which can be evaluated from perturbation theory by requiring finiteness. For instance, a renormalized mass $m_{\text{phys.}}$ can be chosen to be the position of the pole of the corresponding two-point correlation function (particle self-energy), such that the bare mass is $m = Z_m m_R$, where R stands for “renormalized”. Another example is the QED coupling constant, which can be

defined by the large-distance electric charge, e . This is called *on-shell renormalization* for obvious reasons.

Sometimes, it is not possible to find an observable, like mass or charge, to which the bare parameter can be tied. For instance, this is the case for the gluon self-coupling, g , in QCD (see below). In such cases, one can conveniently define the renormalized Lagrangian parameters at an arbitrary renormalization scale μ , given a renormalization prescription, such as *modified minimal subtractions* ($\overline{\text{MS}}$) [45]. This particular scheme has the advantage of being well defined in the massless limit. All bare quantities predicted from the theory are then evaluated in terms of the renormalized (or physical) parameters. For example, the bare gluon self-interaction coupling can be redefined as

$$g = \mu^\varepsilon \cdot Z_g(\mu) \cdot g_R(\mu). \quad (2.7)$$

In (2.7), Z_g depends on μ through g_R – i.e., $Z_g(\mu) \sim (g_R(\mu)/4\pi)^2 \varepsilon^{-1} + \mathcal{O}(1)$ at 1-loop [42, §26.5.3-26.6.1]. The *fixed* bare quantities must, however, not depend on the renormalization scale μ , as it is arbitrary. This fact is expressed in terms of the so-called *renormalization group equations* (RGE). For example, by writing $\mu^\varepsilon = \exp(\varepsilon \log(\mu))$, chain rule tells us

$$\frac{d}{d \log(\mu)} g(\mu, g_R(\mu), \varepsilon) = \frac{dg_R}{d \log(\mu)} \frac{\partial g}{\partial g_R} + \varepsilon g = 0 \Rightarrow \frac{dg_R(\mu)}{d \log(\mu)} = -\varepsilon g \cdot \left(\frac{\partial g}{\partial g_R} \right)^{-1}, \quad (2.8)$$

where the LHS of the second equation is called the β -function. We see that the solution of the RGE relates the parameters defined at two different renormalization scales: The one at which the bare quantity is defined, μ_0 , and the arbitrary one, μ . This freedom can be useful in that it allows to improve the convergence of the perturbation series by making an appropriate choice of the renormalization scale. This is closely related to the notion of running (or effective) couplings [35, 41, 42, §26.6.1].

For the QCD coupling constant $\alpha_s(\mu) := g_R^2(\mu)/4\pi$, the solution of the 1-loop RGE in the $\overline{\text{MS}}$ scheme is [42]

$$\alpha_s(\mu) = \frac{\alpha_s(\mu_0^2)}{1 + \beta_0 \alpha_s(\mu_0^2) \log(\mu^2/\mu_0^2)}, \quad \beta_0 = \frac{11N_c - 2N_f}{3}. \quad (2.9)$$

Here N_c denotes the number of colors and N_f the number of flavors of quarks, which are considered massless here. We observe, that at large scales the effective strong coupling constant

becomes very small, independent of the initial value $\alpha_s(\mu_0^2)$. On one hand, this implies that at high energies QCD behaves as a weakly-interacting theory. This phenomenon reflects the QCD asymptotic freedom. This fact enables the usage of perturbation theory to predict the scattering of strongly-interacting particles at hadron colliders. On the other hand, at low energies, the effective strong coupling becomes large, and the application of perturbation theory is not justifiable. This gives a quantitative explanation to an experimental fact: Free partons are not observed because they are confined into colorless QCD bound states: The *hadrons*. Perturbation theory has nothing to say about confinement, which complicates the theoretical description of hadron collisions. Fortunately, the short-distance and large-distance effects can be disentangled using, for example, *Feynman's Parton Models* [14–16, 46–48], but we won't go into any details here as they won't be immediately important.

The confinement regime is best captured in terms of the *non-perturbative scale of QCD*, Λ_{QCD} , defined as

$$\alpha_s(\mu) = \frac{\alpha_s(\mu_0^2)}{1 + \beta_0 \alpha_s(\mu_0^2) \log(\mu^2/\mu_0^2)} \equiv \frac{\alpha_s(\mu_0^2)}{\beta_0 \alpha_s(\mu_0^2) \log(\mu^2/\Lambda_{\text{QCD}}^2)}. \quad (2.10)$$

Given that a value for Λ_{QCD} only defines $\alpha_s(\mu)$ once one knows which particular approximation μ_0 is being used, Λ_{QCD} is a rough estimate ($\mu \sim 250\text{MeV}$) of the fuzzy boundary between the (higher) energies where the perturbative expansions are good, accurate, and useful, and the (lower) energies where the perturbative approaches don't work well – i.e., beyond which the β -function starts diverging. One can say that for $\mu \ll \Lambda_{\text{QCD}}$ the theory is strongly coupled—implying confinement—, and for $\mu \gg \Lambda_{\text{QCD}}$ it is weakly coupled—implying asymptotic freedom. For $\mu \ll \Lambda_{\text{QCD}}$, this implies the color charges of QCD is *not* experimentally measurable! If it wasn't for *hadronization* [49, 50] and *top quark weak decay* [51] (see Footnote 3 for some basic intuition), we'd be able to observe a lone quark, and so to measure its charge and, up to a messier convention hassle than with electric charges, its “sign” – i.e., color – from high-energy collisions.

2.1.4 Color Stripped Amplitudes

IN THIS SECTION, we illustrate that the color structure of pure gluon amplitudes is factorizable and, therefore, one can usually focus on *color stripped amplitudes* [33, 34, 42].

In the last section, we saw that complications are experienced in gauge theory calculations because, in part, expressions need to be gauge invariant. This forces the theory to not just carry spacetime labels, but also gauge group ones. For a $SU(N_c)$ Yang-Mills theory, the state of a particle is given by a vector in some vector space on which elements of $SU(N_c)$ act as linear (in fact unitary) operators. We say the particle “transforms under some representation of $SU(N_c)$ ”. For example, $SU(N_c)$ -gluons, $A = A^a T^a$, are the basis states of the $SU(N_c)$ Lie algebra itself. That is, gluons will transform under the *adjoint* representation of $SU(N_c)$ (see [37, p.240-242] for the complete story), labeled by a color Roman index $a = 1, 2, \dots, N_c^2 - 1$ – i.e., $A = A^a T^a \rightarrow A^a (g \cdot T^a \cdot g^{-1}) = g \cdot A \cdot g^{-1}$, $g \in SU(N_c)$. Since the T^a are $(N_c \times N_c)$ -matrices, so is any element of $SU(N_c)$ by exponentiation. Each of these elements can act on column vectors by matrix multiplication. This gives a N_c -dimensional representation of $SU(N_c)$: The *fundamental* representation. The $SU(N_c)$ -quarks transform under this representation of $SU(N_c)$ and, because it is N_c -dimensional, we say quarks come in N_c colors. For example, in QCD where $N_c = 3$, there are eight (e.g., Gell-Mann) 3×3 hermitian matrices, $T^{1 \leq a \leq 8}$, so there exists eight gluon fields $A^{1 \leq a \leq 8}$. The quarks **red** $= (1, 0, 0)^\top$, **green** $= (0, 1, 0)^\top$ and **blue** $= (0, 0, 1)^\top$, will transform under the 3-dimensional fundamental representation.

Now, to avoid a proliferation of factors of $\sqrt{2}$ in the amplitudes, we normalize these such that $\text{tr}(T^a T^b) = \delta^{ab}$. The special unitary group is a Lie group and the Lie algebra that generates it near the identity is by definition

$$[T^a, T^b] = i f^{abc} T^c. \quad (2.11)$$

where the f^{abc} are referred as the structure constant. We shall abbreviate $T = (T^a)_i^j$ and $f = f^{abc}$ whenever it is not confusing. The T -commutators satisfy a Jacobi identity and so do the f 's

$$f^{ade} f^{bcd} + f^{bdc} f^{cad} + f^{cde} f^{abd} = 0. \quad (2.12)$$

At the tree-level, we can read off from the Feynman rules above that the group theory manifests itself for each quark-gluon vertex by one factor of T and for each 3-gluon vertex by a factor of f , while for 4-gluon vertices it is with contracted pairs of f 's. It is the quark and gluon propagators that will contract many of the indices together and many of these combinations will end up as factors of “1” or vanishing due to our choice of T -normalization. We can simplify the color structure of the amplitudes further by noticing that color factors in the Feynman rules can all be replaced by linear combinations of strings of T 's due to the following identity [41]

$$f^{abc} = -i\text{Tr}(T^a[T^b, T^c]). \quad (2.13)$$

However, as the T 's are generators, they will form a complete set of traceless Hermitian matrices. Algebraically, it implies the $\text{SU}(N_c)$ -Fierz identity [41]

$$\sum_{a=1}^{N_c^2-1} (T^a)^{\bar{j}}_i (T^a)^{\bar{l}}_k = \delta_i^{\bar{l}} \delta_k^{\bar{j}} - \frac{1}{N_c} \delta_i^{\bar{j}} \delta_k^{\bar{l}}. \quad (2.14)$$

We can interpret the term proportional to $1/N_c$ as the subtraction of the $\text{U}(N_c)$ traces in which $\text{SU}(N_c)$ is canonically embedded by the additional constraint that its elements preserve volumes – i.e., $\det(A) = 1$. This indeed ensures the tracelessness of the T 's, as contracting (2.14) with δ_j^i shows us. For the interested reader, in reference [34], Dixon gives a nice Feynman diagrammatic interpretation of identities such as (2.13) and (2.14). We also already see from (2.14) why it can be computationally appealing to consider theories with a large number of colors as the second term in the right hand side drops off. However, there's a price to pay when we take $N_c \rightarrow \infty$: We lose non-planarity [36, 52, 53, §6].

Mathematically, a graph is said to be *planar* if it *can* be drawn on a sphere without selfcrossings. This “topological” definition implies that any tree and 1-loop graph is planar, because it is not restrictive on the ordering of the external legs (if any). However, as we are about to see, color stripping the amplitudes forces us to fix a specific ordering for the external legs. Thus, instead of thinking about planarity topologically, it will be more useful to think about it in terms of planar/non-planar *channels*. For example, in 4-point processes, the s - and t -channels are planar, while the u -channel is non-planar (see Fig. 2.2). This illustrates

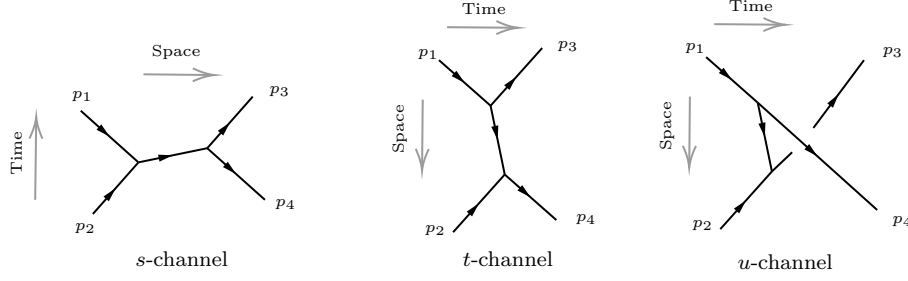


Figure 2.2: s -, t - and u -channel exchanges for a 4-point process.

that a planar topology, here $\begin{array}{c} \diagup \quad \diagdown \\ \hline \diagdown \quad \diagup \end{array}$, can have non-planar channels. Consequently, given an ordering of the external legs, a color stripped amplitude is *planar* if and only if it has no non-planar channels. In particular, the latter characterization implies that planar amplitudes have *right hand cut* singularities only [54] – i.e., planar graphs can only depend on *consecutive* Mandelstam invariants $s_{ij} := (p_i + p_j)^2$.

Now, with the help of (2.14), we can simplify further sums of double-traces appearing, for example, if we only have external gluons [55]

$$\sum_a \text{tr}(T^{a_1} \dots T^{a_k} T^a) \text{tr}(T^a \dots T^{a_{k+1}} T^{a_n}) = \text{tr}(T^{a_1} \dots T^{a_k} T^{a_{k+1}} \dots T^{a_n}) - \frac{1}{N_c} \text{tr}(T^{a_1} \dots T^{a_k}) \text{tr}(T^{a_{k+1}} \dots T^{a_n}), \quad (2.15)$$

and, sums of strings of generators terminated by fundamental indices, for example, if we have external quarks

$$\sum_a \text{tr}(T^{a_1} \dots T^{a_k} T^a) (T^a \dots T^{a_{k+1}} T^{a_n})_i^{\bar{j}} = (T^{a_1} \dots T^{a_k} T^{a_{k+1}} \dots T^{a_n})_i^{\bar{j}} - \frac{1}{N_c} \text{tr}(T^{a_1} \dots T^{a_k}) (T^{a_{k+1}} \dots T^{a_n})_i^{\bar{j}}. \quad (2.16)$$

For pure gluon scatterings, one can check by hand that the terms with $1/N_c$ all cancel among themselves after summing over all the permutations. However, we can deduce that without doing any computation. Indeed, notice that the term would be absent if the gauge groups were $U(N_c) \simeq SU(N_c) \times U(1)$ rather than just $SU(N_c)$ as the constraint on the traces are removed. Moreover, for the same reason photons do not self-couple⁴, the auxiliary $U(1)$ photon field does not couple to gluons. Therefore, the $1/N_c$ term only has to be retained

⁴This is because $U(1)$ is abelian and the additional $U(1)$ Lie algebra generator is proportional to the identity matrix – i.e., $(T_{U(1)}^a)_i^{\bar{j}} = \frac{1}{\sqrt{N_c}} \delta_i^{\bar{j}}$.

only for amplitudes where a gluon can couple to a fermion line at both ends, given quarks interact with the photons as they are electrically charged. This shows gluonic amplitudes must contain only single traces. We write the full n -gluon tree-level amplitudes as [33]

$$\mathcal{A}_n^{\text{tree}} = g^{n-2} \sum_{\sigma \in \mathcal{S}_n/\mathcal{C}_n} \text{tr}(T^{a_{\sigma(1)}} T^{a_{\sigma(2)}} \dots T^{a_{\sigma(n)}}) A_n^{\text{tree}}[\sigma(1), \sigma(2), \dots, \sigma(n)], \quad (2.17)$$

where $\mathcal{S}_n/\mathcal{C}_n$ is the permutation group of n letters modulo cyclic ones. It is easy to see that there are exactly $(n-1)!$ such permutations. The A_n^{tree} are the *color-stripped* and cyclic invariant (sub)amplitudes depending *only* on one ordering of the external particles, making them color independent. In particular, color independency implies that A_n^{tree} is gauge invariant, because they behave like in abelian theory – i.e., they satisfy a Ward-like identity [56]. Moreover, it is easy to see that A_n^{tree} satisfies a reflection property

$$A_n^{\text{tree}}(1, 2, \dots, n) = (-1)^n A_n^{\text{tree}}(n, \dots, 2, 1). \quad (2.18)$$

An additional property worthwhile noting is what happens when we take *one* of the T -generators proportional to the identity, i.e., $(T_{\text{SU}(N_c)}^a)_i^{\bar{j}} \rightarrow (T_{\text{U}(1)}^a)_i^{\bar{j}} = \frac{1}{\sqrt{N_c}} \delta_i^{\bar{j}}$. Physically, this corresponds to replacing one of the gluon by a photon. From there, it is not so hard to show that the sum of $(n-1)$ -color-stripped amplitudes vanishes

$$A_n^{\text{tree}}(1, 2, 3, \dots, n) + A_n^{\text{tree}}(2, 1, 3, \dots, n) + A_n^{\text{tree}}(2, 3, 1, \dots, n) + \dots + A_n^{\text{tree}}(2, 3, \dots, 1, n) = 0. \quad (2.19)$$

For obvious reasons, this is known as the U(1) decoupling identity. This is an indication that the trace-basis is actually overcomplete. Indeed, the overcompleteness gives rise to many other linear relations among color-stripped tree-level amplitudes known as the *Kleiss-Kuijff relations* [57, 58]. An interesting homologically based proof of such relations is given [59]. Note that for tree amplitudes involving quarks, analogous formulas can be derived where instead of a trace, the string of matrices will be terminated by the specific T 's in the quark-quark-gluon vertices.

With the previous prescriptions, we can write the color-ordered Feynman rules for QCD, they are readily obtained by the usual Feynman rules just by imposing a given ordering – i.e., they are given in Fig. 2.1, but without a $\sqrt{2}igf^{abc}$ factor.

As final comment to this section, we note that this color-ordering decomposition can be extended to higher loops and multiplicities. For instance, in [60], the trace basis for all-loop 4-point amplitudes is derived, while in [61], it is the 5-point that is derived. Similar expressions can be obtained by freezing the number of loops and taking arbitrary multiplicity – e.g., at 1-loop, we note amplitudes of gluons have double-trace terms as well as single-trace terms – e.g., see [62, Eq. 4] or [55]. The 2-loop 5-point case for any $SU(N_c)$ gauge theory is discussed in [63, Eq. 1].

2.1.5 Spinor-Helicity Formalism

A MATHEMATICAL TOOL that as been seen to tremendously simplifies computations in gauge theory is the so-called *spinor-helicity formalism* [33]. At the tree-level, for instance, it was shown by Parke and Taylor in the late 80’s that any color ordered n -gluon amplitude could be written in a one line spinor-helicity expression [64]. Here, we provide a brief summary of this formalism.

The helicity of a particle is the projection of its spin \mathbf{S} on the direction of its 3-momentum \mathbf{p} , and the states $\psi_{\pm s}$ with helicity $\pm s$ are defined as

$$\frac{\mathbf{S} \cdot \mathbf{p}}{|\mathbf{p}|} \psi_{\pm s} = \pm s \psi_{\pm s}. \quad (2.20)$$

The helicity of *massless* particles is a Lorentz invariant, as its spin is and $|\mathbf{p}|$ is characterized only by the particle frequency. In such a case, helicity and chirality eigenstates coincide. For massive particles helicity eigenstates can be constructed relative to a chosen reference frame. Because we are interested in scatterings at high energies, we shall focus on the massless spinor-helicity formalism, although a massive generalization can be considered – e.g., see [65–67].

For a null vector $p_\mu = (p_0, p_1, p_2, p_3)$, satisfying $p_\mu p^\mu = 0$, we can derive a spinor representation. This is done mathematically by going from the usual 4-vector representation of $SO(1, 3)$ to the locally equivalent⁵ to the $(1/2, 1/2)$ -representation of $SL(2, \mathbb{C})$ [42, §10.1.2].

⁵The Lorentz group $SO(1, 3)$ is locally isomorphic to $SU(2) \times SU(2)$, whose finite dimensional representations are labeled by weights (p, q) , taking integer or half-integer values. This isomorphism is true locally

A central contraction for us will be

$$p_{\alpha\dot{\beta}} \equiv p_{\mu}\sigma^{\mu}_{\alpha\dot{\beta}} = \begin{pmatrix} p^{+} & (\mathbf{p}^{\perp})^{\star} \\ \mathbf{p}^{\perp} & p^{-} \end{pmatrix}, \quad (2.21)$$

where $p^{\pm} = p^0 \pm p^3$ and $\mathbf{p}^{\perp} = p^1 + ip^2$. The $\text{SL}(2, \mathbb{C})$ -action on $p_{\alpha\dot{\beta}}$ is by conjugation – i.e., $p_{\alpha\dot{\beta}} \rightarrow p'_{\alpha\dot{\beta}} := \Lambda_{\mathbb{C}}^{\top} \cdot p_{\alpha\dot{\beta}} \cdot \Lambda_{\mathbb{C}}$, for any $\Lambda_{\mathbb{C}} \in \text{SL}(2, \mathbb{C})$ –, from which equivalence classes $\det(p'_{\alpha\dot{\beta}}) = \det(p_{\alpha\dot{\beta}})$ are determined. This also implies that Pauli matrices transform equivalently as 4-vectors under the usual Lorentz transformation and as 2×2 matrices under $\text{SL}(2, \mathbb{C})$ -conjugation – i.e., $\sigma_{\mu}\Lambda^{\mu}_{\nu} = \Lambda_{\mathbb{C}}^{\top} \cdot \sigma_{\nu} \cdot \Lambda_{\mathbb{C}}$. It is straightforward to see that whenever p is null, $\det(p_{\alpha\dot{\beta}}) = 0$. Moreover, if $\det(p_{\alpha\dot{\beta}}) = 0$, then $p_{\alpha\dot{\beta}}$ can be written as the Kronecker product of two 2-vectors

$$p_{\alpha\dot{\beta}} = \lambda_{\alpha}\tilde{\lambda}_{\dot{\beta}}. \quad (2.22)$$

This means a momentum 4-vector should be viewed as an object with one each of the positive- (undotted-) and negative- (dotted-) chirality labels of the $\text{SL}(2, \mathbb{C})$ -spinor representations. In physics language, this is equivalent to say that λ_a and $\tilde{\lambda}_{\dot{b}}$ are, respectively, positive-chirality and negative-chirality Weyl spinors.

Although the explicit component forms of the spinors are not needed in most cases, we will see later that for limit parameterizations – e.g., collinear limits –, they turn out to be useful. Hence, we give their explicit form

$$\lambda_{\alpha} \equiv \begin{pmatrix} -z \frac{\mathbf{p}^{\perp}}{\sqrt{p^{-}}} \\ z \sqrt{p^{-}} \end{pmatrix} \quad \text{and} \quad \tilde{\lambda}_{\dot{\beta}} \equiv \begin{pmatrix} -\frac{1}{z} \frac{(\mathbf{p}^{\perp})^{\star}}{\sqrt{p^{-}}} \\ \frac{1}{z} \sqrt{p^{-}} \end{pmatrix}^{\top}. \quad (2.23)$$

In this decomposition, it is understood that $\mathbf{p}^{\perp} = \exp(i\text{Arg}(\mathbf{p}^{\perp}))\sqrt{p^{+}}\sqrt{p^{-}}$. In (2.23), z is an unfixed parameter accounting the non-uniqueness of this representation. In other words, we have a rescaling freedom

$$\lambda_{\alpha} \rightarrow z\lambda_{\alpha}, \quad \tilde{\lambda}_{\dot{\beta}} \rightarrow \frac{1}{z}\tilde{\lambda}_{\dot{\beta}}. \quad (2.24)$$

because it happens at the level of their Lie algebras. The positive-chirality spinor representation is $(1/2, 0)$, while the negative chirality spinor representation is $(0, 1/2)$, a notation reminiscent of the $\mathfrak{su}(2) \oplus \mathfrak{su}(2)$ exponentiation into the universal $\text{SL}(2, \mathbb{C})$ -covering of $\text{SO}(1, 3)$ – i.e., $\text{SO}(1, 3) \simeq \text{SL}(2, \mathbb{C})/\mathbb{Z}_2$ [38].

In the literature, this action of this symmetry is called the little group scaling. This is in fact a “subgroup” of the Lorentz group transforming the spinors and invisible at the level of the momentum. In some cases, it is useful to fix z for the problem convenience. For instance, when $p^\mu \in \mathbb{R}^{1,3}$ and $p^+ > 0$, we can set $z \in \text{U}(1)$, from which it follows that

$$\lambda_\alpha = (\tilde{\lambda}_{\dot{\beta}})^*, \quad (2.25)$$

where the “ \star ” operation stands for complex conjugation. Nevertheless, one is often interested in the holomorphic properties of the scattering amplitudes – e.g., for crossing symmetry – and we, consequently, usually avoid such a choice. Another choice one can make that is sometimes computationally helpful is $z = \sqrt{p^-}$. With this choice, we get rid of the square roots in (2.23).

Moreover, as usual when we deal with spinor objects, we can use the Levi-Civita tensors

$$\varepsilon^{\alpha\beta} = \begin{pmatrix} 0 & 1 \\ -1 & 0 \end{pmatrix}, \quad \varepsilon^{\dot{\alpha}\dot{\beta}} = \begin{pmatrix} 0 & 1 \\ -1 & 0 \end{pmatrix}, \quad \varepsilon_{\alpha\beta} = \begin{pmatrix} 0 & -1 \\ 1 & 0 \end{pmatrix}, \quad \varepsilon_{\dot{\alpha}\dot{\beta}} = \begin{pmatrix} 0 & -1 \\ 1 & 0 \end{pmatrix}, \quad (2.26)$$

to raise and lower the spinor indices⁶

$$\lambda^\alpha = \varepsilon^{\alpha\beta} \lambda_\beta, \quad \lambda_\alpha = \varepsilon_{\alpha\beta} \lambda^\beta, \quad \lambda^{\dot{\alpha}} = \varepsilon^{\dot{\alpha}\dot{\beta}} \lambda_{\dot{\beta}}, \quad \text{and} \quad \lambda_{\dot{\alpha}} = \varepsilon_{\dot{\alpha}\dot{\beta}} \lambda^{\dot{\beta}}. \quad (2.27)$$

Now, given p_i for arbitrary $i \in \mathbb{N}$ is a null vector, we denote the corresponding spinor by λ_i . We can make our notation less notationally bulky by introducing the following “braket” notation

$$\langle ij \rangle := \lambda_i^\alpha \lambda_{j\alpha}, \quad \text{and} \quad [ij] := \tilde{\lambda}_{i\dot{\alpha}} \tilde{\lambda}_j^{\dot{\alpha}}. \quad (2.28)$$

This shows spinors of the same chirality contract consistently via epsilon tensors. Conversely, chirality forbids invariants of the form $\langle ij \rangle := \lambda_i^\alpha \tilde{\lambda}_j^{\dot{\alpha}}$ to exist – i.e., they vanish [33]. The

⁶Recalling that physical left/right Weyl spinors $\lambda^\alpha/\lambda^{\dot{\alpha}}$ are Graßmann-odd, the antisymmetric tensor $\varepsilon_{\alpha\beta}/\varepsilon_{\dot{\alpha}\dot{\beta}}$ can be viewed as a metric on spinors. It is an invariant tensor under $\text{SL}(2, \mathbb{C})$, which can be seen by how the symplectic form (see (2.28)), $\langle \lambda_1, \lambda_2 \rangle := \lambda_1^1 \lambda_2^2 - \lambda_1^2 \lambda_2^1 \equiv \lambda_1^\top \cdot \varepsilon \cdot \lambda_2$, transforms under $\text{SL}(2, \mathbb{C})$

$$\langle \lambda_1, \lambda_2 \rangle = \lambda_1^\top \cdot \varepsilon \cdot \lambda_2 = \langle \Lambda_{\mathbb{C}} \lambda_1, \Lambda_{\mathbb{C}} \lambda_2 \rangle = \lambda_1^\top \cdot (\Lambda_{\mathbb{C}}^\top \cdot \varepsilon \cdot \Lambda_{\mathbb{C}}) \cdot \lambda_2, \quad \Lambda_{\mathbb{C}} \in \text{SL}(2, \mathbb{C}) \Leftrightarrow \varepsilon = \Lambda_{\mathbb{C}}^\top \cdot \varepsilon \cdot \Lambda_{\mathbb{C}}.$$

This statement in the usual $\text{SO}(1,3)$ representation may be more familiar; the 4×4 real Lorentz transformation, $x^\mu = \Lambda^\mu_\nu x^\nu$, preserves the Lorentz-invariant Minkowski bilinear form $\Lambda^\top \cdot \eta \cdot \Lambda = \eta$. Hence, if we have an irreducible representation, λ^α , of $\text{SL}(2, \mathbb{C})$, we can transform it with ε and this will give one in the same class: It doesn’t matter whether we use λ^α or λ_α because both quantities represent the same physical thing.

definitions in (2.28) are sensitive to the order of the spinors. For example,

$$\langle ij \rangle = \varepsilon^{\alpha\beta} \lambda_{i\beta} \lambda_{j\alpha} = \varepsilon^{\beta\alpha} \lambda_{i\alpha} \lambda_{j\beta} = \varepsilon^{\beta\alpha} \lambda_{j\beta} \lambda_{i\alpha} = -\varepsilon^{\alpha\beta} \lambda_{j\beta} \lambda_{i\alpha} = -\langle ji \rangle. \quad (2.29)$$

Similarly, $[ij] = -[ji]$. From the above, it is now clear that $\langle ij \rangle = [ij] = 0$, whenever $i = j$.

Note that due to the little-group rescaling, these angle and square brackets are not uniquely defined. In what follows, it will be useful to have a “parity-flipped” set of Pauli matrices, $\bar{\sigma}^{\mu, \dot{\alpha}\beta} := (\sigma^0, -\sigma^i)^{\dot{\alpha}\beta}$, which is related to the usual ones via

$$\bar{\sigma}^{\mu, \dot{\beta}\delta} = \varepsilon^{\delta\alpha} \varepsilon^{\dot{\beta}\dot{\alpha}} \sigma_{\alpha\dot{\alpha}}^{\mu}. \quad (2.30)$$

When there will be no risk of confusion, we may drop the spinor indices and write (2.30) as $\bar{\sigma}^{\mu} = (\varepsilon \cdot \sigma^{\mu} \cdot \varepsilon^{\top})^{\top}$, where $\varepsilon := i\sigma^2$ is defined in (2.1). The σ and $\bar{\sigma}$ matrices satisfy orthonormal relations in both chiral and spacetime indices

$$\text{tr}(\sigma^{\mu} \bar{\sigma}^{\nu}) = -2\eta_{\mu\nu} \quad \text{and} \quad \sigma_{\mu, \alpha\dot{\alpha}} \bar{\sigma}^{\mu, \dot{\beta}\beta} = -2\delta_{\alpha}^{\beta} \delta_{\dot{\alpha}}^{\dot{\beta}}. \quad (2.31)$$

We can use the orthonormal relation to recover the original null-vector p_i from the spinors

$$p_i^{\nu} = \frac{1}{2} (\tilde{\lambda}_{i, \dot{\beta}} \bar{\sigma}^{\nu, \dot{\beta}\alpha} \lambda_{i, \alpha}) = \frac{1}{2} (\tilde{\lambda}_i \bar{\sigma}^{\nu} \lambda_i), \quad (2.32)$$

where we identified λ with λ_{α} and $\tilde{\lambda}$ with $\tilde{\lambda}_{\dot{\beta}}$. In a similar fashion, the spinors allow us to construct new intermediate null-vectors such that

$$(\lambda_i \tilde{\lambda}_j)^{\nu} = \frac{1}{2} (\tilde{\lambda}_{j, \dot{\beta}} \bar{\sigma}^{\nu, \dot{\beta}\alpha} \lambda_{i, \alpha}) = \frac{1}{2} (\tilde{\lambda}_j \bar{\sigma}^{\nu} \lambda_i), \quad (2.33)$$

which makes clear that

$$(\lambda_i \tilde{\lambda}_j)_{\nu} \sigma_{\alpha\dot{\beta}}^{\nu} = \lambda_{i, \alpha} \tilde{\lambda}_{j, \dot{\beta}} \quad \text{and} \quad p_i^{\nu} = (\lambda_i \tilde{\lambda}_i)^{\nu}. \quad (2.34)$$

One important identity that follows from (2.29) after taking double contractions of (2.33) is

$$\langle ik \rangle [\ell j] = -2(\lambda_i \tilde{\lambda}_j)^{\nu} (\lambda_k \tilde{\lambda}_{\ell})_{\nu}. \quad (2.35)$$

It is also easy to see this equation holds using the standard Pauli matrix identities

$$\begin{aligned} \langle ik \rangle [\ell j] &= (\varepsilon^{\alpha\beta} \lambda_{i, \beta} \lambda_{k, \alpha}) (\varepsilon^{\alpha\beta} \tilde{\lambda}_{\ell, \dot{\alpha}} \tilde{\lambda}_{j, \dot{\beta}}) \\ &= (\lambda_k^{\top} \cdot \varepsilon \cdot \lambda_i) (\tilde{\lambda}_{\ell} \cdot \varepsilon \cdot \tilde{\lambda}_j^{\top}) = (\lambda_k^{\top} \cdot \varepsilon \cdot \lambda_i) (\tilde{\lambda}_{\ell} \cdot \varepsilon \cdot \tilde{\lambda}_j^{\top})^{\top} \\ &= (\lambda_i \tilde{\lambda}_j)_{\mu} (\lambda_k^{\top} (\bar{\sigma}^{\mu})^{\top} \tilde{\lambda}_{\ell}^{\top}) = (\lambda_i \tilde{\lambda}_j)_{\mu} (\tilde{\lambda}_{\ell} \bar{\sigma}^{\mu} \lambda_k) \\ &= \text{tr}(\sigma^{\nu} \bar{\sigma}^{\mu}) (\lambda_i \tilde{\lambda}_j)_{\mu} (\lambda_k \tilde{\lambda}_{\ell})_{\nu} = -2(\lambda_i \tilde{\lambda}_j)^{\nu} (\lambda_k \tilde{\lambda}_{\ell})_{\nu}. \end{aligned} \quad (2.36)$$

When we take $k = j$ and $i = \ell$ in (2.35), we see that, if all momenta are outgoing,

$$s_{ij} = (p_i + p_j)^2 = \langle ij \rangle [ij], \quad (2.37)$$

and likewise for higher-point kinematic invariants. This also allows one to write

$$\langle ij \rangle = \exp(i\phi_{ij})\sqrt{s_{ij}} \quad \text{and} \quad [ij] = \exp(-i\phi_{ij})\sqrt{s_{ij}}, \quad (2.38)$$

for some phase ϕ_{ij} . There are numerous other identities one can derive that makes the spinor formalism a very useful language for calculations in scattering amplitudes. For example, we already saw that the on-shell conditions are built-in these variables. Another example of a particularly useful identity is the Schouten's identity. It follows from the basic fact that 3 vectors in a plane cannot be all linearly independent. Therefore, if we have 3 spinors λ_i , λ_j and λ_k , it exists some a and b such that $\lambda_i = a\lambda_j + b\lambda_k$, which can be used to construct spinor products

$$\langle ik \rangle = a\langle jk \rangle \quad \text{and} \quad \langle ij \rangle = b\langle kj \rangle. \quad (2.39)$$

This implies

$$\langle i\ell \rangle = a\langle j\ell \rangle + b\langle k\ell \rangle = \frac{\langle ik \rangle}{\langle jk \rangle}\langle j\ell \rangle + \frac{\langle ij \rangle}{\langle kj \rangle}\langle k\ell \rangle \Rightarrow \langle ij \rangle\langle k\ell \rangle + \langle jk \rangle\langle i\ell \rangle + \langle ki \rangle\langle j\ell \rangle = 0. \quad (2.40)$$

This identity is particularly useful when one wants to make tree-level amplitudes look nicer, but as it is a quadratic relation, it does not straightforwardly help to eliminate spinor products by naively using it.

The momentum conservation condition for the scattering of n -massless particles also takes a quadratic form in these variables

$$\sum_{i=1}^n (\lambda_i \tilde{\lambda}_i)_\nu = 0 \Rightarrow 2(\lambda_i \tilde{\lambda}_j)^\nu \left(\sum_{i=1}^n (\lambda_i \tilde{\lambda}_i)_\nu \right) = 0 \Rightarrow \sum_{i=1}^n \langle ki \rangle [ij] = 0, \quad \forall k, j, \quad (2.41)$$

making it harder to use in comparison its formulation where it is the linear sum of external momenta that vanishes.

When we will talk about parameterizations of limits for the 2-loop 5-gluon scattering in latter sections, we will find it useful to have already noted that for four⁷ null-vectors p_i , p_j ,

⁷The discussion can easily be generalized to five momenta, but for the sake of the illustration we choose to work with just four.

p_k and p_ℓ , we have

$$\text{tr}(\sigma^\alpha \bar{\sigma}^\beta \sigma^\gamma \bar{\sigma}^\sigma) = 2(\eta^{\alpha\beta} \eta^{\gamma\sigma} + \eta^{\alpha\sigma} \eta^{\gamma\beta} - \eta^{\alpha\gamma} \eta^{\beta\sigma} + i\varepsilon^{\alpha\beta\gamma\sigma}), \quad (2.42)$$

where $\varepsilon^{\alpha\beta\gamma\sigma}$ is the totally skew-symmetric tensor and so, by a computation similar to (2.36) using (2.42), we get

$$\langle ij \rangle [jk] \langle k\ell \rangle [\ell i] = 2(p_i \cdot p_\ell)(p_j \cdot p_k) + 2(p_i \cdot p_j)(p_k \cdot p_\ell) - 2(p_i \cdot p_k)(p_j \cdot p_\ell) - 2i\varepsilon(i, j, k, \ell), \quad (2.43)$$

where $\varepsilon(i, j, k, \ell) = \varepsilon^{\alpha\beta\gamma\sigma} p_{1\alpha} p_{2\beta} p_{3\gamma} p_{4\sigma}$. One can check that, under $\varepsilon(i, j, k, \ell) \rightarrow \pm \varepsilon(i, j, k, \ell)$, (2.43) can be rewritten compactly as a chiral trace, $\text{tr} \left(\frac{1 \pm \gamma_5}{2} \not{p}_i \not{p}_j \not{p}_k \not{p}_\ell \right)$. Under the parity action, which is flipping the signs of the spacial momentum vectors (of the helicities)

$$\mathbf{p} : (p^0, \mathbf{p}_i) \mapsto (p^0, -\mathbf{p}_i), \quad (2.44)$$

we observe the Lorentz invariant expression (2.43) is parity-odd. Complimentary, it is often useful to further define the 4×4 matrix $\delta(p_i, p_j, p_k, p_\ell)$ such that

$$\delta(p_i, p_j, p_k, p_\ell)_{nm} := 2p_n \cdot p_m, \text{ for } n, m \in \{i, j, k, \ell\}. \quad (2.45)$$

Its determinant, $\Delta(p_i, p_j, p_k, p_\ell)$, is called the Gram determinant of $\{p_i, p_j, p_k, p_\ell\}$ and it is clearly parity-even since it is a perfect square

$$\Delta(p_i, p_j, p_k, p_\ell) = -\varepsilon(i, j, k, \ell)^2. \quad (2.46)$$

Note that Gram determinants vanishes if the momenta are linearly dependent [68] – e.g., two particles become collinear.

One additional feature of the spinor-helicity formalism is that it makes it easy to construct spin-1 on-shell massless states, like gluons. Given the usual quantum field operator expansions for massless spin-1 particles A_μ (see, e.g., [42, Eq. 8.76]), the helicity eigenstates of vector particles can be constructed in both $\text{SO}(1, 3)$ - or $\text{SL}(2, \mathbb{C})$ -representations

$$\epsilon_{i,+}^\mu = \sqrt{2} \frac{(\lambda_k \tilde{\lambda}_i)^\mu}{\langle ki \rangle} \quad \text{or} \quad \epsilon_{i,+}^{\alpha\dot{\beta}} = \sqrt{2} \frac{\lambda_k^\alpha \tilde{\lambda}_i^{\dot{\beta}}}{\langle ki \rangle} \quad \text{and} \quad \epsilon_{i,-}^\mu = \sqrt{2} \frac{(\lambda_i \tilde{\lambda}_k)^\mu}{[ik]} \quad \text{or} \quad \epsilon_{i,-}^{\alpha\dot{\beta}} = \sqrt{2} \frac{\lambda_i^\alpha \tilde{\lambda}_k^{\dot{\beta}}}{[ik]}, \quad (2.47)$$

where $k \neq i$ denotes an arbitrary reference spinor reflecting gauge invariance – i.e., the freedom in rescaling $\epsilon_{i,\pm} \rightarrow \epsilon_{i,\pm} + \kappa p_i$, for any $\kappa \in \mathbb{C}$. For given helicity h , a choice of λ_k then uniquely determines polarization vectors ϵ_\pm . The last observation finally makes justice to

the name “*spinor-helicity*”: Vector states $(p^\mu, \epsilon_\pm^\mu)$ are equivalent to the spinor-helicity vector states $(\lambda, \tilde{\lambda}, h)$!

Furthermore, as it should be, the little group scaling for the polarizations is

$$\epsilon_\pm \rightarrow t^{\mp 2} \epsilon_\pm. \quad (2.48)$$

Note that this does not spoil the on-shellness of p_i as it is encoded in the Ward identity $p_i^\mu \mathcal{A}_\mu = 0$ [41]. We just need to stick with our choice of k for each external gluon until the very end; summing over all diagrams will kill the k -dependence in the final amplitude \mathcal{A} . As noted in [33], the independence of the choice of reference spinor provides a useful way to check results, in particular when one proceeds by numerical evaluation, where it is fast to verify the stability of the amplitudes under various choices of k . From the $\text{SL}(2, \mathbb{C})$ -representations in (2.47), it is easy to see that

$$p_{i,\alpha\dot{\beta}} \epsilon_{i,+}^{\alpha\dot{\beta}} \sim [ii] = 0, \quad p_{i,\alpha\dot{\beta}} \epsilon_{i,-}^{\alpha\dot{\beta}} \sim \langle ii \rangle = 0, \quad \epsilon_{i,\pm}^2 = 0, \quad \epsilon_{i,+} \cdot \epsilon_{i,-} = -1. \quad (2.49)$$

The first two equations are the spin-1 analogues of the massless Weyl equations. We can check the remaining cases can be written as

$$\epsilon_{i,+}^\mu \epsilon_{i,-}^\nu + \epsilon_{i,-}^\mu \epsilon_{i,+}^\nu = -\eta^{\mu\nu} + \frac{p_i^\mu p_k^\nu + p_i^\nu p_k^\mu}{p_i \cdot p_k}. \quad (2.50)$$

Finally, we note that expressions like (2.43), makes it relatively easy convert spinor-helicity functions into functions of the Mandelstam variables. For example, for a massless 4-point process,

$$\begin{aligned} \frac{\langle 12 \rangle \langle 34 \rangle}{\langle 13 \rangle \langle 24 \rangle} &= \frac{\langle 12 \rangle \langle 34 \rangle [31][42]}{s_{13}s_{24}} = \frac{\langle 21 \rangle [13] \langle 34 \rangle [42]}{s_{13}s_{24}} \\ &= \frac{s_{12}s_{34} + s_{24}s_{13} - s_{23}s_{14}}{2s_{13}s_{24}} = \frac{s^2 - t^2 + (s+t)^2}{2(s+t)^2} \\ &= -\frac{s}{u}, \end{aligned} \quad (2.51)$$

which corresponds to a u -channel exchange.

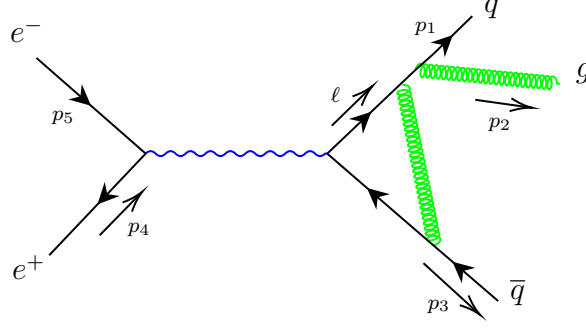


Figure 2.3: Feynman diagram for $e^+e^- \rightarrow qq\bar{q}$, in which the quark q is shown as radiating a gluon g . Time flows horizontally.

2.2 Loop-Integral Methods

IN THIS SECTION, we introduce some modern loop-integral methods. They are seen to hugely facilitate the evaluation of Feynman integrals in QCD and, in particular, our latter study of the double virtual corrections to massless 5-parton master integrals.

2.2.1 d -Dimensional Feynman Integrals

BY DEFINITION, a *Feynman integral* (FI) is the mathematical quantity we associate to a loop-level Feynman diagram (a topology) constructed from the Feynman rules of a given theory. In a *generic* 4-dimensional theory, a L -loop Feynman integral for a topology \mathcal{T} with P propagators typically takes the following form

$$I_{L,\mathcal{T}}(a_1, \dots, a_p) := \int \left(\bigwedge_{i=1}^L \frac{d^4 \ell}{i\pi^2} \right) \frac{c_{\mathcal{T}}(f^{ab}_c f^{cd}_e \dots) n_{\mathcal{T}}(p_i^\mu, \ell_j^\mu, \gamma^\mu, \epsilon^\mu, \dots)}{\prod_{i=1}^P D_i^{a_i}}. \quad (2.52)$$

In (2.52), $c_{\mathcal{T}}$ contains the color structure and is not trivial if we are in a gauge theory, while $n_{\mathcal{T}}$ contains the kinematic structure. The denominators $D := K^2 - m^2$ are the usual propagators. In the expression for the propagator D , K^μ stands for a sum of loop and/or external momenta q_j – i.e., $K^\mu := \sum_j q_j^\mu$.

To illustrate how integrals like (2.52) arise in practice, let's consider a 5-point process: $e^+e^- \rightarrow qq\bar{q}$ (see Fig. 2.3). This is a mixed QED/QCD process. The Feynman rules for QED are given in [42, §26.1]. At high enough energies, we can effectively ignore the masses

of the electron and the light quarks. In a collision experiment, this diagram would eventually contribute to a 3-jet event (see Fig. 1.3 (Left)), where a high transverse momentum gluon is emitted before the hadronization of the quarks takes place. The gluon would later hadronize in its own jet.

The interaction between the QED/QCD sectors is mediated by a [photon](#). From the Feynman rules in Fig. 2.1, one obtains a complicated Feynman integral

$$\begin{aligned} \mathcal{I}_{e^+e^- \rightarrow qg\bar{q}} = & -e^2 g^3 T^a C_F \bar{v}(p_4) \gamma^\mu u(p_5) \frac{1}{(p_1 + p_2 + p_3)^2} \int \frac{d^4 \ell}{(2\pi)^4} \frac{1}{(\ell - p_1 - p_2)^2} \not{\epsilon}(p_2) \\ & \times \frac{\not{p}_1 + \not{p}_2}{(p_1 + p_2)^2} \gamma^\nu \frac{\not{\ell}}{\ell^2} \gamma^\mu \frac{\not{\ell} - \not{p}_1 - \not{p}_2 - \not{p}_3}{(\ell - p_1 - p_2 - p_3)^2} \gamma^\nu v(p_3), \end{aligned} \quad (2.53)$$

where $C_F = (N_c^2 - 1)/(2N_c)$ arises from the [gluon](#) in the loop and is defined through $C_F \delta_{ij} = \sum_a (T^a T^a)_{ij}$. Further $\not{\epsilon}(p_2) = \gamma_\mu \varepsilon^\mu(p_2)$, where $\varepsilon^\mu(p_2)$ is the polarisation vector of the outgoing gluon.

2.2.2 From Tensorial to Scalar Feynman Integrals

OFTEN, Feynman integrals are *tensorial*. We can see that directly from non-abelian gauge theory Feynman rules written in previous sections. For example, it is possible to rewrite (2.53) as

$$\begin{aligned} \mathcal{I}_{e^+e^- \rightarrow qg\bar{q}} = & -e^2 g^3 T^a C_F \bar{v}(p_4) \gamma^\mu u(p_5) \frac{1}{(p_1 + p_2 + p_3)^2 (p_1 + p_2)^2} \bar{u}(p_1) \not{\epsilon}(p_2) (\not{p}_1 + \not{p}_2) \gamma_\nu \gamma_\rho \gamma_\mu \gamma_\sigma \gamma^\nu v(p_3) \\ & \times \int \frac{d^d \ell}{(2\pi)^4} \frac{\ell^\rho (\ell - p_1 - p_2 - p_3)^\sigma}{\ell^2 (\ell - p_1 - p_2)^2 (\ell - p_1 - p_2 - p_3)^2}. \end{aligned} \quad (2.54)$$

This illustrates that, more generally, the integrals (2.52) can involve complicated slashed momenta and tensor arrangements in the numerators. The solution to this obstacle is rather simple, but often involves a tedious amount of tensor algebra. Indeed, it is done by using properties of the Dirac algebra and generalized *Passarino-Velman (or tensor) reduction* [69]. In practice, one is usually able to express any L -loop with arbitrary multiplicity tensor integrals as a linear combination of *constant* tensors with coefficients being scalar Feynman integrals [70]. These are the integrals that would be obtained in a theory of scalar particles

only. For example, one can check that the tensor part of (2.54) contains only terms of the form

$$\begin{aligned} \int \frac{d^d \ell}{(2\pi)^4} \frac{\ell^\mu (\ell - p_1 - p_2 - p_3)^\nu}{\ell^2 (\ell - p_1 - p_2)^2 (\ell - p_1 - p_2 - p_3)^2} \supset & -\frac{1}{2(p_1 \cdot p_3 + p_2 \cdot p_3)^2} p_3^\nu (-p_2^\mu (p_1 \cdot p_3) - p_1^\mu (p_2 \cdot p_3) \\ & + p_3^\mu (p_1 \cdot p_2 + p_1 \cdot p_3 + p_2 \cdot p_3) \\ & - p_1^\mu (p_1 \cdot p_3) + -p_3^\mu (p_1 \cdot p_3) \\ & - p_2^\mu (p_2 \cdot p_3) - p_3^\mu (p_2 \cdot p_3)) \int \frac{d^d \ell}{(2\pi)^4} \frac{1}{\ell^2 (\ell - p_3)^2}. \end{aligned} \quad (2.55)$$

Consequently, the only type of integrals we will have to care about are *scalar integrals*. Up to a choice of normalization factor, they will always take the form [71]

$$G_{L,T}(a_1, \dots, a_{P'}) := \frac{1}{(i\pi^{d/2})^L} \int \bigwedge_{i=1}^L d^d \ell_i \frac{1}{\prod_{i=1}^{P'} D_i^{a_i}}, \quad (2.56)$$

where we still have P propagators, but also new⁸ *irreducible propagators* coming from tensor reduction [73]. The latter are inverse denominators – i.e., $a_i < 0$.

2.2.3 Regularizing Feynman Integrals from Dimensions

WHEN STUDYING INTEGRALS LIKE (2.56), one quickly encounters the several difficulties associated with them; the most worrying one being that many loop integrals diverge. The ceremonial way to make sense of divergent loop integrals is to employ the renormalization machinery that was quickly discussed in a previous section. This allows some physical parameters like the bare coupling constants and the bare masses present in the Lagrangian to be infinite in such a way that they compensate the divergences of the integrals. The physical results of the calculations are therefore finite. In order to make sense of calculations containing divergent integrals we have to choose a regularization scheme. They are nowadays

⁸In fact, there are exactly N such propagators, where $N = P' - P = EL + L(L + 1)/2 - P$ and $P' := |\{\ell_i \cdot q_j\}|$, $q_j \in \{\ell_{1 \leq j \leq L}\} \cup \{p_{1 \leq j \leq E}\}$. In the expression for N , P is the initial numbers of propagators, $E + 1$ is the number of external momenta and L denotes the loop order. Note that since we can always blow-up contact terms [72], we can consider Feynman graphs containing only 3-legged vertices. Hence, $P = 3L + E - 2$ and so $N_{\text{Blow-Up}} = (L - 1)(L + 2E - 4)/2$. Thus, when $L \geq \max(2, 5 - 2E)$, $P' > P$ and there are more scalar products than there are propagators. [73]. In such a case, it is not possible to express all the s_{ij} as linear combinations of the denominators. For diagrams with $E > 1$, this starts from $L = 2$.

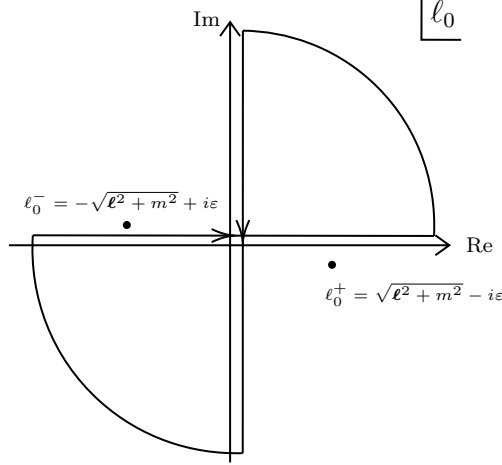


Figure 2.4: Wick rotation. ℓ_0^\pm -poles in Feynman propagators are shown. Integrating over the real axis is then equivalent to integrating over the pole-free imaginary one.

pretty standard and we can find them in any good QFT textbooks such as [35,41,42]. Among all of them, a very celebrated one is the scheme of *dimensional regularization*. It generalizes our usual 4-dimensional integrals to arbitrary \mathbb{Z} -dimension, d , and then analytically continue it by setting $d \rightarrow 4 - 2\varepsilon$, for any $\varepsilon \in \mathbb{C}$. Taking the limit $\varepsilon \rightarrow 0$ at the end of the computation gives the regularized evaluations of the integrals in 4-dimensions.

The dimensional regularization procedure for a given scalar Feynman integral in 4-dimension always goes along the same lines. First, as integration over Riemannian manifolds is easier done than integration over Lorentzian ones, we can exploit the fact that the Minkowski metric and the 4-Euclidean metric are equivalent if the time components of either are allowed to have imaginary values [74]. Practically, this amounts to performing a Wick rotation on each loop momentum: $\ell^0 \rightarrow i\ell_E^0$, where “E” stands for Euclidean. The second step is to drop the $i\varepsilon$ -prescriptions in propagators, because we do not have a pole anymore as long as all the masses are real (see Fig. 2.4). In the third step, we invoke the so-called “Schwinger trick” for which each denominator in the integral is expressed as an integral over a variable x_a measuring the “length” (or proper time) of the corresponding edge of the Feynman diagram

$$\frac{1}{D_i^{a_i}} = \frac{1}{\Gamma(a_i)} \int_{\mathbb{R}_+} x_i^{a_i-1} \exp(-x_i D_i^{a_i}) dx_i. \quad (2.57)$$

Following the derivation done in [75], we see that this step turns each of the d -dimensional loop integrals into a d -fold product of 1-dimensional integrals. In this way, we see that d -dimensions L -loop scalar Feynman integrals are in fact *twisted periods*

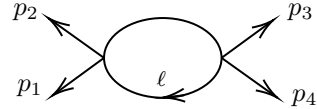
$$G_{L,\mathcal{T}}(a_1, \dots, a_{P'}) = \int_{\mathbb{R}_+^P} \exp(\varepsilon \mathcal{W}) \phi_{a_1, \dots, a_P}, \quad (2.58)$$

where

$$\begin{cases} \mathcal{U} = \det(\mathcal{Q}), \mathcal{F} = \mathcal{U}(c - \mathcal{L}^\top \mathcal{Q}^{-1} \mathcal{L}) \text{ such that } x_a D_a = \ell_i \mathcal{Q}_{ij} \ell_j + 2\mathcal{L}_i \ell_i + \mathcal{C}, \\ \mathcal{W} = \log(\mathcal{F} + \mathcal{U}) + \delta_a \log(x_a), \delta_a \xrightarrow{\forall a} 0, \\ \phi_{v_1, \dots, v_P} = \frac{\Gamma(2-\varepsilon)(\mathcal{F}+\mathcal{U})^{-2}}{\Gamma((L+1)(2-\varepsilon)-|v|-\varepsilon|\delta|)} \bigwedge_{a=1}^P \frac{x_a^{v_a-1} dx_a}{\Gamma(v_a+\varepsilon\delta_a)}. \end{cases} \quad (2.59)$$

This representation is particularly useful for both combinatorial and homological study of Feynman integrals – e.g., see [75–79].

We can see how this works with a simple example [80]. We consider the bubble integral with massless lines



$$= \int \frac{d^d \ell}{i\pi^{d/2}} \frac{1}{\ell^2(\ell-p_1-p_2)^2} = \mathcal{I}.$$

Here the external lines $p_{1 \leq i \leq 4}$ are all massless, which is equivalent to one massive external line on each side, since any massive four-momentum can be written as a sum of two massless 4-momenta. We will rewrite this with the Schwinger variables $x_0 = \ell$, $x_1 = 0$ and $x_2 = p_1 + p_2$ of (2.57) and make the further generalization by authorizing arbitrary powers α_1 and α_2 of the propagators. We easily see

$$\mathcal{I} = \int \frac{d^d \ell}{i\pi^{d/2}} \frac{1}{((-x_0 - x_1)^2)^{\alpha_1} ((-x_0 - x_2)^2)^{\alpha_2}}. \quad (2.60)$$

Note that by our choices of x 's, the only possible Lorentz invariant quantity we can expect at the end of the computation is $s := (p_1 + p_2)^2$ and by dimensional analysis, we see that it will be proportional to $s^{(d-2\alpha)/2}$, where $\alpha = \alpha_1 + \alpha_2$. Indeed, after the integration is carried out (see Appendix B)

$$\begin{aligned} \mathcal{I} &= (-s)^{(d-2\alpha)/2} \frac{\Gamma(\alpha - d/2) \Gamma(d/2 - \alpha_1) \Gamma(d/2 - \alpha_2)}{\Gamma(\alpha_1) \Gamma(\alpha_2) \Gamma(d - \alpha)} \\ &\xrightarrow{\alpha_{1,2} \rightarrow 1, d \rightarrow 4-2\varepsilon} \frac{1}{2\varepsilon} + \frac{1}{2}(-2 \log(-s) - \gamma_E + 2) + \mathcal{O}(\varepsilon), \end{aligned} \quad (2.61)$$

where

$$\gamma_E = \lim_{n \rightarrow \infty} \left(\sum_{j=1}^n \frac{1}{j} - \log(n) \right) \simeq 0.5772156649... \quad (2.62)$$

is the Euler's constant. We see that dimensional regularization captures well the logarithmic UV-divergent behaviour of the IR-finite massive bubble one expects from power counting. Moreover, as the loop-integral has a definite mass dimension, the divergence must be, by hand, multiplied by a kinematic invariant with the corresponding dimension, namely $-s^\varepsilon$. Because this invariant is proportional to a tree-amplitude, we can remove the divergence by modifying the constants (such as the overall coupling factors) of the corresponding tree-amplitudes to absorb it. This modification can, in fact, be translated into what we already mentioned above: The modification of the coupling constants and masses in the Lagrangian. In our particular case, multiplying the associated tree-amplitude by $\varepsilon e^{\gamma_E}(-s)^\varepsilon$ does the trick. Equivalently, one can trade \mathcal{I} for its regulated version

$$\mathcal{I}^{\text{reg}} = \varepsilon e^{\gamma_E}(-s)^\varepsilon \mathcal{I} = 1 + 2\varepsilon + \frac{1}{12}(48 - \pi^2)\varepsilon^2 + \left(-\frac{7\zeta_3}{3} + 8 - \frac{\pi^2}{6} \right) \varepsilon^3 + \mathcal{O}(\varepsilon^4). \quad (2.63)$$

In the case where the kinematic invariant in front of the loop-divergences is not proportional to the tree-loop amplitude, one has to modify the theory by adding new operators to the action in such a way that the divergences can be absorbed.

All the dimensionally regulated n -point 1-loop scalar integrals are known and can be found in [81].

2.2.4 The Landau Equations

LET'S NOW DISCUSS THE SINGULARITY STRUCTURE OF THE FEYNMAN INTEGRALS IN (2.56). It is helpful to use the generalized Feynman identity, where $a := \sum_{i=1}^P a_i$ and $X_i \in [0, 1] \forall i$,

$$\frac{1}{\prod_{i=1}^P A_i^{a_i}} = \frac{\Gamma(a)}{\prod_{i=1}^P \Gamma(a_i)} \int_{[0,1]} \left(\bigwedge_{i=1}^P X_i^{a_i-1} dX_i \right) \frac{\delta\left(1 - \sum_{i=1}^P X_i\right)}{\left(\sum_{i=1}^P A_i X_i\right)^a}, \quad (2.64)$$

on the propagator product. After the dust settles, one sees that (2.56) is rewritten as

$$G_{L,\mathcal{T}}(a_1, \dots, a_{P'}) = \frac{\Gamma(a) e^{\varepsilon L \gamma_E} (\mu^2)^{\varepsilon L}}{(i\pi^{D/2})^L \prod_{i=1}^P \Gamma(a_i)} \int \bigwedge_{i=1}^L d^D \ell_i \int_{[0,1]} \bigwedge_{i=1}^P X_i^{a_i-1} dX_i \\ \times \frac{\left(\prod_{i=P+1}^{P'} (K_i^2 - m_i^2)^{a_i} \right) \delta\left(1 - \sum_{i=1}^P X_i\right)}{\left(\sum_{i=1}^P (K_i^2 - m_i^2) X_i \right)^a}. \quad (2.65)$$

Although this equation, looks complicated, it highlights in a very simple way the *singularity structure* of Feynman integrals. Indeed, given the integrand depends analytically on the integration variables X_i , the system

$$\sum_{i=1}^P (K_i^2 - m_i^2) X_i = 0 \quad \text{with} \quad \sum_{i=1}^P X_i = 1, \quad (2.66)$$

is the *only* potential source of singularity.

A careful analysis of these equations shows that the conditions for the appearance of singularities read

$$\sum_i K_i^\mu X_i = 0 \quad \text{along each loop}, \quad (2.67)$$

and

$$K_i^2 = m_i^2 \quad \text{or} \quad X_i = 0. \quad (2.68)$$

These are known as the *Landau equations*. Considering their importance, these equations deserve some comments [76, 82–84]. Firstly, together with the δ -function constraint, $\sum X_i = 1$, Landau equations impose $DL + P + 1$ conditions on $DL + P$ variables (which are loop momenta and the K_i 's). This means that a solution may exist only for specific values of external momenta. Secondly, if it exists, the solution determines the *Landau surface* for the position of a singularity of G in the space of invariants s_{ij} . This implies the solution may be resolved – e.g., to determine the position of a singularity in the invariant energy s , for fixed momentum transfer variables t and vice versa. Thirdly, the condition $K_i^2 = m_i^2$ enforces *locality* – i.e., the only possible physical poles in scattering amplitudes occur when the momentum of a particle goes on-shell, so the particle propagates. Finally, we note a funny resemblance between (2.67) and the Kirchhoff current law equations for electric

circuits, with momentum K_i playing the role of the current I_i , and X_i that of resistance R_i . Analogously, the second equation in (2.68) looks like a “short circuit singularity” associated with a vanishing resistance allowing charged particles to propagate asymptotically freely.

2.2.5 Algebraic Relations Between Feynman Integrals

FROM THE LAST SECTION, it is not hard to see that the evaluation of most Feynman integrals can be rather difficult. Fortunately for us, it turns out that there are many algebraic relations between Feynman integrals. These relations are useful because they give further and often simpler Feynman integrals from the ones we already know. A very lavish set of such relations can be obtained via the so-called *integration by parts identities* (IBP). They relate different integrals of a given integral topology. An integral topology is the set of all integrals with a given propagator structure, but allowing arbitrary integer powers of the propagators. For example, the set of integrals we get from (2.60) form the bubble integral topology. The use of IBP’s is motivated by the fact that if we differentiate an integral with respect to some loop momentum before integration, the integral vanishes by Stokes’ theorem. Let’s see how this works with an almost trivial example. We consider the family of vacuum bubble integral

$$\text{Bubble Diagram} = \int \frac{d^d K}{(K^2 - m^2)^a} \equiv G(a).$$

Since boundary term vanishes, we write

$$\int d^d K \frac{\partial}{\partial K^\mu} \left(K^\mu \frac{1}{(K^2 - m^2)^a} \right) = 0, \quad (2.69)$$

which yields a *recurrence relation*

$$\int d^d K \left(\frac{d}{(K^2 - m^2)^a} - \frac{-2aK^2}{(K^2 - m^2)^{a+1}} \right) = 0 \xrightarrow{K^2 \rightarrow (K^2 - m^2) + m^2} (d-2a)G(a) - 2am^2G(a+1) = 0. \quad (2.70)$$

The upshot, here, is that there are linear relations between members of an integral family with different a ’s. Similarly, if we consider the family of 1-loop propagator integrals

$$\text{Diagram} = \int \frac{d^d K}{(K^2)^{a_1} ((q-K)^2)^{a_2}} \equiv G(a_1, a_2),$$

we get

$$\int d^d K \frac{\partial}{\partial K^\mu} \left(K^\mu \frac{1}{(K^2)^{a_1} ((q-K)^2)^{a_2}} \right) = 0. \quad (2.71)$$

By performing the differentiation and sending, in order, $K \rightarrow (K-q) + q$, rearranging, and then $2K \cdot q \rightarrow K^2 + q^2 - (K-q)^2$, we find

$$(d - 2a_1 - a_2)G(a_1, a_2) + q^2 a_2 G(a_1, a_2 + 1) - a_2 G(a_1 - 1, a_2 + 1) = 0. \quad (2.72)$$

Note that these two examples show that the coefficients depends on both the dimension and the propagator powers.

More generally, we can find such linear relations by asking [20]

$$\int \bigwedge_{i=1}^L d\ell_i \frac{\partial}{\partial \ell_i^\mu} \left(\frac{q_j^\mu}{\prod_{i=1}^{P'} D_i^{a_i}} \right) = 0, \quad (2.73)$$

for $q_j \in \{p_1, \dots, p_E, \ell_1, \dots, \ell_L\}$. This gives rise to exactly $L(L+E)$ linear relations of the form

$$c_1 G(a_1, \dots, a_{P'} - 1) + \dots + c_m G(a_1 + 1, \dots, a_{P'}) = 0. \quad (2.74)$$

Similarly, since the scalar Feynman integrals should not change under the infinitesimal $\text{SO}(d-1, 1)$ transformation [85]

$$p^\mu \rightarrow p^\mu + \delta p^\mu = p^\mu + \delta \epsilon^\mu_\nu p^\nu, \quad (2.75)$$

with skew-symmetric $\mathfrak{so}(D-1, 1)$ generator $\delta \epsilon^\mu_\nu = -\delta \epsilon^\nu_\mu$, we must have

$$G_{a_1, \dots, a_{P'}}(\{p_i + \delta p_i\}) = G_{a_1, \dots, a_{P'}}(\{p_i\}), \quad (2.76)$$

which we can expand in the $\mathfrak{so}(D-1, 1)$ generators as

$$G_{a_1, \dots, a_{P'}}(\{p_i + \delta p_i\}) = \left(1 + \delta p_1^\mu \frac{\partial}{\partial p_1^\mu} + \dots + \delta p_E^\mu \frac{\partial}{\partial p_E^\mu} \right) G_{a_1, \dots, a_{P'}}(\{p_i\}). \quad (2.77)$$

For skew-symmetric $\delta \epsilon^\mu_\nu \neq 0$, this yields to $D(D-1)/2$ *Lorentz invariance identities* (LI).

$$\sum_{i=1}^E p_i^{[\nu} \frac{\partial}{\partial p_{\mu]i}} G_{a_1, \dots, a_{P'}}(\{p_i\}) = 0. \quad (2.78)$$

However, the LI identities can always be expressed in terms of the IBP relations [20, 86]. Therefore, the IBP's by their own can be used to express *any* integrals in a given topology in terms of a *minimal* set of integrals: A *master integral basis* (MI). In practice, this can be done in various different ways. A very celebrated one is the *Laporta's algorithm* [18, 20, §6.3]. It goes along the following lines:

1. Once a family of integrals is chosen, apply IBP and LI relations to a set of arbitrarily chosen propagator exponents $\mathbf{a} = (a_1, \dots, a_{P'}) \in \mathbb{Z}^{P'}$. These \mathbf{a} are called seeds;
2. Using different seeds yields to relations between different and *unknown* scalar integrals in the family;
3. As the number of relations is observed to grow *faster* than the number of unknown scalar integrals;
4. Once we use enough seeds, *all* the required scalar integrals can be reduced to a basis of integrals, called master integrals (MI), via a Gauß-type elimination

$$G_{L,\mathcal{T}}(a_1, \dots, a_{P'}) = \sum_{j=1}^{\chi} c_j M_{L,\mathcal{T}}^j(a_1^{(j)}, \dots, a_{P'}^{(j)}). \quad (2.79)$$

In the last equation, number, χ , of MI's is determined entirely by the *topology* of the associated moduli space [17]. It was shown in [87], that χ is always finite.

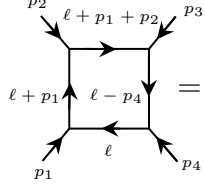
A noteworthy feature of such decomposition is that the set of master integrals is *not* unique at all. In practice, it is a really hard exercise to generate “the best”⁹ basis of MI's *just* from Laporta's algorithm. Hence, we usually start by finding one randomly and changing basis to a more convenient one. By construction, Laporta's algorithm generates a huge number of complicated equations. For high external legs and loop multiplicities, it is therefore necessary to use computer implementations¹⁰ [88–92]. Amelioration of IBPs algorithms is still an active area of research – e.g., see [93].

⁹The definition of “best basis” is flexible in the literature. Nevertheless, for us, it means it makes the differential equations canonical. This will be discussed in incoming sections.

¹⁰However, even for good computers, solving huge systems of linear equations is CPU-, disk-, and RAM-expensive.

2.2.6 Example: IPBs for the Massless Box

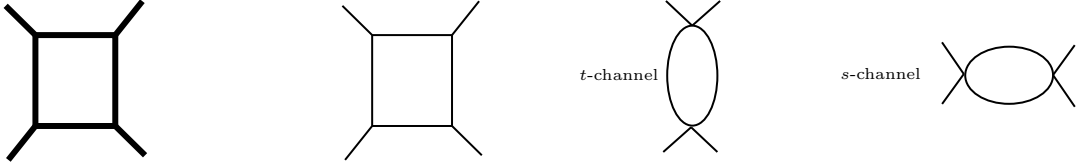
TO ILLUSTRATE WHAT WE DISCUSSED IN THE LAST SECTION, we derive a master integral basis for the massless 4-point 1-loop topology using the C++ implementation KIRA [89]. The integral family is defined by



$$= \int \frac{d^D \ell}{(\ell^2)^{a_0} ((\ell+p_1)^2)^{a_1} ((\ell+p_1+p_2)^2)^{a_2} ((\ell-p_4)^2)^{a_3}} \equiv G_{1,\text{box}}(a_0, a_1, a_2, a_3).$$

In this example, we want to decompose the triangle integral $G_{1,\text{box}}(1, 1, 0, 1)$ and higher-power box $G_{1,\text{box}}(2, 1, 1, 1)$ in terms of MI's. To do so, there are 4 IBP and 6 LI identities we can use. A basis of 3 master integrals is found in less than one second. The explicit IBP's are listed in Appendix A. The resulting basis decomposition is given by

$$G_{1,\text{box}}(a_0, a_1, a_2, a_3) = c_1 G_{1,\text{box}}(1, 1, 1, 1) + c_2 G_{1,\text{box}}(0, 1, 0, 1) + c_3 G_{1,\text{box}}(1, 0, 1, 0)$$



The choice of these three integrals as basis integrals is, as mentioned earlier, not unique and we could also have taken three different integrals. Traditionally, one would choose the integrals that are particularly easy to calculate or have some suitable properties, such as UV-finiteness. The decomposition for the triangle integral and higher-power box in terms of this basis are therefore seen to be

$$G_{1,\text{box}}(1, 1, 0, 1) = \frac{6-2d}{t(d-4)} G_{1,\text{box}}(0, 1, 0, 1), \quad (2.80)$$

and

$$G_{1,\text{box}}(2, 1, 1, 1) = \frac{5-d}{s} G_{1,\text{box}}(1, 1, 1, 1) + \frac{4d^2 - 32d + 60}{st^2(d-6)} G_{1,\text{box}}(0, 1, 0, 1). \quad (2.81)$$

The former decomposition shows that the triangle integral related to the bubble, which explains why it is not appearing in the basis. The latter decomposition shows that higher powers in the denominator can be removed.

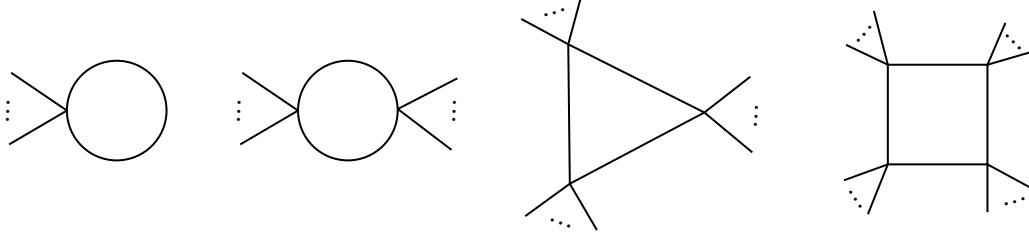


Figure 2.5: Basis obtained from integral reduction for 1-loop integrals.

The attentive reader may have noticed that, for all the examples given, the coefficients c_j of (2.116) are rational functions of the dimension and of the kinematic invariants. This is a manifestation of the fact that, for 1-loop integrals, it is always possible to reduce any n -point Feynman integral as a sum ansatz with respect to the four basis integrals and a rational function \mathcal{R} [69, 80]. These four basis integrals are tadpoles (T), bubbles (B), triangles (Δ), and boxes (\square) with an arbitrary number of external legs of the original diagram at each vertex, see Fig. 2.5

$$\mathcal{A}_{n\text{-point}}^{1\text{-loop}} \supset \mathcal{I}_{n\text{-point}}^{1\text{-loop}} = \mathcal{R} + \sum_{j_\square} c_{j_\square}^\square \mathcal{I}_{j_\square}^\square + \sum_{j_\Delta} c_{j_\Delta}^\Delta \mathcal{I}_{j_\Delta}^\Delta + \sum_{j_B} c_{j_B}^B \mathcal{I}_{j_B}^B + \sum_{j_T} c_{j_T}^T \mathcal{I}_{j_T}^T + \mathcal{O}(\delta), \quad (2.82)$$

where the c 's are coefficients to be determined and the small δ -corrections coming from the subleading pentagon integrals contributions [94]. Note that this expansion is valid at the *integrand* level too, but only for $n \geq 5$. The explanation is that, in the $n \leq 4$ cases, there are not enough external momenta to construct a four-dimensional integrand basis. However, in these cases it can be argued that scalar products of ℓ with vectors that are perpendicular to the external momenta – e.g., see [80, Eq. 3.36] –, lead to numerators that vanish, but just after integration – e.g., see [80, Eq. 3.70]. Thus, (2.82) is valid at the integrand level for generic n , provided additional transverse degrees of freedom living in the integration kernel are introduced for $n \leq 4$.

Integral reductions like (2.82) can also be found for more than 1-loop. One example is the planar 2-loop diagram with massless internal propagators. Here, only diagrams with eleven or fewer propagators can be reduced using this technique [94, 95]. The reason for this limitation is practical; the bound $L \geq \max(2, 5 - 2E)$ saturates fast passed $L = 1$ (see Footnote 8). Thus, in contrast to the 1-loop case, for $L > 1$ there are also diagrams

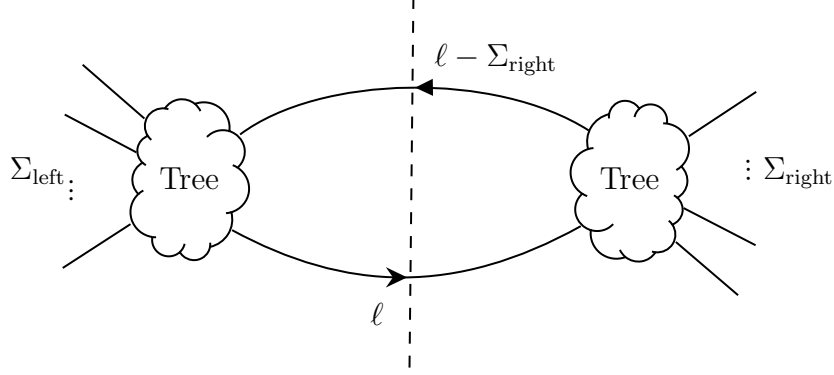


Figure 2.6: Visualization of 1-loop unitary cut. External particles are all outgoing.

with loop-dependent irreducible propagators, obscuring the general ansatz for such *complete* integral reductions.

2.2.7 Recycling Tree Amplitudes: Unitary Cuts

UNITARY CUTS are a useful tool in different ways to calculate Feynman loop integrals. The first application of unitary cuts one is usually exposed to in a QFT course, is the so-called *optical theorem* [35, 41, 42]. It gives a relation between the imaginary part of the loop amplitudes $\mathcal{A}^{1\text{-loop}}$ and the integral over tree amplitudes.

Broadly speaking [33, 80], it says that the imaginary part of the loop amplitude, which probes its branch cut structure, is related to the pole structure of the amplitude integrand across the unitary cuts of interest (see Fig. 2.6)

$$\text{Im}\mathcal{A}^{1\text{-loop}} = \frac{1}{2} \int d^4\ell \delta(\ell^2) \Theta(\ell^0) \delta((\ell - \Sigma_{\text{left}})^2) \Theta((\ell - \Sigma_{\text{left}})^0) \mathcal{A}_{\text{left}}^{\text{tree}} \mathcal{A}_{\text{right}}^{\text{tree}}. \quad (2.83)$$

One can reconstruct the integrand by analyzing different sets of unitary cuts. It is a bit like “recycling” our knowledge of tree amplitudes to make predictions at the loop-level. Indeed, the only necessary loop-level input is an ansatz for $\mathcal{A}^{1\text{-loop}}$, which is given in (2.82). Note that the $I_{j_\star}^\star$ ’s where the cut propagator is not present will have trivial residue and will therefore vanish on the cut. By plugging the ansatz in the LHS of (2.83), it easy to see that each cut we make generates equations where, on the right hand side, we have integrals over tree-level amplitudes and, on the left hand side, we have linear combinations of the coefficients $c_{j_\star}^\star$.

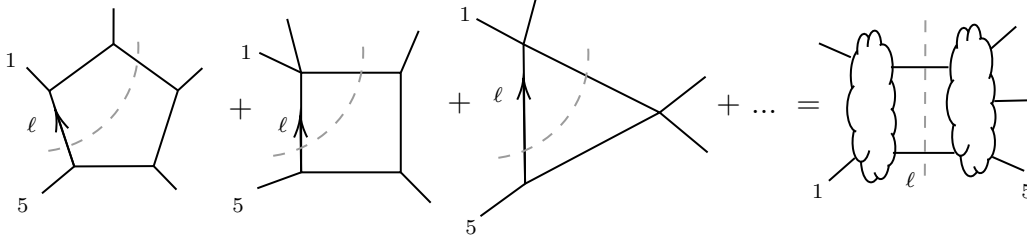


Figure 2.7: The sum of all Feynman diagrams localized on the cut where the propagators $(\ell)^{-2}$ and $(\ell - p_1 - p_2)^{-2}$ go on-shell (left) is equal to the product of two tree-amplitudes (right).

A 5-point example is shown schematically in Fig. 2.7, where the 2-cut is performed on the momenta flowing between 1 and 5 and between 2 and 3. Solving these linear equations gives us the coefficients as a combination of products of tree-amplitudes. The only part which is by construction invisible to this method is the determination of \mathcal{R} . Consequently, \mathcal{R} is often referred to the *non-cut-constructable* part of the scattering amplitudes. Two explicit and pedagogical examples for (i) the box coefficient of an n -point 1-loop amplitude in $d = 4$, and (ii) for the integral coefficients for the fermion-loop correction of the 1-loop 4-gluon $(+, -, +, -)$ -helicity amplitudes are given in [33, p.128-129].

2.2.8 Generalized Unitarity

IT IS POSSIBLE TO INTRODUCE A GENERALIZED VERSION of the method described in the previous section. Indeed, for a 1-loop amplitudes, to use (2.83) we had to cut only two propagators, but it is sometimes useful to cut more ¹¹. Cutting an arbitrary number of propagators therefore generalize our previous notion of unitary cuts. One way to determine the coefficients for a general 1-loop amplitude using *generalized cuts* is to match the amplitude and the expansion in Fig. 2.5, but now on the integrand level.

Let's sketch how this works for 1-loop integrals. Recalling that there is no *fixed* integrand-level analogues of (2.82) for the cases where $n \leq 4$, this means that we need a more general

¹¹However, there's always a maximal number of *useful* cut we can make. For example, because of the expansion in equation (2.82), the maximal number of propagators we can cut at leading order in δ in a 1-loop amplitude is four. Otherwise, the right hand side of the expansion always vanishes.

ansatz. One is given in [80, Eq. 3.125]

$$\begin{aligned} \mathfrak{A}_n^{1\text{-loop}} = & \sum_{1 \leq i_1 \leq i_2 \leq i_3 \leq i_4 \leq n} \frac{\Box_{i_1 i_2 i_3 i_4}(\ell)}{D_{i_1} D_{i_2} D_{i_3} D_{i_4}} + \sum_{1 \leq i_1 \leq i_2 \leq i_3 \leq n} \frac{\Delta_{i_1 i_2 i_3}(\ell)}{D_{i_1} D_{i_2} D_{i_3}} \\ & + \sum_{1 \leq i_1 \leq i_2 \leq n} \frac{B_{i_1 i_2}(\ell)}{D_{i_1} D_{i_2}} + \sum_{1 \leq i_1 \leq n} \frac{T_{i_1}(\ell)}{D_{i_1}}. \end{aligned} \quad (2.84)$$

In regards of what has been said previously, the numerators in (2.84) will also inevitably depend on scalar products of the loop momentum with auxiliary vectors momenta, perpendicular to the external momenta. They are explicitly given in [80, Eq. 3.126-3.129], but their explicit form is not relevant for the present discussion. The trick is to use these auxiliary vectors to determine the coefficients. We start with the maximal number of four cuts, where all but one of the 1-loop integrands vanish to determine the numerators $\Box_{i_1 i_2 i_3 i_4}(\ell)$. We continue and cut three propagators, so that we get contributions of boxes and triangles. Following this logic, we can also get the bubble numerators and the tadpole numerators.

We stress that all we need to know, *a priori*, are the tree-level amplitudes and an ansatz of four topologies (see Fig. 2.5) to determine the whole 1-loop amplitudes, still without the rational part. *No integration is needed.* This is an achievement in comparison to the last method where, for each 2-cut made, we had to perform an integration over tree-amplitudes. Another difference to the 2-cut method is that we also have to allow complex momenta since the solution of setting four propagators to zero is unlikely to be real. Using complex momenta also makes a difference for the tree-amplitudes in the left hand side of equation (2.84), since amplitudes like the 3-point tree-amplitudes for gluons vanish for real momenta but not for general complex momenta¹². They, therefore, now need to be considered.

The methods of generalized unitarity deserve much more attention than what we can offer in this thesis. For example, finding optimal methods to reconstruct these coefficients at

¹²Indeed, for on-shell 3-point amplitudes, $p_1 + p_2 + p_3 = 0$ and so the momenta are strongly constrained: $s_{12} = s_{23} = s_{13} = 0$. Recalling $s_{ij} = \langle ij \rangle [ij]$, we see that the two only possible solutions are $\lambda_1 \sim \lambda_2 \sim \lambda_3$ or $\tilde{\lambda}_1 \sim \tilde{\lambda}_2 \sim \tilde{\lambda}_3$. Taking the former solution, we have $p_1 = \lambda_1 \tilde{\lambda}_1, p_2 = \alpha \lambda_1 \tilde{\lambda}_2$ and $p_3 = -\lambda_1 (\tilde{\lambda}_1 + \alpha \tilde{\lambda}_2)$. This system of momenta has no *non-trivial* real solution as it would require, for example, $\tilde{\lambda}_1 + \alpha \tilde{\lambda}_2 = (\lambda_1)^*$. Therefore, the scattering amplitudes of three *physical* gluons must vanish. That's an important input into *on-shell methods* [33, 34]

arbitrary multiplicities is currently an active area of research – see for example [78], where an interesting dual space is used. See also [93], and [96–98] for reviews.

2.2.9 Leading Singularities and $d \log$ Forms

IT TURNS OUT THAT THE UNITARY CUTS discussed above are not only useful to calculate the coefficients of the amplitudes, but can additionally help to explore the *analytic structure* of Feynman integrals in general. The old-fashioned way of introducing unitary cuts is by replacing propagators with δ -functions. Another interpretation, more geometric, is to understand them as taking contour integrals around the poles of the propagators [67]. It is geometric in the sense that it is equivalent to a product of contour integrals *localizing* around the poles of the propagators. For example, in 4-dimension, whenever it makes sense we can perform 4 cuts and trade the 4 degrees of freedom of the loop momenta ℓ^μ with 4 constraints on propagators, say $D_{1 \leq i \leq 4}$. Explicitly,

$$\text{Cut}_4 \left(\int \int_{\mathbb{R}^{1,3}} \frac{d^d \ell}{D_1^2 D_2^2 D_3^2 D_4^2} \cdot \mathcal{R} \right) = \frac{1}{(2\pi i)} \prod_{i=1}^4 \oint_{D_i=0} \frac{dD_i}{D_i} \cdot \frac{\mathcal{R}(\ell)}{J(\ell)} \Big|_{\ell=\ell^\star}, \quad (2.85)$$

where ℓ^\star is the four-vector solution to $D_i = 0$, $\forall 1 \leq i \leq 4$, \mathcal{R} is the remaining part of the original integrand (depending on other external and loop momenta) and J is the Jacobian accounting for the variables change $\ell^\mu \rightarrow \{D\}_{i=1}^4$

$$J = \det \left(\frac{\partial(D_1, D_2, D_3, D_4)}{\partial(\ell_0, \ell_1, \ell_2, \ell_3)} \right). \quad (2.86)$$

We stress that the $D_{1 \leq i \leq 4}$ ordering is arbitrary. As a result, a different choice than the one we made can lead to a different Jacobian sign, which one may interpret as taking the reverse orientation for the integration contour. Moreover, the ordering of the legs are not fixed from the beginning. Different orderings can lead to a different sign, which is related to the orientation of the contour. This choice of orientation is unimportant at the level of leading singularities. The only difference between calculating unitary cuts and calculating the integral along the real axis is the path on which we integrate. Thus, it seems heuristically reasonable to assume that the quantities we get from the unitary cuts and the Feynman integrals have similar properties. Given that calculating unitary cuts is by construction

much easier than determining the integral, it is most of the time useful to calculate unitary cuts in order to learn something about the properties of the Feynman integral.

Now, if we take the residues for *all* integration variables we obtain the quantity that is referred to as a *leading singularity* (LS) of the integrand. In most loop diagrams, however, the number of propagators is smaller than the number of integration variables. For example, this is the case for the triangle 4-point diagram, where the former is three and the latter is four. A natural question is therefore: How practical are leading singularity methods if there are not enough poles where we can take residues? As a matter of fact, since the propagators are quadratic in the momenta taking the residue at the pole of one propagator creates new factors in the denominator, on which residues can be taken. Leading singularities involving such “pole-under-a-pole” are called *composite leading singularities* [33]. Composite leading singularities resolve the subtlety about defining maximal-cut for certain Feynman integrals and we can take as a theorem that the leading singularities of multi-loop amplitudes are always well-defined.

The idea, now, is to work with leading singularities that are as simple as possible. We introduce the concept of *unit* leading singularities. It is defined such that the maximal-cut residue of the integral is normalized to either -1, 0 or 1. This idea is illustrated in the next subsection.

2.2.10 Example: The Leading Singularities of the Massless Box

WE CONSIDER THE PLANAR MASSLESS BOX. Its integrand is given by

$$dG_{1,\text{box}}(1, 1, 1, 1) = \frac{d^4\ell}{D_1 D_2 D_3 D_4}, \quad (2.87)$$

with $D_1 := \ell^2$, $D_2 := (\ell + p_1)^2$, $D_3 := (\ell + p_1 + p_2)^2$, $D_4 := (\ell - p_4)^2$. A first thing we can do is to profit of the arbitrariness of the loop momentum ℓ over integration to write it as

$$\ell = a_1 \lambda_1 \tilde{\lambda}_1 + a_2 \lambda_2 \tilde{\lambda}_2 + a_3 \lambda_1 \tilde{\lambda}_2 + a_4 \lambda_2 \tilde{\lambda}_1, \quad (2.88)$$

where $(p_{1,2})_{\alpha\dot{\alpha}} = \lambda_{1,2} \tilde{\lambda}_{1,2}$. The variables for which we exchanged the four loop momentum degrees of freedom are $a_{1 \leq i \leq 4}$. Note that since $\langle ij \rangle = 0$, each of the last two terms in

(2.88) are both orthogonal the first two. This makes the four components independent. If we compute the propagators D_i in the a_i variables, we observe dependencies on angle- and square-brackets. To avoid this, we can use p_3^μ as an internal normalization parameter

$$a_3 \rightarrow \frac{\langle 23 \rangle}{\langle 13 \rangle} a_3 \quad \text{and} \quad a_4 \rightarrow \frac{\langle 13 \rangle}{\langle 23 \rangle} a_4. \quad (2.89)$$

Now, we only have to deal with $s, t, a_{1 \leq i \leq 4}$ -dependent expressions

$$\begin{aligned} D_1 &= s(a_1 a_2 - a_3 a_4), \\ D_2 &= s(a_2 + a_1 a_2 - a_3 a_4), \\ D_3 &= s(1 + a_1 a_2 + a_1 + a_2 - a_3 a_4), \\ D_4 &= s(a_1 a_2 + a_2 - a_3 a_4 - a_4) - t(a_1 - a_2 - a_3 + a_4), \\ d^4 \ell &= J \bigwedge_{i=1}^4 da_i. \end{aligned} \quad (2.90)$$

Using (2.88), we can compute the determinant, J , of the Jacobian matrix, \mathbf{J} , by conjugating the metric $\eta^{\mu\nu}$ with the matrix components $\mathbf{J}_i^\mu = \partial_{a_i} \ell^\mu$ – i.e.,

$$J = \det(\mathbf{J}) = \sqrt{-\det(\mathbf{J} \eta \mathbf{J}^\top)} = \sqrt{-\det([\mathbf{J}_i^\mu \mathbf{J}_{j\mu}])}. \quad (2.91)$$

As $[\mathbf{J}_i^\mu \mathbf{J}_{j\mu}]$ is a symmetric matrix, there are only two non-trivial distinct components: $\mathbf{J}_1 \cdot \mathbf{J}_2 = p_1 \cdot p_2 = s/2$ and, using (2.35), $\mathbf{J}_3 \cdot \mathbf{J}_4 = -\frac{1}{2} \langle 12 \rangle [12] = -s/2$. After the dust settles, we see the box integrand Jacobian takes the form

$$J = \pm i \frac{s^2}{4}. \quad (2.92)$$

Combining (2.90) and (2.92), we find

$$dG_{1,\text{box}}(1, 1, 1, 1) = \frac{\bigwedge_{i=1}^4 da_i}{(s(a_1 a_2 - a_3 a_4)(a_1 a_2 + a_2 - a_3 a_4)(1 + a_2 a_1 + a_1 + a_2 - a_3 a_4) \times (s(a_2 a_1 + a_2 - a_4 - a_3 a_4) - t(a_1 - a_2 - a_3 + a_4)))}. \quad (2.93)$$

With a bit of work, we can put (2.93) into a $d \log$ -form. We can naively do this using partial fractions [99]. Using MATHEMATICA, we do so algorithmically by using the `Apart[]` function on (2.93), first, with respect to a_1 . From the output, we can collect $d \log(W_i^{a_1})$, where

$$\begin{aligned} W_i^{a_1} \in \mathcal{A}_{a_1} &= \{a_1 a_2 - a_3 a_4, 1 + a_2 + a_1(1 + a_2) - a_3 a_4, a_2 + a_1 a_2 - a_3 a_4, \\ &\quad s(1 + a_1) a_2 + t(-a_1 + a_2 + a_3 - a_4) - s(1 + a_3) a_4\}, \end{aligned} \quad (2.94)$$

out of each fraction. We repeat this step on $d \log$ -coefficients, but now with respect to a_3 ¹³. The $d \log(W_i^{a_3})$ associated to this step are such that

$$W_i^{a_3} \in \mathcal{A}_{a_3} = \{(s+t)a_2 + ta_3, a_2(1+a_2) + a_3a_4, a_3, 1+a_2+a_3, \\ -ta_2(1+a_2+a_3) + a_4((s+t)a_2 + ta_3)\}. \quad (2.95)$$

Similarly, if we repeat for a_4 and a_2 respectively

$$W_i^{a_4} \in \mathcal{A}_{a_4} = \{a_4 - a_2, a_4(s+t) - t(1+a_2), a_4\}, \quad (2.96)$$

and

$$W_i^{a_2} \in \mathcal{A}_{a_2} = \{sa_2 - t, a_2, 1+a_2\}. \quad (2.97)$$

The analysis indicates the box can also be written as a sum of 44 $d \log$ 4-forms

$$dG_{1,\text{box}}(1, 1, 1, 1) = \frac{1}{st} \sum_{i=1}^{44} c_i d \log(W_{\sigma_{a_2}(i)}^{a_2}) \wedge d \log(W_{\sigma_{a_4}(i)}^{a_4}) \wedge d \log(W_{\sigma_{a_3}(i)}^{a_3}) \wedge d \log(W_{\sigma_{a_1}(i)}^{a_1}). \quad (2.98)$$

where $c_i \in \mathbb{Z}/2\mathbb{Z}$ and $\sigma_{a_j}(i) \in \{1, \dots, |\mathcal{A}_{a_j}|\}$, $\forall i, j$. Using (2.98), it becomes much easier to evaluate (2.85). In fact, the latter example highlights a crucial relation between $d \log$ -forms and leading singularities. Indeed, more generally, in the $d \log$ -decomposition of some integrand $d\Omega$,

$$d\Omega = \sum_{i=1}^N \mathbf{C}_i d \log(\omega_{i_1}) \wedge d \log(\omega_{i_2}) \wedge \dots \wedge d \log(\omega_{i_k}), \quad (2.99)$$

the values of the \mathbf{C}_i 's give the leading singularities of $d\Omega$. For the box, up to a sign, the leading singularity is therefore $1/st$. This fits the result found in [67, 100], yet much more compact as it is a single 4-form expression

$$stdG_{1,\text{box}}(1, 1, 1, 1) = d \log \frac{\ell^2}{(\ell - \ell_\star)^2} \wedge d \log \frac{(\ell + p_1)^2}{(\ell - \ell_\star)^2} \wedge d \log \frac{(\ell + p_1 + p_2)^2}{(\ell - \ell_\star)^2} \wedge d \log \frac{(\ell - p_4)^2}{(\ell - \ell_\star)^2}, \quad (2.100)$$

where $\ell_\star = -\frac{\langle 14 \rangle}{\langle 24 \rangle} \lambda_2 \tilde{\lambda}_1 + \lambda_1 \tilde{\lambda}_1$, which is one of the solutions for $D_{1 \leq i \leq 4} = 0$.

We finally note that $d \log$ -forms were shown to play an important role in a toy theory known as $\mathcal{N} = 4$ *Super Yang-Mills* (SYM) theory. Its particle spectrum as well as many of

¹³Note that we skipped a_2 . This would in fact lead to square root terms and so to branch cuts, which are highly unwanted.

its very basic properties are discussed in [101, 102]; a discussion in the context of scattering amplitudes is given in [33, §5, 6.3, 6.4]. This supersymmetric cousin of QCD [103] makes many things computable due to large amount of symmetry – i.e., superconformal symmetry, dual conformal symmetry and its enhancement to the Yangian. For example, the only non-vanishing contributions in Fig. 2.5 for 1-loop $\mathcal{N} = 4$ SYM amplitudes are the box-integrals [33, §6.3, p.130-131]. Moreover, all of its *planar* amplitudes, [33, Eq. 9.1], can be reformulated with a dual formulation using on-shell diagrams computed as contour integrals over the positive Grassmannian [33, §9.2], a structure in algebraic geometry analogous to a convex polytope [33, §10], that generalizes the idea of a simplex in projective space. Using such objects, it was shown that all planar integrands can be written as d log-forms [104]. This reformulation of the S -matrix is connected to the geometric concept of the *amplituhedron* [105], which, however, is defined in momentum twistor variables (see Appendix C). At a given loop order, they can only be used in the planar limit¹⁴. Since we do not need momentum twistor variables to express diagrams as d log-forms, they turn out to be a useful tool for the analysis of non-planar diagrams in $\mathcal{N} = 4$ SYM and also for the investigation of the question *if* the concept of the amplituhedron is also valid in the non-planar case [104, 106].

For further references on d log-forms and leading singularities, we advert to the recent article [107].

2.3 On the Evaluation of Master Integrals

AS WE SAW, the master integrals are functions of the kinematic invariants constructed from the external momenta, of the masses of the external particles and of the particles running in the loops, as well as of the number of spacetime dimensions. Remarkably, the

¹⁴Given a well-defined ordering of the external lines based on the color-ordering, the region variables $\{y_i\}$, on which momentum twistors depend, are essentially labeling the “regions” that the external lines of the amplitude separate the plane into. When loops are added, there are new “internal” regions; one for each loop. In the planar limit, the region, y_{ℓ_i} , associated with the i^{th} -loop momentum, ℓ_i , is uniquely defined as the corresponding “hole”, while the position of ℓ_i on one of the hole edges isn’t. The region variables (and so the momentum twistors) thus give an unambiguous definition of the loop-momentum *only* in the planar limit.

existence of algebraic relations between master integrals forces them to obey linear systems of first-order differential equations in the kinematic invariants, which can be used for their evaluation. In the most general case, the master integrals are ultimately integrated by using a generalized version of the Picard–Lindelöf theorem. Indeed, the nested structure of the Laurent expansion of the linear system of differential equations leads to an iterative structure for the solution that, order-by-order in $\varepsilon = (4-d)/2$, is written in terms of repeated integrals, starting from the kernels dictated by the homogeneous solution. The transcendentality of the solution is associated to the number of repeated integrations and increases by one unit as the order of the ε -expansion increases. The solution of the system, namely the master integrals, is finally determined by imposing the boundary conditions at special values of the kinematic variables, properly chosen either in correspondence of configurations that reduce the master integrals to simpler integrals or in correspondence of desired thresholds. In this latter case, the boundary conditions are obtained by imposing the regularity of the master integrals around spurious singularities, ruling out divergent behavior of the general solution of the systems. After one obtained a master integral basis from the Laporta’s algorithm described above, convenient manipulations of the basis may be performed. An important fact is that a proper choice of master integral can simplify the form of the systems of differential equations tremendously and, hence, of their solution. A general criterion for determining such optimal sets is not yet known. However, a considerable step in this direction has been made by Henn in [29]. The key observation is that a good choice of master integrals allows us to cast the system of differential equation in a canonical form, where the dependence on ε is factorized from the kinematics of the connection. The integration of a system in canonical form trivializes and the analytic properties of its general solution are manifestly inherited from the differential equation connection, which is the kernel of the iterated integrals. As pointed out in [29], finding an algorithmic procedure which, starting from a generic set of master integrals, leads to one fulfilling a canonical system is a harrowing task. In practice, the quest for the suitable basis of master integrals is determined by qualitative properties required for the solution, such as finiteness in the $\varepsilon \rightarrow 0$ limit, and homogeneous transcendentality,

which turn into quantitative tools like the unit leading singularity criterion and the dlog-representation in terms of Feynman parameters [108], we all discussed in the last few sections.

2.3.1 The (Canonical) Differential Equations

IN THIS SECTION, we give a concise review of [109]. In the previous sections, we started with a family of Feynman integrals, then expanded the required integrals into a master integrals basis. To compute them, we can start by writing a differential equation for each master integrals.

From the very first principles, we need these differential equations to be Lorentz invariant. Thus, we differentiate with respect to the Mandelstam variables, s_{ij} , and not with respect to external momenta p_i^μ . Still, the master integrals rarely have an explicit dependence on the s_{ij} . Instead, they depend on the external momenta p_i . This problem can be sidestepped by expanding the differential operator $\frac{\partial}{\partial s_{ij}}$ in a momenta basis. For a n -particle process, we have

$$\frac{\partial}{\partial s_{ij}} = \sum_{i=1}^{n-1} \left(\sum_{j=1}^{n-1} C_{ij} p_j^\mu \right) \frac{\partial}{\partial p_i^\mu}. \quad (2.101)$$

The coefficients C_{ij} can be determined (not uniquely) by imposing the following minimal constraints

$$\frac{\partial}{\partial s_{ij}} p_{1 \leq i \leq n-1}^2 = 0, \quad \frac{\partial}{\partial s_{ij}} (p_k \cdot p_\ell) |_{k, \ell \notin \{i, j\}} = 0, \quad \frac{\partial}{\partial s_{ij}} (p_i \cdot p_j) = \frac{1}{2}, \quad \sum_{\substack{k=1 \\ k \neq i}}^{n-1} \frac{\partial}{\partial s_{ij}} (p_k \cdot p_j) = -\frac{1}{2}. \quad (2.102)$$

The first of these equations follows from on-shellness, while the others follow from the definition of s_{ij} . For example, for $n = 4$, we would have, given $p_1^2 = p_2^2 = p_4^2 = 0$, $p_1 \cdot p_2 = s/2$, $p_1 \cdot p_4 = t/2$ and $p_2 \cdot p_4 = -(s+t)/2$, the following ansatz for the $\frac{\partial}{\partial t}$ -operator

$$\frac{\partial}{\partial t} = (C_{11} p_1^\mu + C_{12} p_2^\mu + C_{14} p_4^\mu) \frac{\partial}{\partial p_1^\mu} + (C_{21} p_1^\mu + C_{22} p_2^\mu + C_{24} p_4^\mu) \frac{\partial}{\partial p_2^\mu} + (C_{41} p_1^\mu + C_{42} p_2^\mu + C_{44} p_4^\mu) \frac{\partial}{\partial p_4^\mu}, \quad (2.103)$$

with conditions

$$\frac{\partial}{\partial t} p_{1,2,4}^2 = 0, \quad \frac{\partial}{\partial t} (p_1 \cdot p_2) = 0, \quad \frac{\partial}{\partial t} (p_1 \cdot p_4) = \frac{1}{2} \quad \text{and} \quad \frac{\partial}{\partial t} (p_2 \cdot p_4) = -\frac{1}{2}. \quad (2.104)$$

One simple construction is that

$$\frac{\partial}{\partial t} = \left(\frac{1}{2t} p_1^\mu + \frac{1}{2(s+t)} p_2^\mu + \frac{s+2t}{2t(s+t)} p_4^\mu \right) \frac{\partial}{\partial p_4^\mu}, \quad (2.105)$$

and, similarly, for the $\frac{\partial}{\partial s}$ -operator

$$\frac{\partial}{\partial s} = \left(\frac{1}{2s} p_1^\mu + \frac{2s+t}{2s(s+t)} p_2^\mu + \frac{1}{2(s+t)} p_4^\mu \right) \frac{\partial}{\partial p_2^\mu}. \quad (2.106)$$

Another one is given in [109]. By acting on the master integrals with $\partial_{s_{ij}}$ given by (2.101), we act on propagators with $\{\partial_{p_k}\}$. This causes a power increase in the propagators and also new numerator factors coming from the C_{ij} .

As a result, we see that the differentiated master integrals are *still* in the original integral family – i.e., for each k , we have differential equation of the form

$$\frac{\partial}{\partial s_{ij}} M_k(\{p_n\}; \varepsilon) = \sum_{\ell=1}^{\chi} A_{s_{ij}}^{k\ell} M_\ell(\{p_n\}; \varepsilon), \quad (2.107)$$

where each coefficient $A_{s_{ij}}^{k\ell}$ is a \mathbb{Q} -function (analogous to the IBP coefficients) of $\{p_i\}$ and ε .

In a vector notation, this equation will become our principal computational tool

$$\frac{\partial}{\partial s_{ij}} \mathbf{M}(\{p_n\}; \varepsilon) = \mathbf{A}_{s_{ij}}(\{p_n\}; \varepsilon) \mathbf{M}(\{p_n\}; \varepsilon). \quad (2.108)$$

It can be easily shown that (2.108) satisfies an *integrability condition*. That is, we must have

$$\partial_{s_{ij}} \mathbf{A}_{s_{k\ell}} - \partial_{s_{k\ell}} \mathbf{A}_{s_{ij}} - [\mathbf{A}_{s_{ij}}, \mathbf{A}_{s_{k\ell}}] = 0, \quad (2.109)$$

for a solution to exist. Moreover, as $[\mathbf{A}_{s_{ij}}] = \frac{1}{2}[E]$ and $[M_k] = (D + 2(N - P))[E]$, where $[E]$ is an energy unit, dimensional analysis provides an Euler's relation

$$\sum_{s_{ij}} s_{ij} \mathbf{A}_{s_{ij}} = \text{diag}([M_1]/2, \dots, [M_\chi]/2). \quad (2.110)$$

In practice, equations (2.109) and (2.110) provide two very useful ways for checking the correctness of the differential equations. That said, it is often convenient to make a change of integral basis, say $\mathbf{M}' = \mathbf{U} \mathbf{M}$ for some matrix \mathbf{U} . The differential equation transforms as follows

$$\frac{\partial}{\partial s_{ij}} \mathbf{M}'(\{p_n\}; \varepsilon) = \mathbf{B}_{s_{ij}}(\{p_n\}; \varepsilon) \mathbf{M}'(\{p_n\}; \varepsilon), \quad (2.111)$$

where

$$\mathbf{B}_{s_{ij}} = \mathbf{U} \mathbf{A}_{s_{ij}} \mathbf{U}^{-1} + \partial_{s_{ij}} \mathbf{U} \mathbf{U}^{-1}. \quad (2.112)$$

One may recognize this as *gauge transformation*, explaining why we call \mathbf{A} a *connection*. Accordingly, given an initial condition, (2.108) is nothing but a *transport equation*. We also notice some practical issues with (2.108). Firstly, $\mathbf{A}_{s_{ij}}(\{p_i\}; \epsilon)$ is usually very complicated, making physical properties, such as asymptotic behaviors and singularity structure of our master integrals, not so transparent. Secondly, multivariable cases become quickly complicated, given any big system of coupled partial differential equations is hard to solve. Thirdly, the integral function space is not apparent.

Mindful of all that, it seems natural to ask: How can we (i) make the differential equations simpler, and (ii) make the physical and the analytic properties of the integrals visible at the level of the differential equations? In 2013, Henn partially answered these questions by observing that this can often be done by looking for a basis of integrals, which identifies to *uniform transcendental* (UT) functions [29].

The concept of *degree of transcendentality*, \mathcal{T} , is basically a way of “grading” (classifying) functions with weights. For our purposes, the weight of a function corresponds to the number of iterated (contour) integrals it takes to define it. Two prototypical examples we can give are the logarithmic- and the polylogarithmic-functions

$$\mathcal{T}(\log(z)) = 1 \text{ and } \mathcal{T}(\text{Li}_n(z)) = \mathcal{T}\left(\int_{[0,z]} dt \frac{\text{Li}_{n-1}(t)}{t}\right) = n. \quad (2.113)$$

Recall that $\text{Li}_1(z) = -\log(1-z)$. Clearly, $\mathcal{T}(f_1 f_2) = \mathcal{T}(f_1) + \mathcal{T}(f_2)$ and algebraic factors are assigned vanishing degree of transcendentality. Numerical constants such as π and ζ_n are assigned the value of the corresponding function from which they can be derived. Indeed, since $\zeta_n = \text{Li}_n(1)$, we have $\mathcal{T}(\zeta_n) = n$ and because $\zeta_2 = \pi^2/2$, we also have $\mathcal{T}(\pi) = 1$. Similarly, we can see that $\mathcal{T}(\varepsilon) = -1$ from $z^\varepsilon = 1 + \varepsilon \log(z) + \mathcal{O}(\varepsilon^2)$.

Ultimately, we are interested in functions with UT, which are defined as functions that can be written as a sum of terms having all the same degree of transcendentality. Furthermore, if some function f satisfies

$$\mathcal{T}\left(\frac{d}{dz}f(z)\right) = \mathcal{T}(f(z)) - 1, \quad (2.114)$$

then f is referred to as a *pure function*. With this definition, we can see that if we were to multiply a pure function with an algebraic function of z the resulting function would still be of uniform transcendentality but not a pure function anymore, since the derivative would also hit the algebraic function. However, a fact that will turn out to be useful is that, given $\mathcal{T}(\mathbf{f}^{(k)}(z)) = k$, Laurent expansions of the form

$$\mathbf{f}(z) = \sum_k \varepsilon^k \mathbf{f}^{(k)}(z), \quad (2.115)$$

are UT pure vector-valued functions. A strong conjecture that will be exploited in this thesis is that functions with unit leading singularities correspond to integrals that are UT pure functions [29]. In some sense, that's something we already explored while studying the $d \log$ decomposition for the massless box. Indeed, we saw from (2.98) that $\mathcal{T}(G_{1,\text{box}}(1, 1, 1, 1)) = 4$, provided the leading singularity was $1/st$.

Back to our master integrals, it means that we are looking for a change of basis, guided by leading singularities, that allows decomposition of the form

$$M_i(\{p_i\}; \varepsilon) = \varepsilon^{-m} \sum_{j \in \mathbb{Z}_{\geq 0}} \varepsilon^j M_i^{(j)}(\{p_i\}; \varepsilon), \quad (2.116)$$

where $M_i^{(j)}(\{p_i\}; \varepsilon)$ is a pure function of weight j . Note that the IR-behavior of Feynman integrals with massless corners fixes $m = 2L$ [33, Ch. 6]. We are now ready to state and prove an important theorem.

Theorem 2.3.1. (Canonical Form) *Let $\mathbf{M} = \{M_i\}_{i=1}^{\chi}$ be a UT basis of MIs. Then, the ε -dependence for $\mathbf{A}_{s_{ij}}$ is linear*

$$\frac{\partial}{\partial s_{ij}} \mathbf{M}(\{p_m\}; \varepsilon) = \varepsilon \mathbf{A}_{s_{ij}}(\{p_m\}) \mathbf{M}(\{p_m\}; \varepsilon). \quad (2.117)$$

Proof. The proof is a little computation. It goes as follows

$$\begin{aligned} \frac{\partial}{\partial s_{ij}} \mathbf{M}(\{p_m\}; \varepsilon) &= \sum_{i=1}^{n-1} \left(\sum_{j=1}^{n-1} C_{ij} p_j^\mu \right) \frac{\partial}{\partial p_i^\mu} \mathbf{M}(\{p_m\}; \varepsilon), \quad \text{from (2.101)} \\ &= \varepsilon^{-2L} \sum_{k \in \mathbb{Z}_{\geq 0}} \varepsilon^k \left(\sum_{i=1}^{n-1} \left(\sum_{j=1}^{n-1} C_{ij} p_j^\mu \right) \frac{\partial}{\partial p_i^\mu} \mathbf{M}^{(k)}(\{p_m\}; \varepsilon) \right), \quad \text{from (2.116)} \end{aligned}$$

$$\begin{aligned}
&= \varepsilon^{-2L} \sum_{k \in \mathbb{Z}_{\geq 1}} \varepsilon^k \underbrace{\sum_{i=1}^{n-1} \left(\sum_{j=1}^{n-1} C_{ij} p_j^\mu \right) \Delta_{\mu i}}_{\Omega_{s_{ij}}(\{p_m\})} \mathbf{M}^{(k-1)}(\{p_m\}; \varepsilon), \\
&= \varepsilon \Omega_{s_{ij}}(\{p_m\}) \left(\varepsilon^{-2L} \sum_{k' \in \mathbb{Z}_{\geq 0}} \varepsilon^{k'} \mathbf{M}^{(k')}(\{p_m\}; \varepsilon) \right), \quad (k \rightarrow k' + 1) \\
&= \varepsilon \Omega_{s_{ij}}(\{p_m\}) \mathbf{M}(\{p_m\}; \varepsilon), \quad \text{from (2.116),}
\end{aligned}$$

where the third equality follows from purity – i.e., the coefficients are invisible for ∂_{p_i} . Above, $\Delta_{\mu i}$ is labeling a set of $D \times (N - 1)$ binary matrices. The matrix Ω is the “new” connection, independent of ε . We will rename it \mathbf{A} in what follows. \square

As a direct corollary, the integrability condition (2.109) becomes, to leading order,

$$\partial_{s_{k\ell}} \mathbf{A}_{s_{ij}} = \partial_{s_{ij}} \mathbf{A}_{s_{k\ell}} \quad \text{and} \quad [\mathbf{A}_{s_{ij}}, \mathbf{A}_{s_{k\ell}}] = 0. \quad (2.118)$$

The first condition implies that *all* the connections $\mathbf{A}_{s_{ij}}$ are related to the *same* connection Ω via $\mathbf{A}_{s_{ij}} = \partial_{s_{ij}} \Omega$. Consequently, there exists, *locally*, an exact single valued 1-form $\mathbf{A} = d\Omega$. This is a useful fact since it permits to cast (2.117) into a differential form

$$d\mathbf{M}(\{p_n\}; \varepsilon) = \varepsilon d\Omega \mathbf{M}(\{p_n\}; \varepsilon). \quad (2.119)$$

In [110], for example, an algorithm to find one transformation matrix \mathbf{B} casting the differential equation into its canonical form is discussed. Differential forms are suitable for parameterizations. In what follows, we denote by \mathcal{K}_n the space of the kinematics invariants s_{ij} for an n -particle process. For example, parametrizing a path $\gamma : [0, 1] \rightarrow \mathcal{K}_n$ with $0 \leq t \leq 1$, we have

$$\frac{d}{dt} \mathbf{M}(t; \varepsilon) = \varepsilon \frac{d\Omega}{dt} \mathbf{M}(t; \varepsilon). \quad (2.120)$$

Now, supposing the boundary condition $t = 0$, $\mathbf{M}(0; \varepsilon)$ is known (we will get back to that later) to certain orders

$$\mathbf{M}(0; \varepsilon) = \varepsilon^{-2L} \sum_{j \in \mathbb{Z}_{\geq 0}} \varepsilon^j \mathbf{M}^{(j)}(0). \quad (2.121)$$

Then, the canonical DE is solved immediately by Picard's method (or Magnus' theorem [111]) as a path ordered exponential

$$\mathbf{M}(t; \varepsilon) = \mathbb{P} \exp \left(\varepsilon \int_{[0,t]} \boldsymbol{\omega}(t') dt' \right) \mathbf{M}(0; \varepsilon), \quad (2.122)$$

where $\boldsymbol{\omega}(t) = \frac{d\Omega}{dt}$. The iterative solution is therefore given by

$$\mathbf{M}^{(k)}(t; \varepsilon) = \sum_{\ell=0}^k \underbrace{\int_{[0,t]} dt_1 \boldsymbol{\omega}(t_1) \dots \int_{[0,t_{\ell-1}]} dt_{\ell} \boldsymbol{\omega}(t_{\ell})}_{\ell \text{ integrations}} \mathbf{M}^{(n-\ell)}(0; \varepsilon), \quad (2.123)$$

at the k^{th} -step. This kind of integral is homotopy invariant [112, 113]. This means the choice of $\gamma : [a, b] \rightarrow \mathcal{K}_n$ is unimportant as long as the endpoints in \mathcal{K}_n are fixed, given no poles of branch cuts are crossed [114].

We note that if we manage to cast the master integrands into $d \log$ -forms, the connection becomes rather simple

$$d\Omega = \sum_k \mathbf{C}_k d \log(W_k), \quad (2.124)$$

where \mathbf{C}_k are constant matrices and W_k are functions of kinematic variables. We emphasize that the canonical form of the differential equation is obtained automatically when using a $d \log$ integrand basis. The W_k -letters thrive in making explicit the singularity and the analytic structure of the master integrals. It also is computationally appealing to work with (2.124) because the function space it is associated to is fairly simple. At the k^{th} iteration, we would encounter k -fold iterative integrals of the form

$$\mathcal{G}(a_1, a_2, \dots, a_k; z) := \int_{[0,z]} \mathcal{G}(a_2, \dots, a_k; t) \frac{dt}{t - a_1}, \quad \text{with } G(z) := 1, \quad (2.125)$$

for any $z \in \mathbb{C}$ and where the $a_i \in \mathbb{C}$ are determined from the W_i -letters. They are known as *Goncharov's polylogarithms* (or multiple polylogarithms) [20, 30, 113]. When $a_{1 \leq i \leq k} \in \{\pm 1, 0\}$, they degenerate into a pretty handy subset known as *harmonic polylogarithms* (HPL). Feynman integrals evaluating to multiple polylogarithms – i.e., whose connection can be transformed into the form (2.124) – are, roughly speaking, the easiest ones we can obtain. The next-to-easiest Feynman integrals being elliptic Feynman integrals. Such integrals appear, for example, in the massive sunrise diagram. The detailed example is

given in [112, 115]. The next-to-next-to-easiest Feynman integrals are Calabi-Yau Feynman integrals [28, 116]. N- and NN-easiest Feynman integrals won't be discussed here.

2.3.2 Determining a Boundary Constant from Physical Consistency

ONCE A CANONICAL BASIS IS KNOWN, the remaining step before integration is to determine a boundary condition [109, 117]. We determine the required boundary conditions from a physical requirement on how the solutions behave near singular points. The matrices \mathbf{C}_k in (2.124) have integer (positive and/or negative) eigenvalues. We demand that the vector of the solutions evaluated at a singular point of the differential equations is in the kernel of the space spanned by the eigenvectors corresponding to *strictly positive* eigenvalues of the associated \mathbf{C}_k -matrix. We can illustrate the justification of this constraint as follows. Because

$$d\Omega \xrightarrow{W_i \rightarrow 0} \mathbf{C}_i d \log(W_i) + \mathcal{O}(W_i), \quad (2.126)$$

the solution of our differential equations to all orders in the dimensional regulator close to the point $W_i = 0$ behaves like

$$\lim_{W_i \rightarrow 0} \mathbf{M} = W_i^{\varepsilon \cdot \mathbf{C}_i} \cdot \mathbf{M}_{W_i=0}, \quad (2.127)$$

where $\mathbf{M}_{W_i=0}$ is a vector of boundary constants. We can use the spectral decomposition of the c 's and see that

$$W_i^{\varepsilon \cdot \mathbf{C}_i} = \exp(\varepsilon \log(W_i) \mathbf{P} \cdot \mathbf{C}_i^{\text{diag}} \cdot \mathbf{P}^{-1}) = \mathbf{P} \cdot \exp(\varepsilon \log(W_i) \mathbf{C}_i^{\text{diag}}) \cdot \mathbf{P}^{-1}, \quad (2.128)$$

where $\mathbf{C}_i^{\text{diag}}$ is the diagonal matrix with entries being eigenvalues of \mathbf{C}_i . The UV divergences appear in the limit $\varepsilon \rightarrow 0^+$. Therefore, our solution (2.127) to the differential equations would exhibit logarithmic UV-divergences for positive c_i -eigenvalues at $W_i = 0$ for a generic boundary condition. To cure this aporia, we can tune the boundary vector $\mathbf{M}_{W_i=0}$ such that no such divergences are present in our solution, normalizing it with right factors. Of course, the same has to be true for the other singular points of our systems of differential equations. In particular, $\Delta = 0$ defines the hypersurfaces where these divergences need to

be cancelled [118, 119]. To close this chapter, we shall work out an explicit example of how we can use the differential equation program to evaluate master integrals.

2.3.3 Example: Differential Equations for the Massless Box

WE FOUND EARLIER that the basis decomposition for $G_{1,\text{box}}(a_0, a_1, a_2, a_3)$ was given the physical box $G_{1,\text{box}}(1, 1, 1, 1)$, the t -channel bubble $G_{1,\text{box}}(0, 1, 0, 1)$ and the s -channel bubble $G_{1,\text{box}}(1, 0, 1, 0)$. We can *naively* hit these basis elements with (2.106) and find

$$\begin{aligned}\partial_s G_{1,\text{box}}(1, 1, 1, 1) &= \frac{tG_{1,\text{box}}(0, 1, 2, 1)}{2s(s+t)} + \frac{G_{1,\text{box}}(1, 0, 2, 1)}{2(s+t)} - \frac{tG_{1,\text{box}}(1, 1, 1, 1)}{2s(s+t)} \\ &\quad - \frac{G_{1,\text{box}}(1, 1, 1, 1)}{s+t} + \frac{G_{1,\text{box}}(1, 1, 2, 0)}{2(s+t)} - \frac{tG_{1,\text{box}}(1, 1, 2, 1)}{2(s+t)}, \\ \partial_s G_{1,\text{box}}(1, 0, 1, 0) &= \frac{tG_{1,\text{box}}(0, 0, 2, 0)}{2s(s+t)} + \frac{G_{1,\text{box}}(1, -1, 2, 0)}{2(s+t)} - \frac{tG_{1,\text{box}}(1, 0, 1, 0)}{2s(s+t)} \\ &\quad + \frac{G_{1,\text{box}}(1, 0, 1, 0)}{s+t} + \frac{G_{1,\text{box}}(1, 0, 2, -1)}{2(s+t)} - \frac{tG_{1,\text{box}}(1, 0, 2, 0)}{2(s+t)},\end{aligned}\tag{2.129}$$

$$\partial_s G_{1,\text{box}}(0, 1, 0, 1) = 0.$$

This computation can be done in arbitrary dimension with, for example, the help of `FeynCalc` [120]. A similar computation is done with (2.105). Next, we use the box IBPs given in (A.5) and find, after setting $d \rightarrow 4 - 2\varepsilon$ and expanding to leading order in ε ,

$$\begin{aligned}\partial_s G_{1,\text{box}}(1, 1, 1, 1) &= \frac{2(2\varepsilon - 1)(sG_{1,\text{box}}(0, 1, 0, 1) - tG_{1,\text{box}}(1, 0, 1, 0)) - stG_{1,\text{box}}(1, 1, 1, 1)(s + t\varepsilon + t)}{s^2t(s+t)}, \\ \partial_s G_{1,\text{box}}(1, 0, 1, 0) &= -\frac{\varepsilon G_{1,\text{box}}(1, 0, 1, 0)}{s},\end{aligned}\tag{2.130}$$

$$\partial_s G_{1,\text{box}}(1, 0, 1, 0) = 0.$$

Our first differential equation is therefore

$$\partial_s \begin{pmatrix} G_{1,\text{box}}(1, 0, 1, 0) \\ G_{1,\text{box}}(1, 0, 1, 0) \\ G_{1,\text{box}}(1, 1, 1, 1) \end{pmatrix} = \underbrace{\begin{pmatrix} 0 & 0 & 0 \\ 0 & -\varepsilon/s & 0 \\ -\frac{2(1-2\varepsilon)}{st(s+t)} & \frac{2(1-2\varepsilon)}{s^2(s+t)} & -\frac{s+t+\varepsilon t}{s(s+t)} \end{pmatrix}}_{\mathbf{A}_s} \begin{pmatrix} G_{1,\text{box}}(1, 0, 1, 0) \\ G_{1,\text{box}}(1, 0, 1, 0) \\ G_{1,\text{box}}(1, 1, 1, 1) \end{pmatrix}.\tag{2.131}$$

Reproducing the same steps for ∂_t , we find

$$\partial_t \begin{pmatrix} G_{1,\text{box}}(1, 0, 1, 0) \\ G_{1,\text{box}}(1, 0, 1, 0) \\ G_{1,\text{box}}(1, 1, 1, 1) \end{pmatrix} = \underbrace{\begin{pmatrix} -\varepsilon/t & 0 & 0 \\ 0 & 0 & 0 \\ \frac{2(1-2\varepsilon)}{t^2(s+t)} & -\frac{2(1-2\varepsilon)}{st(s+t)} & -\frac{s+\varepsilon s+t}{t(s+t)} \end{pmatrix}}_{\mathbf{A}_t} \begin{pmatrix} G_{1,\text{box}}(1, 0, 1, 0) \\ G_{1,\text{box}}(1, 0, 1, 0) \\ G_{1,\text{box}}(1, 1, 1, 1) \end{pmatrix}. \quad (2.132)$$

Note that the Euler's condition (2.110) is verified. However, it is easy to verify that $[\mathbf{A}_s, \mathbf{A}_t] \neq 0$ and the basis we got naively from Laporta's algorithm is not canonical. Furthermore, *only* 2 out of 3 eigenvalues of these matrices are linear in ε . This means that \mathbb{Q} -transforming the basis is not enough to get a canonical form [109]. We need to find a new one. As discussed earlier, we do so by choosing integrals with constant (unit) leading singularity. In the exact same fashion, we computed the leading singularity of $G_{1,\text{box}}(1, 1, 1, 1)$, we can compute those for $G_{1,\text{box}}(1, 0, 2, 0)$ and $G_{1,\text{box}}(0, 1, 0, 2)$. They are respectively given by s and t . We therefore propose the following basis [109]

$$\begin{cases} \mathbf{M}_1 = \varepsilon^2 (e^{\varepsilon\gamma_E}(-s)^\varepsilon) st G_{1,\text{box}}(1, 1, 1, 1), \\ \mathbf{M}_2 = \varepsilon (e^{\varepsilon\gamma_E}(-s)^\varepsilon) s G_{1,\text{box}}(1, 0, 2, 0), \\ \mathbf{M}_3 = \varepsilon (e^{\varepsilon\gamma_E}(-s)^\varepsilon) t G_{1,\text{box}}(0, 1, 0, 2). \end{cases} \quad (2.133)$$

The different powers of ε are dictated by the number of ε we need to cancel either the soft and collinear divergences due to the presence of massless corners (for the box) or the UV-divergences (for the two bubbles) [33]. The extra factor $e^{\varepsilon\gamma_E}(-s)^\varepsilon$ conveniently normalizes dimensionality within dimensional regularization. In particular, the factor $(-s)^\varepsilon$ is set to make all these integrals dimensionless.

Note that (2.133) is dilatation invariant – i.e., they each depend only on the ratio $x = t/s$.

This means the only *active* variable is x , so

$$d \begin{pmatrix} \mathbf{M}_1 \\ \mathbf{M}_2 \\ \mathbf{M}_3 \end{pmatrix} = \partial_x \begin{pmatrix} \mathbf{M}_1 \\ \mathbf{M}_2 \\ \mathbf{M}_3 \end{pmatrix} dx = -\frac{s}{x} \partial_s \begin{pmatrix} \mathbf{M}_1 \\ \mathbf{M}_2 \\ \mathbf{M}_3 \end{pmatrix} ds = \varepsilon \begin{pmatrix} \frac{-dx}{x(1+x)} & \frac{2dx}{1+x} & \frac{-2dx}{x(1+x)} \\ 0 & 0 & 0 \\ 0 & 0 & \frac{-dx}{x} \end{pmatrix} \begin{pmatrix} \mathbf{M}_1 \\ \mathbf{M}_2 \\ \mathbf{M}_3 \end{pmatrix}. \quad (2.134)$$

This basis looks promising for many reasons: (i) the eigenvalues are linear in ε , (ii) the coefficients of the connection are rational in $\{x, 1+x\}$, which implies that the function space is

characterized by harmonic polylogarithms, and (iii) the good singularity structure is already visible in the connection – i.e., $x \rightarrow 0 \Leftrightarrow t \rightarrow 0$, $x \rightarrow \infty \Leftrightarrow s \rightarrow 0$ and $x \rightarrow -1 \Leftrightarrow u \rightarrow 0$. Because the planar box topology is not complicated, we can determine fully two elements of the basis without using the differential equation approach (see Appendix B). We can use this information about the subtopologies, (2.134) as well as the planar constraint, $u \neq 0$, to evaluate the physical box $G(1, 1, 1, 1)$. The first thing we need is an initial condition. Take it to be at $x \rightarrow 1$ since the point is regular with

$$\varepsilon^2 \begin{pmatrix} \mathbf{M}_1(1) \\ \mathbf{M}_2(1) \\ \mathbf{M}_3(1) \end{pmatrix} = \begin{pmatrix} C_0 \\ -1 \\ -1 \end{pmatrix} + \varepsilon \begin{pmatrix} C_1 \\ 0 \\ 0 \end{pmatrix} + \varepsilon^2 \begin{pmatrix} C_2 \\ \pi^2/12 \\ \pi^2/12 \end{pmatrix} + \varepsilon^3 \begin{pmatrix} C_3 \\ 7\zeta_3/3 \\ 7\zeta_3/3 \end{pmatrix} + \varepsilon^4 \begin{pmatrix} C_4 \\ 47\pi^4/1440 \\ 47\pi^4/1440 \end{pmatrix} + \mathcal{O}(\varepsilon^5), \quad (2.135)$$

where $C_{0 \leq i \leq 4}$ are to be determined. This can be done by plugging

$$\mathbf{M}(x) = \frac{1}{\varepsilon^2} \sum_{k \in \mathbb{Z}_{\geq 0}} \varepsilon^k \mathbf{M}^{(k)}(x), \quad (2.136)$$

into the DE and solve for the C 's by imposing $u \neq 0$ at each order in ε . At weight 0, this is trivial

$$\begin{pmatrix} \mathbf{M}_1^{(0)}(t) \\ \mathbf{M}_2^{(0)}(t) \\ \mathbf{M}_3^{(0)}(t) \end{pmatrix} = \begin{pmatrix} C_0 \\ -1 \\ -1 \end{pmatrix}. \quad (2.137)$$

At weight 1, we need to evaluate one integral

$$\begin{aligned} \begin{pmatrix} \mathbf{M}_1^{(1)}(t) \\ \mathbf{M}_2^{(1)}(t) \\ \mathbf{M}_3^{(1)}(t) \end{pmatrix} &= \begin{pmatrix} C_1 \\ 0 \\ 0 \end{pmatrix} + \int_1^t \begin{pmatrix} \frac{-dx}{x(1+x)} & \frac{2dx}{1+x} & \frac{-2dx}{x(1+x)} \\ 0 & 0 & 0 \\ 0 & 0 & \frac{-dx}{x} \end{pmatrix} \cdot \begin{pmatrix} C_0 \\ -1 \\ -1 \end{pmatrix} \\ &= \begin{pmatrix} C_1 + \log(t)(2 - C_0) + (\log(1+t) - \log(2))(C_0 - 4) \\ 0 \\ \log(t) \end{pmatrix} \end{aligned} \quad (2.138)$$

$$\xrightarrow{x \rightarrow -1 \text{ finite} \Rightarrow C_0=4} \begin{pmatrix} C_1 - 2 \log(t) \\ 0 \\ \log(t) \end{pmatrix}.$$

At weight 2,

$$\begin{aligned} \begin{pmatrix} M_1^{(2)}(t) \\ M_2^{(2)}(t) \\ M_3^{(2)}(t) \end{pmatrix} &= \begin{pmatrix} C_2 \\ \pi^2/12 \\ \pi^2/12 \end{pmatrix} + \int_1^t \begin{pmatrix} \frac{-dx}{x(1+x)} & \frac{2dx}{1+x} & \frac{-2dx}{x(1+x)} \\ 0 & 0 & 0 \\ 0 & 0 & \frac{-dx}{x} \end{pmatrix} \cdot \begin{pmatrix} C_1 - 2 \log(t) \\ 0 \\ \log(t) \end{pmatrix} \\ &= \begin{pmatrix} C_2 - C_1(\log(t) + \log(1+t)) \\ \pi^2/12 \\ \pi^2/12 - \log^2(t)/2 \end{pmatrix} \\ &\xrightarrow{x \rightarrow -1 \text{ finite} \Rightarrow C_1=0} \begin{pmatrix} C_2 \\ \pi^2/12 \\ \pi^2/12 - \log^2(t)/2 \end{pmatrix}. \end{aligned} \tag{2.139}$$

At weight 3, polylogarithms and ζ -values start appearing

$$\begin{aligned} \begin{pmatrix} M_1^{(3)}(t) \\ M_2^{(3)}(t) \\ M_3^{(3)}(t) \end{pmatrix} &= \begin{pmatrix} C_3 \\ 7\zeta_3/3 \\ 7\zeta_3/3 \end{pmatrix} + \int_1^t \begin{pmatrix} \frac{-dx}{x(1+x)} & \frac{2dx}{1+x} & \frac{-2dx}{x(1+x)} \\ 0 & 0 & 0 \\ 0 & 0 & \frac{-dx}{x} \end{pmatrix} \cdot \begin{pmatrix} C_2 \\ \pi^2/12 \\ \pi^2/12 - \log^2(t)/2 \end{pmatrix} \\ &= \begin{pmatrix} C_3 - (C_2 - \frac{\pi^2}{6}) \log(t) + \frac{1}{3} \log^3(t) + C_2(\log(1+t) - \log(2)) + \frac{\pi^2}{3}(\log(1+t) - \log(2)) \\ + \frac{3\zeta_3}{2} - \log^2(t) \log(1+t) - 2 \log(t) \text{Li}_2(-t) + 2 \text{Li}_3(-t) \\ \pi^2/12 - \log^2(t)/2 \end{pmatrix} \\ &\xrightarrow{x \rightarrow -1 \text{ finite} \Rightarrow C_2 = -\frac{4\pi^2}{3}} \begin{pmatrix} C_3 + \frac{1}{3} \log^3(t) - \log^2(t) \log(1+t) - 2 \log(t) \text{Li}_2(-t) \\ + \frac{7\pi^2}{6} \log(t) + \pi^2 \log(2/(1+t)) + 2 \text{Li}_3(-t) + \frac{3\zeta_3}{2} \\ 7\zeta_3/3 \\ \frac{1}{12}(2 \log^3(t) - \pi^2 \log(t) + 28\zeta_3) \end{pmatrix}. \end{aligned} \tag{2.140}$$

For $k > 3$, the Goncharov's polylogarithms are evaluated analytically using **GiNac** [121] and **PolyLogTools** [31], provided we have an ansatz for the transcendental numbers appearing.

At $k = 4$, we find $C_3 = 77\zeta_3/6$, in accordance with [109]. Below, we write the solution for

our UT basis of MIs, in terms of “classical” functions/numbers up to weight 3

$$\begin{aligned}
\varepsilon^2 \begin{pmatrix} \mathbf{M}_1(t) \\ \mathbf{M}_2(t) \\ \mathbf{M}_3(t) \end{pmatrix} &= \begin{pmatrix} 4 \\ -1 \\ -1 \end{pmatrix} + \varepsilon \begin{pmatrix} -2\log(t) \\ 0 \\ \log(t) \end{pmatrix} + \varepsilon^2 \begin{pmatrix} -\frac{4\pi^2}{3} \\ \pi^2/12 \\ \pi^2/12 - \log^2(t)/2 \end{pmatrix} \\
&+ \varepsilon^3 \begin{pmatrix} \frac{34\zeta_3}{3} + \frac{1}{3}\log^3(t) - \log^2(t)\log(1+t) - 2\log(t)\text{Li}_2(-t) \\ +\frac{7\pi^2}{6}\log(t) + \pi^2\log(2/(1+t)) + 2\text{Li}_3(-t) \\ \hline 7\zeta_3/3 \\ \frac{1}{12}(2\log^3(t) - \pi^2\log(t) + 28\zeta_3) \end{pmatrix} + \mathcal{O}(\varepsilon^4).
\end{aligned} \tag{2.141}$$

We see from the last expression that as $\varepsilon \rightarrow 0$, it is enough to truncate $\mathcal{O}(\varepsilon^3)$ and higher contributions on the RHS.

Conversely, given we know both the explicit connection and the boundary constants $\mathbf{M}(0)$, we implemented a code in MATHEMATICA that evaluates $\mathbf{M}(t)$ for any values of t . This is, in essence, the code we will use to compute the DE constants in Chapter 4.

Chapter 3

Scattering Of 5-Gluon at 2-Loop

AS ADVERTISED IN THE INTRODUCTION, owing to the performance of the LHC, we have accessed an era of precision high-energy physics. Some of the most recently studied processes in particle colliders were 3-light-particles- and jet-production [122–124]. These can both be used, for instance, to test the strong interaction predictions at high-energies and to determine α_s . From the *theoretical* viewpoint, predictions with compatible precision are needed, which minimally requires perturbative QCD calculations up to the NNLO. In this chapter, we present an overview of the significant advances that have been made in the past few years toward the resolution of NNLO five asymptotically light partons amplitudes.

3.1 Setup and Preliminaries

3.1.1 The Kinematic Space of $2 \rightarrow 3$ Scatterings

THE MAIN OBJECTIVE OF THIS THESIS is the evaluation of the master integrals contributing to NNLO five massless partons scattering amplitudes by “moving” between overlapping kinematic sectors. Before we delve into this problem, we first briefly discuss the kinematics of these processes and introduce some quantities that will be relevant in the following sections. We follow the conventions initially introduced in [125]. The associated momenta are all subject to on-shellness, $p_{1 \leq i \leq 5}^2 = 0$, and we put the kinematic on crossing-symmetric grounds

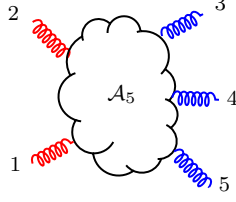


Figure 3.1: A 5-gluon process.

by assuming they are all incoming such that momentum conservation reads $\sum_{i=1}^5 p_i^\mu = 0$. The physical scattering region of $2 \rightarrow 3$ processes (see 3.1) is described by 5 independent Mandelstam variables $s_{ij} = (p_i + p_j)^2$, which we choose to be cyclically ordered

$$X = \{s_{12}, s_{23}, s_{34}, s_{45}, s_{15}\} \text{ with } s_{\textcolor{red}{i}\textcolor{blue}{j}}, s_{\textcolor{blue}{i}\textcolor{red}{j}} \geq 0 \text{ and } s_{\textcolor{red}{i}\textcolor{red}{j}} \leq 0. \quad (3.1)$$

These variables are not sufficient to characterize the kinematics of the scattering process [126]. Indeed, there is an additional parity label, generalizing the one discussed in Section 2.1.5, which can be captured by the parity-odd Levi-Civita contraction

$$\text{tr}_5 := 4i\varepsilon_{\alpha\beta\gamma\delta} p_1^\alpha p_2^\beta p_3^\gamma p_4^\delta = \text{tr}(\gamma_5 \not{p}_4 \not{p}_5 \not{p}_1 \not{p}_2). \quad (3.2)$$

This is necessary to have if we assume spacetime parity, as $s_{ij} \xrightarrow{\text{p}} s_{ij}$, but $\text{tr}_5 \xrightarrow{\text{p}} -\text{tr}_5$. As they indicate possible linear dependencies, is also useful to introduce Gram determinants when discussing kinematics of scattering processes. For $(n+1)$ -legged processes, they are generically given by the determinants, $\Delta(p_1, \dots, p_n)$, of the Gram matrix $\delta(p_1, \dots, p_n)$ defined as

$$\delta(p_1, \dots, p_n) = [2p_i \cdot p_j]_{1 \leq i, j \leq n}. \quad (3.3)$$

Another useful and easily verifiable property $\Delta(p_1, \dots, p_n)$ satisfies is invariance under shifts of any of the p_i by any of the other momenta. It is also parity-even by construction. We can expand both (3.2) and (3.3) (for $n = 5$) in terms of spinor-helicity variables and notice [126]

$$\Delta(p_1, \dots, p_4) = [12]\langle 23\rangle[34]\langle 41\rangle - \langle 12\rangle[23]\langle 34\rangle[41] = (\text{tr}_5)^2. \quad (3.4)$$

In other words, tr_5 is *always* the square root of a polynomial in the Mandelstam variables in X . Note, also, that for $p_{1 \leq i \leq 5} \in \mathbb{R}^{1,3}$, $\Delta(p_1, \dots, p_4) \leq 0$. To see this, we can write $\Delta(p_1, \dots, p_4) = 2 \det(V^\top(p_1, \dots, p_4) \eta V(p_1, \dots, p_4)) = -\det^2(V)$, where $V(p_1, \dots, p_4)$ is a 4×4

matrix whose columns are the vectors p_i^μ . This is a particular condition the kinematics of processes with $n = d - 1$ satisfy.

We close this section with a brief comment on the analytic structure of the master integrals that will be present. They evaluate to functions of the Mandelstam variables s_{ij} with a complicated branch cut structure. More precisely, the integrals we compute have branch cuts starting at zeroes of $s_{ij} \in X$. This makes the possibility of crossing the real axis really hard to see in practice. Nevertheless, we think taking appropriate scaling limits can make these branch cuts a lot easier to locate and avoid as we move in the kinematic space. Below, methods to control the approach to such limits will be discussed. We will also refer as “physical region” any region for which there is a physical configuration of momenta with timelike (positive) and spacelike (negative) Mandelstam variables. For example, Euclidean regions where $s_{ij} > 0$, $\forall i, j$ would not be considered physical, given this corresponds to a process with no initial (or final) states to scatter.

3.1.2 Massless 5-particle 2-loop Topologies and their IBPs

TO OBTAIN THE REDUCTION OF FEYNMAN INTEGRALS for 2-loop 5-gluon scattering amplitudes, we only need to consider integrals that originate from the four topologies shown in Fig. 3.2 [127, 128]. All the other Feynman integrals are 1-loop-like, and can be dealt with much easier. To explain what kind of Feynman integrals we need to reduce, we will focus on the DP-topology, which turns out to be the most complicated one. With two loop momenta ℓ_1 and ℓ_2 , as labeled in Fig. 3.2, a complete¹ set of propagators can be chosen as

$$\begin{aligned} D_1 &= \ell_1^2, \quad D_2 = (\ell_1 + p_2)^2, \quad D_3 = (\ell_1 + p_1 + p_2)^2, \quad D_4 = \ell_2^2, \quad D_5 = (\ell_2 + p_4)^2, \\ D_6 &= (\ell_1 + \ell_2 + p_1 + p_2 + p_4)^2, \quad D_7 = (\ell_1 + \ell_2 - p_3)^2, \quad D_8 = (\ell_1 + \ell_2)^2, \\ D_9^{(\text{ISP})} &= (\ell_2 + p_2)^2, \quad D_{10}^{(\text{ISP})} = (\ell_2 + p_1)^2, \quad D_{11}^{(\text{ISP})} = (\ell_2 + p_3)^2. \end{aligned} \tag{3.5}$$

¹Note that for $L = 2$ and $E = 4$, the number of irreducible scalar products (ISP) is $N = 3$.

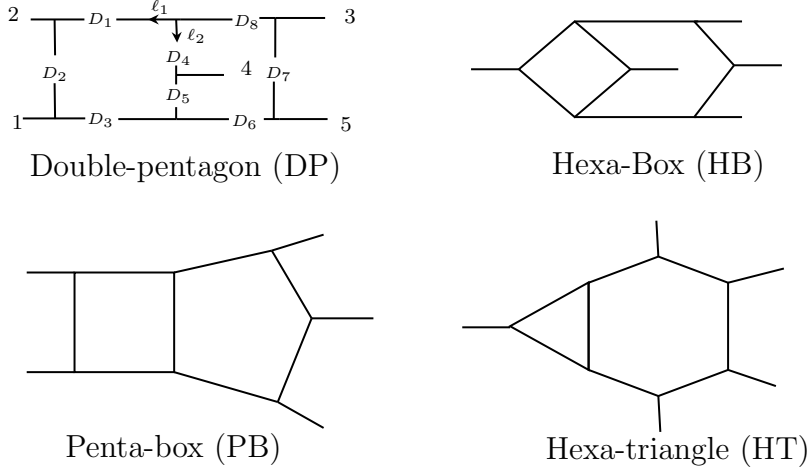


Figure 3.2: All the 8-propagator families.

where the first eight are inverse propagators and the last three are irreducible scalar products (ISP). Then, the family of integrals defined by the DP-topology are expressed as

$$G_{\text{DP}}(a_1, \dots, a_9) = \int \frac{d^d \ell_1 d^d \ell_2}{(i\pi)^d} \frac{D_9^{-a_9} D_{10}^{-a_{10}} D_{11}^{-a_{11}}}{D_1^{a_1} \dots D_8^{a_8}}, \quad (3.6)$$

where the indexes $a_1, \dots, a_8 \in \mathbb{Z}$ and $a_9, a_{10}, a_{11} \in \mathbb{N}_0$. It turns out that all the master integrals for the massless 2-loop 5-particle topologies in 3.2 are known [129]. For the DP-topology, there are 108 master integrals [130, 131], for the HB-topology, there are 73 master integrals [132–134], for the PB-topology, there are 61 master integrals [127, 135] and, finally, for the HT-topology, there are only 28 master integrals [128]. However, the raw computer output is not necessarily a basis of canonical integrals. So, to ultimately evaluate these integrals using the differential equations approach, we need to perform a change of basis. The choice of transition matrix is strongly guided by the knowledge of the leading singularities. At $L = 2$, they suggest the canonical basis of master integrals evaluates to a special kind of iterated integrals, known as the *pentagon functions* [125]. This was confirmed in [130, 131]. The upshot is that the only necessary inputs are the ingredients – the alphabet $\{W_i\}$ – needed to generate these pentagon functions.

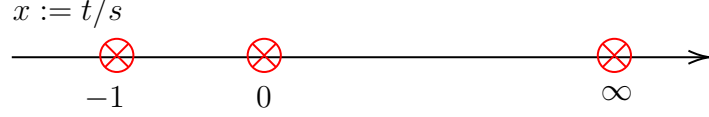


Figure 3.3: Massless 4-point process singularity structure.

| Letter | s -notation | p -notation | Cyclic |
|----------|---|---|--------|
| W_1 | s_{12} | $2p_1 \cdot p_2$ | $+(4)$ |
| W_6 | $s_{34} + s_{45}$ | $2p_4 \cdot (p_3 + p_5)$ | $+(4)$ |
| W_{11} | $s_{12} - s_{45}$ | $2p_3 \cdot (p_4 + p_5)$ | $+(4)$ |
| W_{16} | $s_{45} - s_{12} - s_{23}$ | $2p_1 \cdot p_3$ | $+(4)$ |
| W_{21} | $s_{34} + s_{45} - s_{12} - s_{23}$ | $2p_3 \cdot (p_1 + p_4)$ | $+(4)$ |
| W_{26} | $\frac{s_{12}s_{23}-s_{23}s_{34}+s_{34}s_{45}-s_{12}s_{15}-s_{45}s_{15}-\sqrt{\Delta}}{s_{12}s_{23}-s_{23}s_{34}+s_{34}s_{45}-s_{12}s_{15}-s_{45}s_{15}+\sqrt{\Delta}}$ | $\frac{\text{tr}[(1-\gamma_5)\not{p}_4\not{p}_5\not{p}_1\not{p}_2]}{\text{tr}[(1+\gamma_5)\not{p}_4\not{p}_5\not{p}_1\not{p}_2]}$ | $+(4)$ |
| W_{31} | $\sqrt{\Delta}$ | $\text{tr}[\gamma_5\not{p}_1\not{p}_2\not{p}_3\not{p}_4]$ | |

Figure 3.4: 2-loop massless 5-point (pentagon) alphabet.

3.1.3 Function Space and the Pentagon Alphabet

IN THIS SECTION, we will follow [125], where the authors bootstrapped the form the pentagon alphabet. They use, essentially, two guiding lines to do so. Firstly, since, by definition, the master integrals know about the kinematics, $W_i = W_i(s)$. Secondly, by locality, the branch points of the master integrals must correspond to physical and spurious singularities. Consequently, the zero loci of letters encode, by construction, all possible singularities of the amplitudes. We enforce that the form of this alphabet is not unique [136, §5.1].

A prototypical example is to consider a 4-point massless process, where the singularities from Landau equations read as $s = 0, t = 0, u = -s - t = 0$, see Fig. 3.3. The differential equations are generated by a single letter $x = t/s$. The alphabet for massless 5-point processes at 2-loop is listed in Fig. 3.4. We first observe from the third column that the

letters $W_{1 \leq i \leq 25}$ contains information about all the physical, soft and collinear divergences of the scattering amplitudes. Furthermore, since $\sqrt{\Delta} \in i\mathbb{R}$ in physical regions, the letters $W_{26 \leq i \leq 30}$ are pure phases and, in fact, they can be written as product ratios of four alternating angle- and square-brackets. For example,

$$W_{30} = \frac{\langle 34 \rangle [45] \langle 51 \rangle [13]}{[34] \langle 45 \rangle [51] \langle 13 \rangle}. \quad (3.7)$$

The remaining $W_{26 \leq i \leq 30}$ are obtained by cyclic permutations of $\{1, 2, 3, 4, 5\}$ of spinor entries in (3.7). More generally, this form is particularly convenient to see how they transform under the \mathcal{S}_5 -action. Intuitively, the phases are needed because they ensure the alphabet reproduces the singularities on *all* sheets, recalling that Feynman integrals are usually multi-valued objects. Finally, the inclusion W_{31} is justified by the need of a parity label. It also measures, in some sense, the distance with the physical point where Δ is evaluated and the boundary of the physical region.

Some additional comments can be made on the pentagon alphabet: (i) we note it splits into $\mathbb{Z}/5\mathbb{Z}$ -orbits, (ii) it is closed under the symmetric group \mathcal{S}_5 action (see [125, Ap. A]), reflecting non-planarity, and (iii) it splits into parity *odd* and *even* parts – i.e.,

$$\Delta \leq 0 \Rightarrow (\sqrt{\Delta})^* = -\sqrt{\Delta} \Rightarrow W_i^* = W_i^{-1} \Rightarrow \log(W_i^*) = -\log(W_i), \text{ for } 26 \leq i \leq 30. \quad (3.8)$$

Further properties of this alphabet are discussed in [137]. The pentagon functions, $G(X)$, we get out of the differential equation can be nicely written as \mathbb{Q} -linear combinations of iterated integrals, defined over the pentagon alphabet

$$\mathcal{S}[G(X)] = \alpha_I \cdot [W_{i_1} \otimes \dots \otimes W_{i_{n-1}} \otimes W_{i_n}](X) = \alpha_I \int_{\gamma} d \log(W_{i_n}(\xi)) [W_{i_1} \otimes \dots \otimes W_{i_{n-1}}](\xi), \quad (3.9)$$

where $\alpha_I \in \mathbb{C}$, with $I = \{i_1, \dots, i_{n-1}, i_n\}$, and γ is an integration contour connecting X_0 to X . Summation over repeated indices is assumed. The first tail of tensor products in (3.9) defines a weight n element of the symbol representation, $\mathcal{S}[G(X)]$, of the function $G(X)$ [138]. The symbol itself does not contain the information of the integration contour or of the values that the iterated integral has to take at the boundary points. These integration constants have to be provided once the symbol is known and it then becomes, in principle, possible to express the function itself in terms of explicit functions such as (Goncharov) polylogarithms. The

main advantage of working with symbols is their ability to capture the main combinatorial and analytic properties of iterated integrals, while being significantly easier to deal with. In particular, if the function $G(X)$ is defined via a differential equation, its symbol is, in a sense, the general solution to the differential equation – i.e., the solution up to integration constants. However, in this thesis, these constants are exactly what we are looking for, so we will need to go beyond the symbolic representations of the MI's.

Given a symbol, we can always lift to functions, we just need to specify a boundary point. For example, if we choose the boundary point be $s_{ii+1} = -1 \forall i$ and let $Z := \frac{s_{34}}{s_{12}}$. Then,

$$\begin{aligned} \frac{W_3}{W_1} \otimes \frac{W_{13}}{W_1} &= \frac{s_{34}}{s_{12}} \otimes \left(1 - \frac{s_{34}}{s_{12}}\right) \\ &= Z \otimes (1 - Z) \\ &= \int_1^Z d\log(1 - Z') \int_1^{Z'} d\log(Z'') \\ &= -\text{Li}_2(1 - Z). \end{aligned}$$

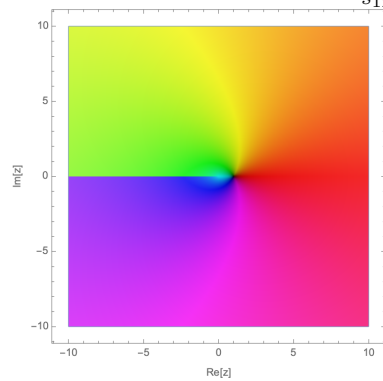


Figure 3.5: Color plot of $-\text{Li}_2(1 - Z)$.

We note that the first entry² of the symbol contains the information about its branch cuts (see Fig. 3.5). Further constraints, on the arguments that may appear as symbol arguments are given in [139] – e.g., the first and second entry conditions – but will not be discussed here.

3.2 Kinematic Sectors

THIS SECTION IS DEDICATED to the description of two important kinematic limits, the *multi-Regge kinematics* (MRK) and the *collinear kinematics*.

²It is the one associated with the last integral to perform in the iteration.

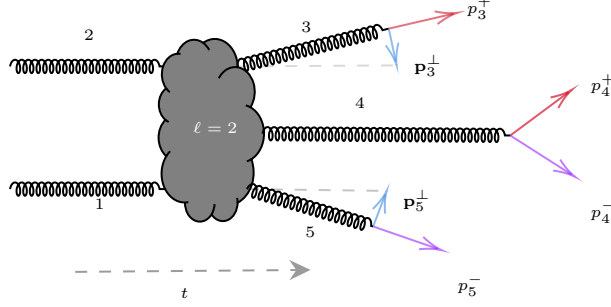


Figure 3.6: Visualization of the 5-point multi-Regge kinematics. Each particle has its own light-cone frame.

3.2.1 The Multi-Regge Kinematics

THE MULTI-REGGE KINEMATICS is defined as a scattering process where the final state particles are strongly ordered in rapidity, $\tanh(R) = p_i^\parallel/p_i^0$, and have comparable transverse momenta. A general treatment of such kinematics for $2 \rightarrow 2 + (n - 4)$ processes is given in [140]. We will focus on how it works for $n = 5$. We work in the s_{12} -channel and assume, without loss of generality, that we are in a reference frame where the momenta of the incoming state gluons p_1 and p_2 lie on the z -axis before colliding, implying $p_1^+ = p_2^- = \mathbf{p}_1^\perp = \mathbf{p}_2^\perp = 0$. Usually, it is useful to associate a physical limit with a symmetry of the physical process. Here, the multi-Regge limit grants that our physical setting is invariant under $SO(1,3)$ -boosts along the z -direction. Similar ideas can be applied for collinear limits – e.g., see [141]. Using light cones coordinates $p_j = (p_j^+, p_j^-, \mathbf{p}_j^\perp)$, where $p_j^\pm := p_j^0 \pm p_j^3$ and $\mathbf{p}_j^\perp := p_j^1 + ip_j^2$, we have

$$|p_3^+| \gg |p_4^+| \gg |p_5^+|, \quad |p_3^-| \ll |p_4^-| \ll |p_5^-|, \quad \text{and} \quad |\mathbf{p}_3^\perp| \sim |\mathbf{p}_4^\perp| \sim |\mathbf{p}_5^\perp|. \quad (3.10)$$

To quantify these orderings, we use an infinitesimal positive parameter ϵ , which regulates the size of the light-cone components as

$$|p_1^-| \sim |p_2^+| \sim |p_3^+| \sim |p_5^-| \sim \mathcal{O}(\epsilon^{-1}), \quad (3.11)$$

$$|p_4^-| \sim |p_4^+| \sim |\mathbf{p}_3^\perp| \sim |\mathbf{p}_4^\perp| \sim |\mathbf{p}_5^\perp| \sim \mathcal{O}(1), \quad (3.12)$$

$$|p_3^-| \sim |p_5^+| \sim \mathcal{O}(\epsilon), \quad (3.13)$$

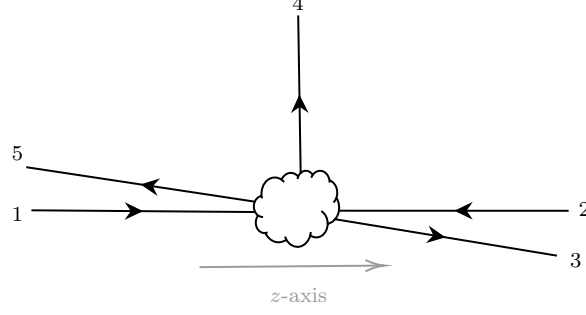


Figure 3.7: Collider geometry for 5-point processes at high energies.

For us, this is conveniently pictured in Fig. 3.6, even though the physical geometry of the collision much more looks like Fig. 3.7.

Formally, this is done by setting

$$p_j^\mu = \left(p_j^+ \epsilon^{j+\frac{1}{2}(-n-3)} \quad p_j^- \epsilon^{\frac{n+3}{2}-j} \quad \sqrt{|p_j^-|} \sqrt{|p_j^+|} e^{i\phi_j} \quad \sqrt{|p_j^-|} \sqrt{|p_j^+|} e^{-i\phi_j} \right)^\top, \quad 3 \leq j \leq n, \quad (3.14)$$

and momentum conservation implies

$$p_1^\mu = \left(0 \quad -\sum_{j=3}^n p_j^- \epsilon^{\frac{n+3}{2}-j} \quad 0 \quad 0 \right)^\top, \quad (3.15)$$

$$p_2^\mu = \left(-\sum_{j=3}^n p_j^+ \epsilon^{j+\frac{1}{2}(-n-3)} \quad 0 \quad 0 \quad 0 \right)^\top, \quad (3.16)$$

$$\sum_{j=3}^n \mathbf{p}_i^\perp = 0. \quad (3.17)$$

Above, $\phi_j := \text{Arg}(\mathbf{p}_j^\perp)$. Note that these formulas work for any $n > 2$. To relate to light-cone coordinates, we can go in the $\text{SL}(2, \mathbb{C})$ -representation, where $p_i^\mu = \sigma_{\alpha\dot{\alpha}}^\mu p_{i,\alpha\dot{\alpha}}$ with $p_{i,\alpha\dot{\alpha}} := \lambda_{i,\alpha} \tilde{\lambda}_{i,\dot{\alpha}}$. We can easily see the correct spinors read

$$\lambda_1 = \left(0 \quad \sqrt{|p_1^-|} \epsilon^{\frac{3-n}{4}} \right), \quad (3.18)$$

$$\lambda_2 = \left(\sqrt{|p_2^+|} \epsilon^{\frac{3-n}{4}} \quad 0 \right), \quad (3.19)$$

$$\lambda_j = \left(\sqrt{|p_j^+|} \epsilon^{\frac{j}{2}-\frac{n}{4}-\frac{3}{4}} \quad \sqrt{|p_j^-|} e^{i\phi_j} \epsilon^{-\frac{j}{2}+\frac{n}{4}+\frac{3}{4}} \right), \quad 3 \leq j \leq n. \quad (3.20)$$

Under reality of momenta condition, recall that $\lambda_i^* = \tilde{\lambda}_i$. At leading order, it is not hard to verify that the Mandelstam variables are given by

$$s_{12} = p_1^- p_2^+ \equiv s/\epsilon^2, \quad (3.21)$$

$$s_{23} = -|\mathbf{p}_3^\perp|^2 \equiv t_1, \quad (3.22)$$

$$s_{15} = -|\mathbf{p}_5^\perp|^2 \equiv t_2, \quad (3.23)$$

$$s_{34} = p_3^+ p_4^- \equiv s_1/\epsilon, \quad (3.24)$$

$$s_{45} = p_4^+ p_5^- \equiv s_2/\epsilon, \quad (3.25)$$

where $z, \bar{z} \in \mathbb{C}$ are defined such that

$$z\bar{z} := -\frac{t_1 s}{s_1 s_2} \quad \text{and} \quad (1-z)(1-\bar{z}) := -\frac{t_2 s}{s_1 s_2}. \quad (3.26)$$

Note that when we fix the other parameters and take the second scaling defined by $z \rightarrow \epsilon_1 z$ (and similarly for \bar{z}) for $\epsilon \ll \epsilon_1$, gluons 2 and 3 become collinear, which we denote by $(2||3)$. Similarly, if z and \bar{z} are near the identity, gluons 1 and 5 are (almost) collinear. Hence, this parametrization already embeds certain collinear limits. This is consistently visible from how the MRK parameters relate to light-cone momenta under the constraints of momentum conservation and on-shellness. Indeed, given $e_{1,2} = s_{1,2}/s$,

$$\begin{aligned} s &:= p_5^- \cdot p_3^+, \quad e_1 := p_4^-/p_5^-, \quad e_2 := p_4^+/p_3^+, \\ z &:= 1 + \exp(-i(\phi_4 - \phi_5)) \frac{\sqrt{p_5^-} \sqrt{p_5^+}}{\sqrt{p_4^-} \sqrt{p_4^+}}. \end{aligned} \quad (3.27)$$

We observe that, for example, as $(1||5)$, $p_5^+ \rightarrow \epsilon_1^2 p_5^+$ which indeed corresponds to $z \rightarrow 1 + \mathcal{O}(\epsilon_1)$. At the leading order in the MRK, the Gram determinants becomes

$$\Delta = \epsilon_5^2 \xrightarrow{\epsilon \rightarrow 0} \frac{s_1^2 s_2^2 (z - \bar{z})^2}{\epsilon^4} + \mathcal{O}(\epsilon^{-3}). \quad (3.28)$$

Since $\Delta \leq 0$, we deduce, choosing the positive branch of the square root, that $(z - \bar{z})^2 \leq 0$ and so $z - \bar{z}$ is purely imaginary. Thus, in the physical region, z and \bar{z} are related by complex conjugation, explaining the notation. Hence, the multi-Regge physical s_{12} -channel region is defined by

$$s \geq 0, \quad s_1 \geq 0, \quad s_2 \geq 0, \quad \text{and} \quad z^* = \bar{z}. \quad (3.29)$$

In the physical region, the pentagon alphabet reduces nicely to only 12 letters, factoring into the following decoupled orbits

$$\mathcal{A}_{\text{MRK}} = \{\epsilon\} \cup \{s e_1 e_2\} \cup \{s, e_1, e_2, e_1 + e_2, e_1 - e_2\} \cup \{z, \bar{z}, 1 - z, 1 - \bar{z}, z - \bar{z}, 1 - z - \bar{z}\}. \quad (3.30)$$

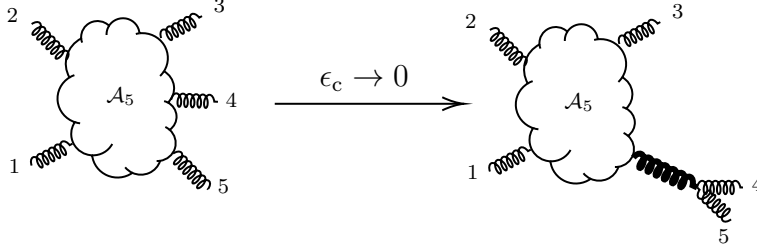


Figure 3.8: Visualization of the 5-point collinear limit.

The functional structure of massless 2-loop five particles amplitudes is therefore *extremely* simple in the MRK and this makes the symbols particularly handy. As Δ is a perfect square, a choice of branch for $\pm\sqrt{\Delta}$ is needed. By choosing the $+$ -branch, z needs to lie in the upper half of the complex plane, namely $\text{Im}(z) > 0$. Furthermore, we know from the symbols that for certain non-planar Feynman integrals contributing to the amplitudes, discontinuities (and even divergence) appears at $\sqrt{\Delta} = 0$. This hypersurface corresponds to $z = \bar{z}$, namely $\text{Im}(z) = 0$. Because of this reason, it is important to be careful and always have $\text{Im}(z) > 0$ and $\text{Im}(\bar{z}) < 0$ when we move in the kinematic space. The loci of the alphabet will tell us the singularity structure of the corresponding master integrals. Here, we expect from locality physical singularities at $z = 0, z = 1, e_1 = 0, e_2 = 0$ and $s = 0$. However, some letters of the alphabet vanish at $z + \bar{z} = 1, z = \bar{z}$ and $e_1 = e_2$. These singularities have no physical meaning and therefore are spurious.

3.2.2 Collinear Kinematics

IN THIS SECTION, we discuss the approach a collinear configuration from a generic initial physical configuration. We will parametrize the limit where gluons 4 and 5 become collinear, but this discussion is completely general and could be applied to any other pairs of legs, timelike or spacelike separated. Let ϵ_c be the parameter we sent to zero as we approach $(4\parallel 5)$ (see Fig. 3.8). To control the collinear behaviour, we trade the two light-like momenta $p_{4,5}^\mu$ for the two light-like vectors P and R . The former defines the “collinear direction”, while the latter defines an auxiliary vector that can be fine-tuned depending on how we want to approach the limit. We, furthermore, ask for $P \xrightarrow{\epsilon_c \rightarrow 0} p_4 + p_5$ and use the following spinor

decomposition

$$\lambda_4 = \sqrt{\zeta}\lambda_P - \epsilon_c\sqrt{1-\zeta}\lambda_R, \quad \tilde{\lambda}_4 = \lambda_4^*. \quad (3.31)$$

$$\lambda_5 = \sqrt{1-\zeta}\lambda_P + \epsilon_c\sqrt{\zeta}\lambda_R, \quad \tilde{\lambda}_5 = \lambda_5^*. \quad (3.32)$$

Then, the associated momenta are easily seen to be given by

$$p_4 = \zeta P - \underbrace{\epsilon_c\zeta(1-\zeta)(\lambda_P\tilde{\lambda}_R + \lambda_R\tilde{\lambda}_P)}_{\text{transverse component}} + \epsilon_c^2(1-\zeta)R, \quad (3.33)$$

$$p_5 = (1-\zeta)P + \epsilon_c\zeta(1-\zeta)(\lambda_P\tilde{\lambda}_R + \lambda_R\tilde{\lambda}_P) + \epsilon_c^2\zeta R. \quad (3.34)$$

Notice that in the collinear limit, the transverse momentum components of p_4 and p_5 are the same, but with opposite signs. This reflects something we physically expect as $\epsilon_c \rightarrow 0$, namely $|\mathbf{p}_4^\perp/(p_4^+ + p_4^-)| \rightarrow |\mathbf{p}_5^\perp/(p_5^+ + p_5^-)|$. Moreover, using this parameterization, gluons 4 and 5 are exchanged by sending $\zeta \rightarrow 1 - \zeta$.

Using spinor identities (see Section 2.1.5), one can verify that our parameterization have all the expected properties of a collinear process – i.e.,

$$p_4 \xrightarrow{\epsilon_c \rightarrow 0} \zeta P, \quad p_5 \xrightarrow{\epsilon_c \rightarrow 0} (1-\zeta)P, \quad (3.35)$$

$$p_4 + p_5 = P + \epsilon_c^2 R. \quad (3.36)$$

$$\langle 45 \rangle = \epsilon_c \langle PR \rangle, \quad [45] = \epsilon_c [PR], \quad (3.37)$$

$$s_{45} = 2\epsilon_c^2 P \cdot R, \quad (3.38)$$

$$k^\perp \cdot P = k^\perp \cdot R = 0, \quad (3.39)$$

$$(k^\perp)^2 \leq 0. \quad (3.40)$$

In the next section, we will see that there are intermediate parameters suitable to link both MRK and collinear parameterizations.

3.3 Pure Master Integrals in a MRK-background

TO FIND THE SOLUTION of the canonical differential equation (2.117) in the MRK, we consider the $\epsilon \rightarrow 0$ boundary condition together with the following system of differential

equations [126]

$$\begin{cases} \partial_\epsilon \mathbf{M}(y, \epsilon; \varepsilon) = \varepsilon \mathbf{A}_\epsilon(y, \epsilon) \mathbf{M}(y, \epsilon; \varepsilon), \\ \partial_y \mathbf{M}(y, \epsilon; \varepsilon) = \varepsilon \mathbf{A}_y(y, \epsilon) \mathbf{M}(y, \epsilon; \varepsilon). \end{cases} \quad (3.41)$$

Here, $y \in \mathcal{A}_{\text{MRK}} - \{\epsilon\}$ and ε is the t' Hooft dimensional regularization parameter. We saw earlier the canonical differential equation exhibits the singularity structure of the Feynman integrals (see Section 2.2.4) and, as a consequence of locality, it must only have regular poles in Mandelstam variables. For 2-loop 5-point processes, this is already visible from the pentagon alphabet. This condition guarantees that the matrix \mathbf{A}_x , where $x \in \{\epsilon, y\}$, has, *at worst*, a pole of order one. Hence, for each singular point of the system, we can find a gauge transformation $\mathbf{U}(y, \epsilon; \varepsilon)$ such that the gauge equivalent system of differential equations has a connection which has leading behavior of $\mathcal{O}(x^{-1})$, as $x \rightarrow 0$. This is similar to what we discussed in Section 2.3.2.

For the ϵ -differential equation, we use U such that the gauge equivalent form of \mathbf{A}_ϵ can be expanded as

$$\mathbf{A}_\epsilon(y, \epsilon) \rightarrow \mathbf{A}'_\epsilon(y, \epsilon) = \frac{\mathbf{A}_0}{\epsilon} + \sum_{i \geq 0} \epsilon^i \mathbf{A}_{i+1}(y), \quad (3.42)$$

where the residue \mathbf{A}_0 is a constant \mathbb{Q} -matrix, independent of y – i.e., the coefficients of $d \log(\epsilon)$ in (2.124) are rational numbers. We recall that \mathbf{A}_ϵ and \mathbf{A}'_ϵ are related via (2.112) – i.e.,

$$\varepsilon \frac{\mathbf{A}_0}{\epsilon} + \mathcal{O}(\epsilon^0) = \mathbf{U}^{-1}(y, \epsilon; \varepsilon) (\varepsilon \mathbf{A}_\epsilon(y, \epsilon) - \partial_\epsilon) \mathbf{U}(y, \epsilon; \varepsilon). \quad (3.43)$$

On the other hand, the solution to the second differential equation is regular in the MRK parameter ϵ , since $y \neq \epsilon$. To solve (3.43), it is useful to assume U is smooth enough to represent it formally as a Taylor polynomial in ϵ

$$\mathbf{U}(y, \epsilon; \varepsilon) = \mathbb{1} + \sum_{k \geq 1} \epsilon^k \mathbf{U}_k(y; \varepsilon). \quad (3.44)$$

In particular, we choose it such that it becomes the identity as $\epsilon \rightarrow 0$. At LO in $\epsilon \rightarrow 0$, the gauge equation (3.43) reduces to $\mathbf{A}_\epsilon(y, \epsilon = 0) = \mathbf{A}'_\epsilon(y, \epsilon = 0) = \mathbf{A}_0/\epsilon$. Plugging (3.42) in

(3.43), we find a contiguous equation

$$\varepsilon \mathbf{A}_k(y) + \varepsilon \mathbf{U}_k(y; \varepsilon) \mathbf{A}_0 - \varepsilon \mathbf{A}_0 \mathbf{U}_k(y; \varepsilon) - k \mathbf{U}_k(y; \varepsilon) + \varepsilon \sum_{j=1}^{k-1} \mathbf{A}_{k-j}(y) \mathbf{U}_j(y; \varepsilon) = 0, \quad \forall k \geq 1. \quad (3.45)$$

Since the right hand side is trivial, this relation tells us that $k \mathbf{U}_k(y; \varepsilon) \sim \mathcal{O}(\varepsilon) \forall k$, indicating that a second expansion, this time in $\varepsilon \rightarrow 0$, would be convenient. We take

$$\mathbf{U}_k(y; \varepsilon) = \sum_{j \geq 1} \varepsilon^j \mathbf{U}_{k,j}(y). \quad (3.46)$$

Putting (3.46) in (3.45) and comparing order by order in ε gives us a recursion relation

$$\begin{cases} \mathbf{U}_{k,1} = \frac{1}{k} \mathbf{A}_k(y), \\ \mathbf{U}_{k,j} = \frac{1}{k} \left[\mathbf{A}_0 \mathbf{U}_{k,j-1}(y) - \mathbf{U}_{k,j-1} \mathbf{A}_0 + \sum_{\ell=1}^{k-1} \mathbf{A}_{k-\ell}(y) \mathbf{U}_{\ell,j-1} \right]. \end{cases} \quad (3.47)$$

This can be solved order by order simultaneously in both ε and ϵ . Its solution is a formal double sum expression for the gauge transformation U [126]

$$\mathbf{U}(y, \epsilon; \varepsilon) = \mathbb{1} + \sum_{k \geq 1} \sum_{j \geq 1} \epsilon^k \varepsilon^j \mathbf{U}_{k,j}(y). \quad (3.48)$$

Given a canonical basis of master integrals, \mathbf{A}_ϵ is obtained explicitly by plugging the basis into the first equation of (3.41). Using the result, we plug (3.47) and (3.48) and via (3.43), \mathbf{A}_0 can be obtained. Because $\mathbf{A}_0 \neq \mathbf{A}_0(\epsilon)$, we have

$$\left[\mathbf{A}_0, \int \mathbf{A}_0 d \log(\epsilon) \right] = 0, \quad (3.49)$$

and the solution of the ϵ -differential equation is of the form $\epsilon^{\varepsilon \mathbf{A}_0} \mathbf{c}$. This gives enough information to solve this part of the system in the MRK

$$\begin{cases} \partial_\epsilon \mathbf{M}'(y, \epsilon; \varepsilon) = \varepsilon \frac{\mathbf{A}_0}{\epsilon} \mathbf{M}'(y, \epsilon; \varepsilon) + \mathcal{O}(\epsilon^0), \\ \partial_y \mathbf{M}'(y, \epsilon; \varepsilon) = \varepsilon \mathbf{A}'_y(y, \epsilon) \mathbf{M}'(y, \epsilon; \varepsilon), \end{cases} \quad (3.50)$$

where $\mathbf{M}' = \mathbf{U} \mathbf{M}$. To solve the system (3.50), we integrate it along the piecewise path

$$(\epsilon = 0, y = y_0) \xrightarrow{\text{(I)}} (\epsilon = 0, y) \xrightarrow{\text{(II)}} (\epsilon, y), \quad (3.51)$$

for some y_0 lying in the s_{12} -channel. In other words, what we first do is to restore the y -dependence and then the ϵ one. Hence, the integration along path (I) is given by

$$\mathbf{M}'(y, \epsilon = 0; \varepsilon) = \mathbb{P} \exp \left(\varepsilon \int_{\gamma(\text{I})} \mathbf{A}'_y(y', \epsilon = 0) dy' \right) \mathbf{M}'(y = y_0, \epsilon = 0; \varepsilon), \quad (3.52)$$

and integrating further along path (II), with initial condition given by (3.52), yields

$$\mathbf{M}'(y, \epsilon; \epsilon) = \epsilon^{\epsilon \mathbf{A}_0} \mathbf{M}'(y, \epsilon = 0; \epsilon) = \epsilon^{\epsilon \mathbf{A}_0} \mathbb{P} \exp \left(\epsilon \int_{\gamma(\text{II})} \mathbf{A}'_y(y', \epsilon = 0) dy' \right) \mathbf{M}'(y = y_0, \epsilon = 0; \epsilon), \quad (3.53)$$

where $\mathbf{M}'(y = y_0, \epsilon = 0; \epsilon)$ is the boundary constant of

$$\partial_y \mathbf{M}'(y, \epsilon = 0; \epsilon) = \epsilon \mathbf{A}'_y(y, \epsilon = 0) \mathbf{M}'(y = y_0, \epsilon = 0; \epsilon), \quad (3.54)$$

and where $\mathbf{A}'_y(y, \epsilon = 0) = \mathbf{A}_y(y, \epsilon = 0)$, from (3.44). We can, finally, go back to the original basis and get

$$\mathbf{M}(y, \epsilon; \epsilon) = \mathbf{U}(y, \epsilon; \epsilon) \epsilon^{\epsilon \mathbf{A}_0} \mathbb{P} \exp \left(\epsilon \int_{\gamma(y_0 \rightarrow y)} \mathbf{A}_y(y', \epsilon = 0) dy' \right) \mathbf{M}(y = y_0, \epsilon = 0; \epsilon). \quad (3.55)$$

Intuitively, we can see the solution as an “initial condition transporter” from $y_0 \rightarrow y$. The latter expression contains divergent logarithms of ϵ , generated by the matrix exponential $\epsilon^{\epsilon \mathbf{A}_0}$. The transformation matrix $\mathbf{U}(y, \epsilon; \epsilon)$ is responsible for power correction in ϵ according to (3.48), as we tried to exemplify in Section 2.3.3 to get to (2.133).

In this thesis, the initial condition was chosen to be in the s_{12} -channel near $(2||3)$ within a dominant MRK background. It is derived following the outline of Section 2.3.2. Indeed, dropping $\log(s)$, $\log(s_1)$ and $\log(s_2)$ from the connection, the initial condition is fixed by requiring the answer is finite after we take the MRK limit, followed by the $(z, \bar{z}) \rightarrow (0, 0)$ limits.

3.4 A Numerical Method for Crosschecks

IN THIS SECTION, we describe a method we used to systematically avoid integrating harder than HPL’s Goncharov polylogarithms [136]. See also [24, 142]. For us, it permits crosschecking numerically our analytic evaluation of the master integrals, based on a method discussed in the last section.

We start with the differential equation in its canonical form along a univariate path (see (2.120)). We only consider paths that are straight lines. This is achieved by making the

letters time dependant by setting

$$W_i(t) := W_{i,\text{initial}} + t(W_{i,\text{final}} - W_{i,\text{initial}}), \quad (3.56)$$

for $t \in [0, 1]$, where the $W_i(0) = W_{i,\text{initial}}$'s are assumed to be known and $W_i(1) = W_{i,\text{final}}$ are the letters evaluated where we wish to transport our initial condition. The *only* active parameter is t . Consequently, the relevant connection is simply

$$\dot{\Omega}(t) = \sum_k \mathbf{C}_k \frac{d}{dt} \log(W_k(t)). \quad (3.57)$$

The iterative solution is still given in (2.123). In general, the form of the symbol alphabet can make it a daunting task to compute everything only in terms of HPLs and polylogarithms. Furthermore, it can also be complicated to accurately handle both spurious and physical branch points. As we saw in the section on the multi-Regge kinematics, a step that is seen to help in both of these problems is to rationalize the alphabet by using appropriate parameterizations. Another trick that helps is to consider locally valid solutions written in terms of power series

$$\mathbf{M}^{(i)}(t) = \sum_{k=0}^{N_e-1} \chi_k(t) \mathbf{M}_k^{(i)}(t), \quad (3.58)$$

where, again, $t \in [0, 1]$, N_e is the number of segments $S_k = [t_k - r_k, t_k + r_k)$, with center t_k and radius r_k , with which we cover $[0, 1]$ and

$$\chi_k(t) = \begin{cases} 1 & t \in S_k, \\ 0 & \text{otherwise.} \end{cases} \quad (3.59)$$

The solution $\mathbf{M}_k^{(i)}$ is valid in S_k . Indeed, since such solution can easily be constructed from series expansions of the integrand in (2.123), the series have finite radii of convergence and so the solutions are valid only locally. Note, also, that the weight- i final solution is given by $\mathbf{M}^{(i)}(1) = \mathbf{M}_{N_e-1}^{(i)}(1)$, while the initial one is given by our initial condition – i.e., $\mathbf{M}^{(i)}(0) = \mathbf{M}_0^{(i)}(0)$.

There are two things we now need to understand how to do. Firstly, how to construct local solutions? Secondly, how to perform the segmentation? To address the former question, we first note that the matrix $\dot{\Omega}(t)$ determines the form of the series expansion of the integrand.

As our alphabet contains both simple poles and square root branch cuts, the series expansion around t_k takes the form

$$\dot{\Omega}(t)\Big|_{t \rightarrow t_k} = \sum_{j=-2}^{\infty} \omega_{j,k} (t - t_k)^{j/2}, \quad (3.60)$$

where $\omega_{j,k}$ are constant matrices. The latter expression just means the series solution takes the form of half-integer power series with logarithmic singularity structure

$$\mathbf{M}_k^{(i)}(t) = \bar{c}_k^{(i)} + \sum_{j=-2}^{\infty} \omega_{j,k} \int dt (t - t_k)^{j/2} \mathbf{M}_k^{(i-1)}(t). \quad (3.61)$$

At $k = 0$, the local solution $\mathbf{M}_0^{(i)}(t)$ matches the known boundary condition at $t = 0$ – i.e., $\mathbf{M}_0^{(i)}(0) = \mathbf{M}^{(i)}(0)$. The remaining integration constants are then iteratively determined exploiting the continuity of the full solution, (3.58), at the boundary of each segment

$$\mathbf{M}_k^{(i)}(t_k - r_k) = \mathbf{M}_{k-1}^{(i)}(t_{k-1} + r_{k-1}), \quad \forall k \in \{1, 2, \dots, N_e - 1\}, \quad (3.62)$$

which exists by construction. In this way, the integration constants in each local solution can be determined from $\mathbf{M}^{(i)}(0)$.

To make the solution (3.61) practical, we usually truncate the infinite series. This must, however, be done with care for the numerical error to remain under our control. Consequently, we choose to work with the constraint that segments should never be larger than half the radius of convergence of the associated solution. We emphasize that the segmentation will be the same for all weight- i .

To address the latter question, we choose segments $S_k^0 := [t_k - r_k, t_k + r_k)$ such that

$$[0, 1] \subset \bigcup_{k=0}^{N_e-1} S_k^0. \quad (3.63)$$

The choice of (t_k, r_k) is primarily dictated by the set of singular points of the differential equation (2.120), call it \mathcal{S} . These are the singularities of the $\log(W_i)$'s. These singularities can either be real or complex. If $x \in \mathcal{S}$ is complex, we can avoid complex arithmetic by considering $\{\text{Re}(s) - \text{Im}(s), \text{Re}(s), \text{Re}(s) + \text{Im}(s)\}$ for each such singularities. Given our constraint of only using series solutions in half of their radius of convergence, it is sufficient to consider points in $t_k \in \mathcal{S}$ such that $t_k \in (-2, 3)$.

Therefore, to each t_k , we associate a radius r_k , chosen to be half the distance between t_k and the closest point in $\bar{\mathcal{S}} = \mathcal{S} \cup \{-2\} \cup \{3\}$. If this procedure is not covering $[0, 1]$, we add segments centered at regular points in the middle of the uncovered intervals lying in $(-2, 3)$ that overlaps with $[0, 1]$. For example, the m^{th} such regular point, say between S_k^0 and S_{k+1}^0 for some k , is given by

$$t_{m,\text{regular}}^1 = \frac{\partial_{\text{right}} S_k^0 + \partial_{\text{left}} S_{k+1}^0}{2}. \quad (3.64)$$

When $S_{k+1}^0 = \emptyset$, we replace $\partial_{\text{left}} S_{k+1}^0$ by 3. The associated radii are chosen to be

$$r_{m,\text{regular}}^1 = \min_{s \in \bar{\mathcal{S}}} \left\{ \left| \frac{t_{m,\text{regular}}^1 - s}{2} \right| \right\}. \quad (3.65)$$

If, again, this additional step is not covering $[0, 1]$, the procedure continues algorithmically until it does. At the n^{th} step, the m^{th} regular center is given by

$$t_{m,\text{regular}}^n = \frac{\partial_{\text{right}} S_k^i + \partial_{\text{left}} S_\ell^j}{2}, \quad (3.66)$$

where $0 \leq i, j \leq n-1$ and $(\partial_{\text{right}} S_k^i, \partial_{\text{left}} S_\ell^j)$ is any yet uncovered subinterval of $[0, 1]$, defined from previously generated segments. The corresponding radius is given by

$$r_{m,\text{regular}}^n = \min_{1 \leq i \leq n-1, 1 \leq k_i \leq N_e(i), s \in \bar{\mathcal{S}}} \left\{ \left| t_{m,\text{regular}}^n - \partial_{\text{right}} S_{k_i}^i \right|, \left| t_{m,\text{regular}}^n - \partial_{\text{left}} S_{k_i}^i \right|, \left| \frac{t_{m,\text{regular}}^n - s}{2} \right| \right\}, \quad (3.67)$$

where $N_e(i)$ is the number of segments obtained from step i . We note that if \mathcal{S} does not contain any point $t_k \in (-2, 3)$, there is a single regular expansion point at $t_0 = 1/2$. Finally, we note that the segmentation procedure we described may have produced segments with no overlap with $[0, 1]$, which we simply remove.

We finally note that the choice of the constraint on the radius of convergence can be made either weaker or stronger. The price to pay is, respectively, to slow down the convergence (which is usually unwanted) or to deal with a bigger number of segments (which slows down the algorithm).

Chapter 4

Original Contributions

COMPUTING THE SCATTERING AMPLITUDES for massless 5-point 2-loop processes requires the analytic expressions for the integral topologies presented in Fig. 3.2 in all of the $5!$ permutations. This means one has to evaluate at least $5! \times (108 + 73 + 61 + 28) = 32400$ master integrals prior computing an amplitude. Using differential equations, there are two obvious ways to proceed. The first one being to work simultaneously with all the $5!$ permutations of each topology and consider a set of differential equations for each of them and solve them directly in physical region. This was the approach used by Chicherin and Sotnikov in [143]. The other option is to evaluate the master integrals in one ordering and obtain the others by permuting legs. Our goal is to explore the latter option and, more explicitly, to find the integration constants of such permutations using multiple scaling limits, each corresponding to a path in the kinematic space relating two different limiting kinematic configurations. An important constraint in the choice of scaling limits is that paths they describe in the kinematic space are generated *only* by HPLs. This constraint ensures that using scaling limits makes the *analytic* evaluation of the solutions fast and simple. Our method is, therefore, the suitable one to use to prove analytically the existence of a “web of computational highways” in the kinematic space relating *all* evaluated master integrals contributing, ultimately, to full NNLO 5-parton scattering amplitudes correction at high energies.

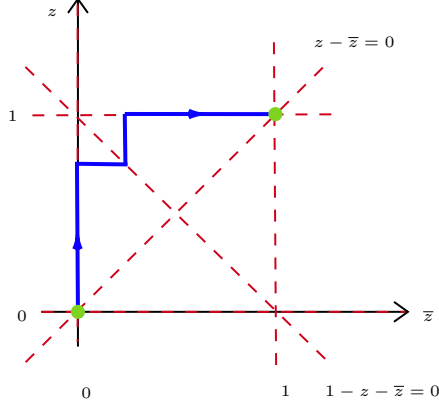


Figure 4.1: Blowing up the path connecting $(0,0)$ and $(1,1)$ with a small corner around $(1,0)$.

4.1 θ -parameterization: A Bridge Between Limits

AS MENTIONED ABOVE, the way we will move between different sectors of the kinematic space using differential equations is by using various scaling limits. Each limit is parametrized in a certain way and induce, via the connection, branch cuts, or boundaries, in the kinematic space. When several of such boundaries intersect, it is important to clarify how the singular boundary is approached. In mathematical language, one can perform a *blowup* that resolves singular intersections of boundaries. For example, in the MRK limit, $1 - z, \bar{z}$ and $1 - z - \bar{z}$ intersect at $(z, \bar{z}) = (1, 0)$; thus one has to specify how exactly this point is approached. The problem of a potential ambiguity can be avoided by switching to appropriate variables that resolve the way the singularity is approached. The variable transformations can also be understood as choosing more sophisticated paths near the origin to connect the boundary values. An example is illustrated in Fig. 4.1.

That said, the MRK and the collinear parameterizations, as discussed in the previous sections, by construction describe *different* kinematic sectors within the s_{12} -channel. At leading order in both ϵ_{MRK} and ϵ_c , we easily see that the regions of validity of neither parameterization overlap clearly in the kinematic space (see Fig. 4.2). The way out of this problem is to use an intermediate and more flexible parameterization that will allow the transport of points in the MRK asymptotic to points in the collinear one (see Fig. 4.3).

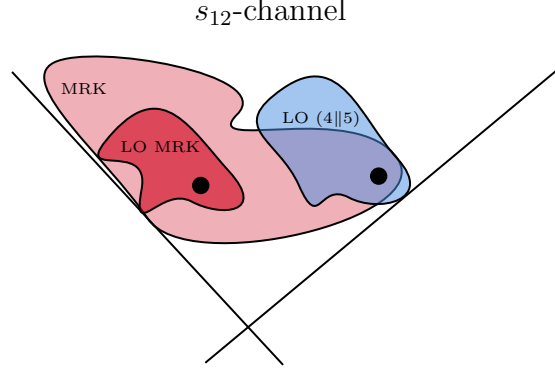


Figure 4.2: At leading order, the MRK and $(4||5)$ parameterizations won't overlap. Without leading order truncation, the MRK alphabet is not practical for computation and cannot be used to transport points (black dots) from truncated MRK to truncated collinear regions.

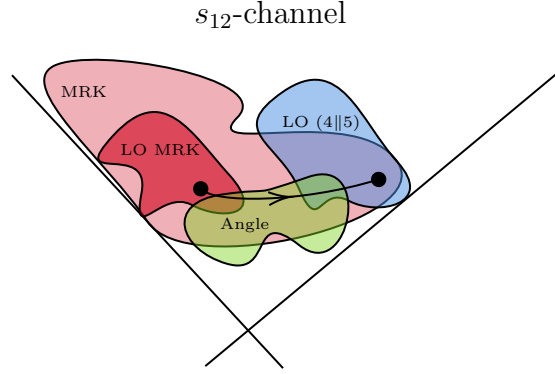


Figure 4.3: Connecting asymptotics.

In the case where we want to control the approach of $(4||5)$ starting from a configuration in the multi-Regge asymptotic, we propose the following spinor parameterization

$$\lambda_4 = \sqrt{\sqrt{2}(p_5^- + p_4^-)} \zeta(\theta_4, 1)^\top \quad \text{and} \quad \lambda_5 = \sqrt{\sqrt{2}(p_5^- + p_4^-)} (1 - \zeta)(\theta_5, 1)^\top. \quad (4.1)$$

where $\zeta := p_4^- / (p_5^- + p_4^-)$ is the collinear momentum fraction. It is easy to see that the corresponding bispinors are

$$p_4 = p_4^- \begin{pmatrix} \theta_4 \tilde{\theta}_4 & \theta_4 \\ \tilde{\theta}_4 & 1 \end{pmatrix} \quad \text{and} \quad p_5 = p_5^- \begin{pmatrix} \theta_5 \tilde{\theta}_5 & \theta_5 \\ \tilde{\theta}_5 & 1 \end{pmatrix}. \quad (4.2)$$

In these variables, our 5 independent 2-particle invariants are given by

$$s_{12} = \frac{(\theta_4 \tilde{\theta}_4 p_4^- + \theta_5 \tilde{\theta}_5 p_5^- + p_3^+) \left(\theta_4 \tilde{\theta}_4 (p_4^-)^2 + p_4^- (\theta_4 \tilde{\theta}_5 p_5^- + \tilde{\theta}_4 \theta_5 p_5^- + p_3^+) + p_5^- (\theta_5 \tilde{\theta}_5 p_5^- + p_3^+) \right)}{p_3^+},$$

$$\begin{aligned}
s_{23} &= -\frac{(\theta_4 p_4^- + \theta_5 p_5^-)(\tilde{\theta}_4 p_4^- + \tilde{\theta}_5 p_5^-)(\theta_4 \tilde{\theta}_4 p_4^- + \theta_5 \tilde{\theta}_5 p_5^- + p_3^+)}{p_3^+}, \\
s_{34} &= \frac{p_4^-(\theta_4 \tilde{\theta}_4 p_4^- + \tilde{\theta}_4 \theta_5 p_5^- + p_3^+)(\theta_4 \tilde{\theta}_4 p_4^- + \theta_4 \tilde{\theta}_5 p_5^- + p_3^+)}{p_3^+}, \\
s_{45} &= p_4^- p_5^- (\theta_4 - \theta_5)(\tilde{\theta}_4 - \tilde{\theta}_5), \\
s_{15} &= -\frac{\theta_5 \tilde{\theta}_5 p_5^- \left(\theta_4 \tilde{\theta}_4 (p_4^-)^2 + p_4^- (\theta_4 \tilde{\theta}_5 p_5^- + \tilde{\theta}_4 \theta_5 p_5^- + p_3^+) + p_5^- (\theta_5 \tilde{\theta}_5 p_5^- + p_3^+) \right)}{p_3^+}.
\end{aligned}$$

Note that there are five parameters, but two of them, namely the angles, are complex.

4.2 Moving Between Regions: An Example

OUR GOAL BEING to find the analytic constants between *all* the permuted diagrams, we start with a vector of constants determined for specific kinematic setting and from it, we recover its permuted version by moving along paths generated by multiple scaling limits of the letters in the DEs. These limits are our kinematics limits. The only constraints on the choices of scaling limits is that each paths they describe leads to HPLs. Using such limits makes the analytic evaluation of the solutions fast. By construction, it also induces a “network” of “computational highways” between *all* the integrals (ultimately) contributing to the whole scattering amplitudes.

In this section, we sketch how to, given an initial configuration, we can permute two *timelike separated* gluons for the double pentagon (DP) topology. Without loss of generality, we will exchange gluons 4 and 5. As mentioned earlier, we take our initial condition near $(2||3)$ in dominant MRK background – i.e., $\varepsilon_{\text{MRK}} \ll z \ll 1$. This corresponds to the left Feynman diagram in Fig. 4.4. Then we consider angle-parameterizations for 4 and 5 spinors given in (4.1). The idea is to use various scaling limits within a MRK background to approach the $(4||5)$ (see the right diagram in Fig. 4.4) limit with HPLs (see the bottom diagram in Fig. 4.4).

The procedure we are about to describe is schematically represented in Fig. 4.5 and the endpoints ordering of the first row are summarized in Fig. 4.6. In terms of the spinor

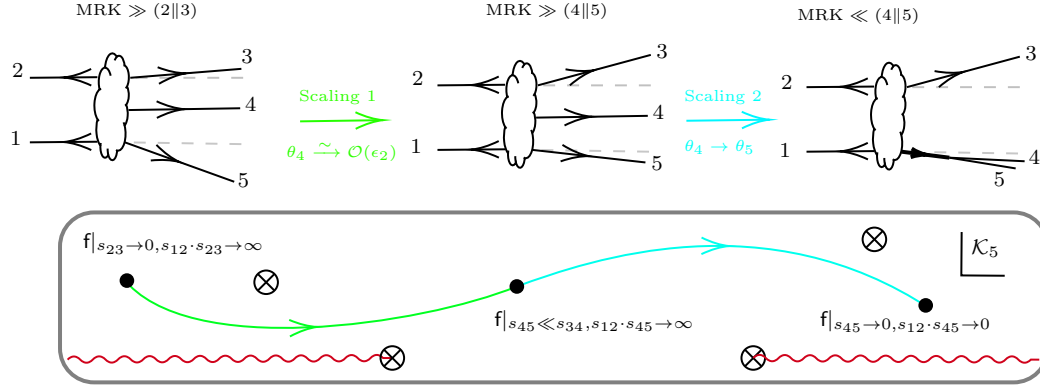


Figure 4.4: $(4||5)$ approach within a MRK background.

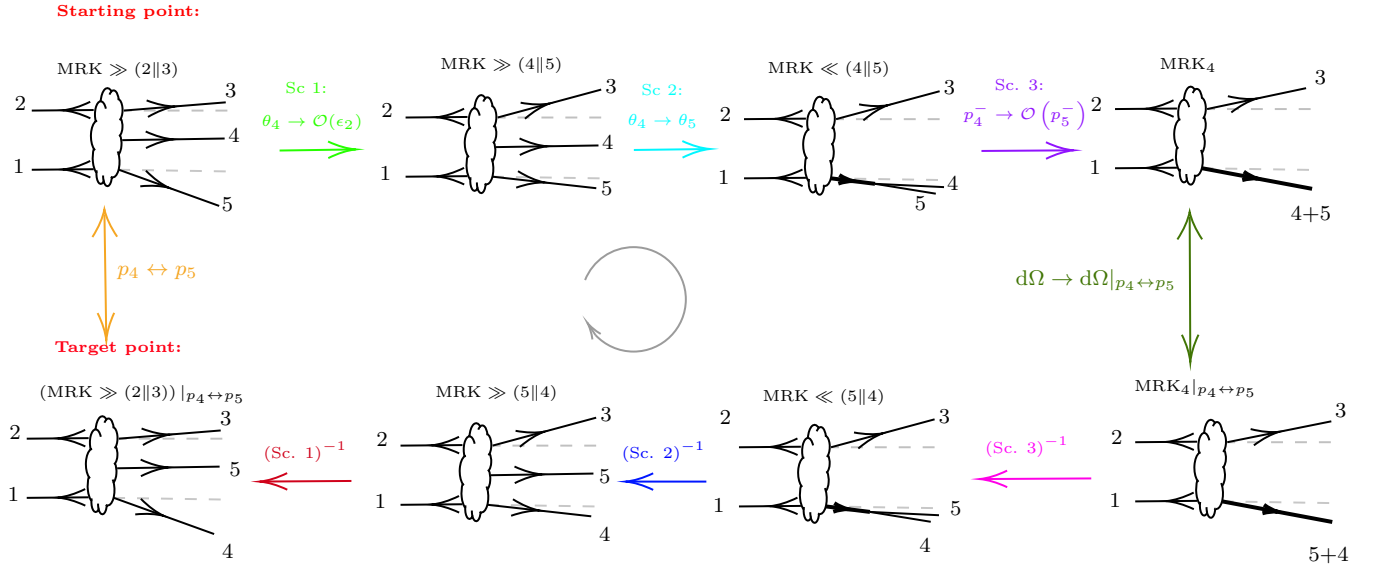


Figure 4.5: The schematic web of HPLs to follow in order to permute 4 and 5 analytically.

$$\begin{cases} |p_5^-| \sim |p_3^+| \sim \mathcal{O}(\epsilon_0^{-1}), \\ |\theta_4| \sim |p_4^-| \sim \mathcal{O}(1), \\ |\theta_5| \sim \mathcal{O}(\epsilon_0), \\ \epsilon_0 \ll 1, \\ p_4^- \theta_4 \rightarrow -p_5^- \theta_5 \text{ (or } z \rightarrow 0). \end{cases} \xrightarrow{\text{Sc. 1}} \begin{cases} |p_5^-| \sim |p_3^+| \sim \mathcal{O}(\epsilon_0^{-1}), \\ |p_4^-| \sim \mathcal{O}(1), \\ |\theta_4| \sim \mathcal{O}(\epsilon_2), \\ |\theta_5| \sim \mathcal{O}(\epsilon_0), \\ \epsilon_0 \ll \epsilon_2 \ll 1. \end{cases} \xrightarrow{\text{Sc. 2}} \begin{cases} |p_5^-| \sim |p_3^+| \sim \mathcal{O}(\epsilon_0^{-1}), \\ |p_4^-| \sim \mathcal{O}(1), \\ \theta_4 = \theta_5 + \mathcal{O}(\epsilon_3), \\ \epsilon_3 \ll \epsilon_0 \ll 1. \end{cases} \xrightarrow{\text{Sc. 3}} \begin{cases} |p_4^-| \sim |p_5^-| \sim |p_3^+| \sim \mathcal{O}(\epsilon_0^{-1}), \\ \theta_4 = \theta_5 + \mathcal{O}(\epsilon_3), \\ \epsilon_3 \ll \epsilon_0 \ll 1. \end{cases}$$

Figure 4.6: Scale orderings for the first row of Fig. 4.5.

parameters, we initially have the following orderings

$$\begin{cases} |p_5^-| \sim |p_3^+| \sim \mathcal{O}(\epsilon_0^{-1}), \\ |\theta_4| \sim |p_4^-| \sim \mathcal{O}(1), \\ |\theta_5| \sim \mathcal{O}(\epsilon_0), \end{cases} \quad (4.3)$$

with $p_4^- \theta_4 \rightarrow -p_5^- \theta_5$ (or $\mathbf{p}_4^\perp \rightarrow -\mathbf{p}_5^\perp$), as $z \rightarrow \epsilon_1$, with $\epsilon_0 \ll \epsilon_1 \ll 1$. We want to approach (4||5) from this initial kinematic setting. While fixing p_4^-, p_5^- and θ_5 , we approach (4||5) using the following map

$$\theta_4(t_1) := -\frac{(1-t_1)p_5^- \theta_5}{p_4^-} + \epsilon_1 \theta_4, \quad 0 \leq t_1 \leq 1, \quad (4.4)$$

where $\theta_4 := \theta_4(t_1 = 0)$ and where it is understood that $\epsilon_0 \ll \epsilon_1 \ll 1$. We then do similarly for $\tilde{\theta}_4$. These maps yield HPLs only, as the symbols arguments lie in $\{t_1, 1-t_1\}$. At $t_1 = 1$, where $(z, \bar{z}) \rightarrow (\epsilon_1^{-1}, \epsilon_1^{-1})$, our orderings become

$$\begin{cases} |p_5^-| \sim |p_3^+| \sim \mathcal{O}(\epsilon_0^{-1}), \\ |p_4^-| \sim \mathcal{O}(1), \\ |\theta_4| \sim \mathcal{O}(\epsilon_1), \\ |\theta_5| \sim \mathcal{O}(\epsilon_0), \end{cases} \quad (4.5)$$

describing a dominant MRK background with a subleading (4||5) one. Next, to make (4||5) dominant, we need to send $\theta_4 \rightarrow \theta_5 + \epsilon_2$, where $\epsilon_2 \ll \epsilon_0 \ll \epsilon_1 \ll 1$. To do this, we need a “blow up” that enables ones to put θ_4 and θ_5 on comparable footing (order)

$$\omega = \theta_4/\theta_5. \quad (4.6)$$

This has to be done in a similar fashion for $\tilde{\omega} = \tilde{\theta}_4/\tilde{\theta}_5$. The resulting LO alphabet letters reducing to

$$\mathcal{A}_{\theta_4 \rightarrow \theta_5} = \{\epsilon_0\} \cup \{p_5^-, p_3^+, p_4^-\} \cup \{\omega, \tilde{\omega}, 1-\omega, 1-\tilde{\omega}, 1-\omega-\tilde{\omega}, \omega-\tilde{\omega}\}. \quad (4.7)$$

Note the resemblance with the initial MRK alphabet in (3.30). The blowup steps are performed by taking ω and $\tilde{\omega}$ from ∞ to 1. In practice, for example, this is done by the following

change of variable

$$\theta_4 \rightarrow \frac{\theta_5}{t_2 + \Lambda}, \quad 0 \leq t_2 \leq 1, \quad \Lambda \rightarrow 0^+. \quad (4.8)$$

Once we integrated up to $t_2, \tilde{t}_2 = 1$, orderings are

$$\begin{cases} |p_5^-| \sim |p_3^+| \sim \mathcal{O}(\epsilon_0^{-1}), \\ |p_4^-| \sim \mathcal{O}(1), \\ |\theta_5| \sim \mathcal{O}(\epsilon_0), \\ \theta_4 = \theta_5 + \mathcal{O}(\epsilon_3), \end{cases} \quad (4.9)$$

where it is understood that $\epsilon_3 \ll \epsilon_0 \ll 1$. The last step, once we are at $t_2, \tilde{t}_2 \rightarrow 1$, is to put p_4 and p_5 on comparable footing to permute them safely. That is, we want to achieve the following orderings

$$\begin{cases} |p_4^-| \sim |p_5^-| \sim |p_3^+| \sim \mathcal{O}(\epsilon_0^{-1}), \\ \theta_4 = \theta_5 + \mathcal{O}(\epsilon_3), \\ \epsilon_3 \ll \epsilon_0 \ll 1. \end{cases} \quad (4.10)$$

Again, this is achieved by blowing up the momenta ratio

$$R = p_4^- / p_5^-, \quad (4.11)$$

from 0 to 1. More generically, we checked that when $R \sim \mathcal{O}(1)$, even at LO, permuting the 4 and 5 labels locally in our parameters – i.e., $p_4^- \leftrightarrow p_5^-$ – reproduces the action of $\sigma_{45} \in \mathcal{S}_5$ on the W_i in *any* kinematic. This shows our end point is an appropriate one to flip gluon 4 and 5. The remaining steps amounts of performing backward the steps we just described, but with the 4 and 5 labels changed. At the end of the day, one gets the integration constants for the diagram corresponding to our initial one, but with gluon 4 and 5 permuted. In particular, the input and output of the calculation being vectors of length 108, we found it sufficient to only stress that the constants appearing as master integrals' vector entries for both unpermuted and permuted diagram lie in the same set of transcendental numbers, graded by their weights (from 0 to 4) – i.e.,

$$\{\mathbf{M}_{1 \leq i \leq 108}^{(\text{DP:12345})}, \mathbf{M}_{1 \leq i \leq 108}^{(\text{DP:12354})}\} \subset \mathbb{Q} \cup i\pi\mathbb{Q} \cup \pi^2\mathbb{Q} \cup \{i\pi^3\mathbb{Q}, \zeta_3\mathbb{Q}\} \cup \{\pi^4\mathbb{Q}, i\pi\zeta_3\mathbb{Q}\}. \quad (4.12)$$

4.3 Permuting Spacelike Separated Gluons: A Word on Analytic Continuation

IN THE LAST SECTION, we discussed how two timelike separated gluons can be flipped by tracing out an appropriate path in the kinematic space \mathcal{K}_5 . We still have to discuss how flipping spacelike separated can happen. By definition, in doing so, some of the multiple particle invariants will change signs. The first step to achieve this is to add a small imaginary part to the relevant Mandelstams – i.e.,

$$s_{ij} \rightarrow s_{ij} + i0. \quad (4.13)$$

Once this is done, they can be analytically continued into the complex plane. The goal is then to trace out the appropriate paths in the complexified kinematic space that reproduce correctly these sign changes, while being careful we are not crossing any branch cut along the way. In our case, we are only dealing with massless particles, which implies that all branch cuts start at the origins in $s_{i,i+1}$ and $s_{i,i+1,i+2}$ [144].

A minimal requirement indicating we are doing the analytic continuation correctly, is to enforce phase prescriptions on paths endpoints. These prescriptions are easily fixed for any multi-particle invariants within the multi-Regge kinematics. To see this, we invoke the dual (region) variables defined in C, where their underlying geometric interpretation is described. For a $2 \rightarrow (N - 2)$ scattering process, we have, in these variables,

$$s_{i+1,\dots,j} := (p_{i+1} + \dots + p_j)^2 = y_{ij}^2, \quad (4.14)$$

where $y_{ij} = y_i - y_j$ and $1 \leq i, j \leq N$. When the limit where $(p_i || p_{i+1})$ is approached, we see that the region variables “collide” – i.e., $y_{i-1} \rightarrow y_{i+1}$. Given the strong rapidity orderings of the MRK, gluons 1 and N are nearly collinear. Because they are spacelike separated in the initial leg ordering, the region variables can only collide in the transverse space – i.e., $y_1^\perp \xrightarrow{\sim} y_{N-1}^\perp$. We note that momentum conservation allows one to shift

$$\mathbf{p}_i^\perp \rightarrow \mathbf{p}_i^\perp = \mathbf{y}_{i-1}^\perp - \mathbf{y}_{i-2}^\perp, \quad (4.15)$$

for $3 \leq i \leq N$, as

$$\sum_{i=3}^N \mathbf{p}_i^\perp = -\mathbf{y}_1^\perp + \mathbf{y}_{N-1}^\perp, \quad (4.16)$$

goes to zero to arbitrary precision. The non-trivial dynamics will then take place in the transverse space with respect to the two high-energy incoming particles described by the shifted \perp -region variables (4.15) of the $N - 2$ produced particles. The space of kinematic configurations in the two-dimensional transverse space of a scattering of N particles in MRK is captured by the moduli space $\mathfrak{M}_{0,N-2}$ of Riemann spheres with $N - 2$ marked points – e.g., see [140].

Let's now see how the signs of multi-particle invariants relate. Without loss of generality, we suppose gluons 1 and 2 are incoming with positive energy and the signs of the energies of the remaining gluons are not fixed. A particular physical region is therefore defined by specifying $\text{sign}(p_i^0)$, for $3 \leq i \leq N$. This initial information about 2-particle invariants is telling which pairs of gluons are timelike and spacelike separated. Moreover, recalling

$$s_{ij} = p_i^0 p_j^0 (1 - \cos(\theta_{ij})), \quad (4.17)$$

and so $\text{sign}(s_{ij}) = \text{sign}(p_i^0) \text{sign}(p_j^0)$ for massless particles, we see that each 2-particle invariant has a *unique* sign in a given physical region. What about multi-particle invariants? To answer this question, we first note that, in the MRK, where $s_{ij} \simeq p_i^+ p_j^-$ for $3 \leq i < j \leq N$, the strong ordering in rapidities makes $s_{i,i+1}$ more relevant than $s_{i,i+j}$, for any $j > 1$ – i.e., all invariants made of k consecutive final state momenta will be comparable in size

$$s_{i,i+1,\dots,i+k} \simeq s_{i,i+k}, \quad (4.18)$$

and much larger than invariants made of $(k - 1)$ consecutive momenta. It therefore follows that

$$y_{ij}^2 \prod_{\ell=i+2}^{j-1} |\mathbf{p}_\ell^\perp|^2 = s_{i+1,\dots,j} \prod_{\ell=i+2}^{j-1} |\mathbf{p}_\ell^\perp|^2 \simeq \prod_{k=i+1}^{j-1} s_{k,k+1}, \quad 2 \leq i < j \leq N. \quad (4.19)$$

Using (4.19) and the fact that $|\mathbf{p}_\ell^\perp|^2 > 0$, we deduce that the sign of any multi-particle invariant in the MRK is *also* fixed by the energy signs of the external momenta

$$\text{sign}(s_{i+1,\dots,j}) = \text{sign}(p_{i+1}^0) \text{sign}(p_j^0). \quad (4.20)$$

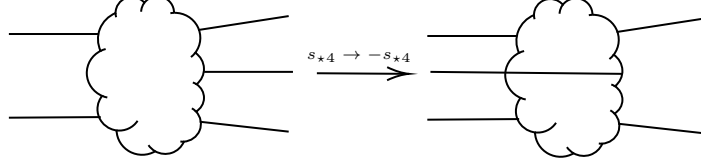


Figure 4.7: Putting gluon 4 into the past.

The analytic continuation follows from $s_{i+1,\dots,j} \rightarrow s_{i+1,\dots,j} + i0$, or equivalently by making $s_{i+1,\dots,j}$ multi-valued – i.e., the rule any future/past-mixing kinematic path must reproduce is the following

$$s_{i+1,\dots,j} = |s_{i+1,\dots,j}| \exp(-i\pi\phi_{ij}), \quad (4.21)$$

where

$$\phi_{ij} := \begin{cases} 1 & \text{if } s_{i+1,\dots,j} > 0, \\ 0 & \text{if } s_{i+1,\dots,j} < 0. \end{cases} \quad (4.22)$$

Let's now sketch how we can use the above to define appropriate paths to follow to flip spacelike separated gluons. Here, we illustrate how to put gluon 4 into the past (see Fig. ??). All the 2-particle invariants containing $\{4\}$ are linked by a constraint

$$s_{14} + s_{24} + s_{34} + s_{45} = 0, \quad (4.23)$$

reducing the number of independent 4-variables to three. This suggests a good choice for our five independent variable is s_{14}, s_{34} and s_{45} in the background defined by s_{12} and s_{23} . Initially, $s_{12}, s_{34}, s_{45} \geq 0$ and $s_{23}, s_{14} \leq 0$. Once gluon 4 is put in the past, s_{34}, s_{45} and s_{14} change signs. Our goal is to parameterize a set of paths reproducing these signs changes. The difficulty is that, since s_{34}, s_{45} and s_{14} are related by (4.23), transporting a variable in the kinematic space will change the positions of the others; if no extra care is given, branch cuts could be crossed resulting in wrong spurious constants in the final answer. To decouple some of the 2-invariant, we can use kinematic limits. For example, in an effective 4-soft dominating MRK background, once both $(1||4)$ - and $(4||5)$ -limits are approached ($|s_{14}| \sim |s_{45}| \ll |s_{34}| \sim |s_{24}| \ll |s_{23}| \sim \mathcal{O}(1) \ll |s_{12}|$) we can check that the only coupled letter in

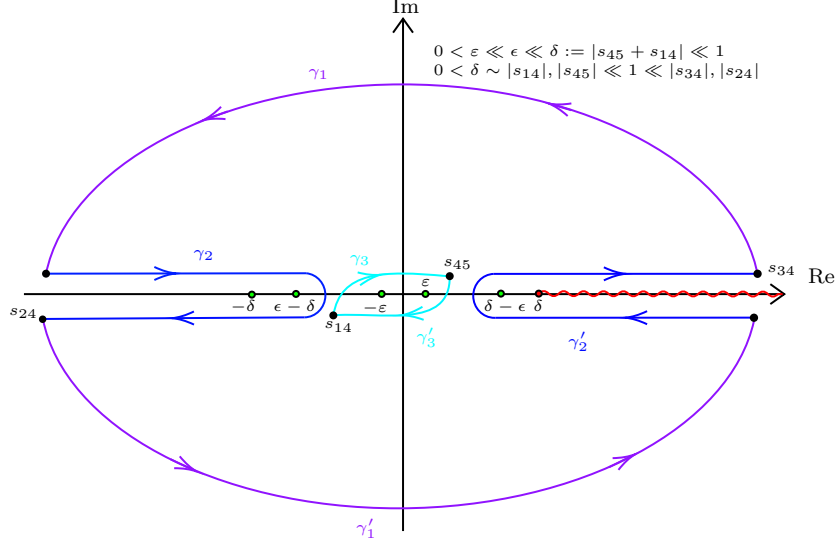


Figure 4.8: Complex section of \mathcal{K}_5 along the $s_{14} + s_{24} + s_{34} + s_{45} = 0$ hyperplane, in the limit where $s_{14}, s_{45} \rightarrow 0$ in a controlled manner. We sketch the (minimal) paths needed for the flipping.

the symbols is $s_{14} + s_{45} \leq 0$. It is negative due to the strong ordering in rapidities, while its norm, $\delta := |s_{14} + s_{45}|$, must be small compared to s_{12} by the effective softness of gluon 4.

Now, a sketch of the paths to follow for the flipping is given in Fig. 4.8. In the first step, we integrate s_{34} and s_{24} along large radius circles γ_1 and γ_1' , while keeping s_{14} and s_{45} fixed. In the second step, s_{34} and s_{24} are taken, by following γ_2 and γ_2' , from the upper-half-plane (UHP) and the lower-half-plane (LHP) to the LHP and the UHP, respectively, while s_{14} and s_{45} are still kept fixed. Finally, we follow γ_3 and γ_3' to change the sign of the remaining small invariants. The target configuration is therefore $s_{12}, s_{14} \geq 0$ and $s_{23}, s_{34}, s_{45} \leq 0$, as predicted by (4.21).

We close this section by noting that once we know how to flip a pair of spacelike and a pair of timelike separated adjacent gluons, we can, in principle, find any other permutation by composition. This reflects the fact that \mathcal{S}_5 is 2-generated. There are therefore many ways to crosscheck a result using our approach.

Chapter 5

Summary and Conclusion

IN THE FIRST PART OF THIS THESIS, we gave a pedagogical review of some modern techniques used to study scattering amplitudes in the context of gauge theories. Among those, we discussed integral reduction, generalized unitarity and differential equation methods. For each new concept, we tried to illustrate the core ideas with the prototypical massless box diagram.

In the second part of this thesis, we investigated in more details some features of 5-point 2-loop amplitudes. Our study focused on their characteristic master integrals (see Fig. 3.2). Before our project started, their phenomenological applications were conceivably still requiring supplemental efforts. Indeed, to the author’s knowledge, the analytic expressions that could be found in the literature – e.g., see [145] – were mostly valid only in unphysical Euclidean regions with all negative 2-particle invariants, whereas the physical scattering region requires some of them to be positive. In [145], the authors reconstructed the analytic form of the coefficients of pentagon functions, but not of the master integrals themselves. The former are, of course, unconcerned with the signs of invariants as they have no physical meaning. The latter, however, do depend on the region. As this wasn’t a conceptual problem given the methods used in [145], Chicherin and Sotnikov recently repeated the reconstruction in all physical regions [143]. For the first time, a complete analytic calculation of the Feynman integrals required for the computation of massless 5-particle 2-loop scattering amplitudes

was given. They worked simultaneously with all the $5!$ permutations of each topology and consider a set of differential equations for each of them. Then, they directly solved them in each of the 10 physical regions defined in [137, Tab. 1], sidestepping the difficulty of analytic continuation.

Although this approach has some obvious advantages, it fails, by construction, to make clear a piece of information the authors think is worthwhile to dig for: *The analytic structure of 2-loop 5-point amplitudes*. The goal of the method presented in this thesis is therefore to reproduce the results they have already acquired, but with considerable additional insights on the hidden analyticity structure. Ultimately, it would expose analytically a conjectured network of paths in the kinematic space relating all the permuted configurations, only with harmonic polylogarithms (HPL).

To do so, we employed the method of canonical differential equations with connections generated by a basis set of transcendental functions: The pentagon functions. Then we considered paths in the kinematic space obtained from multiple-scaling limits relating permuted configurations (see Fig. 4.5). The canonical differential equations were evaluated along these paths with the help of a code we wrote in MATHEMATICA. This code makes multiple uses of `PolyLogTools` [31]. Provided analytic continuation and the corresponding paths, the method is sufficient to evaluate all the integral constants contributing to both planar and non-planar massless 5-point 2-loop amplitudes in the whole physical phase space. A numerical method for fast crosschecks was discussed in Section 3.4.

Finally, we would like to mention that the application of the techniques discussed in higher multiplicities amplitudes seems to be also plausible. This is, of course, assuming a canonical set of master integrals is known. Conceptually no significant new complications should appear as the increase in complexity is only expected to come from the addition of new scales. We are looking forward to tackling such challenges in the near future.

Appendix A

The Massless Box IBPs

THE FOUR IBP's generated by KIRA [89] for the massless 4-point box topology are obtained after reducing 432 equations. The results are

$$\begin{aligned} 0 = & (-a_1 - a_2 + d - a_3 - 2a_0)G_{1,\text{box}}(0, 0, 0, 0) - a_1G_{1,\text{box}}(-1, 1, 0, 0) - a_3G_{1,\text{box}}(-1, 0, 0, 1) \\ & - a_2G_{1,\text{box}}(-1, 0, 1, 0) + sa_2G_{1,\text{box}}(0, 0, 1, 0), \end{aligned} \tag{A.1}$$

$$\begin{aligned} 0 = & (a_0 - a_1)G_{1,\text{box}}(0, 0, 0, 0) - a_0G_{1,\text{box}}(1, -1, 0, 0) + a_1G_{1,\text{box}}(-1, 1, 0, 0) \\ & + a_3G_{1,\text{box}}(0, 0, 0, 1) + a_2G_{1,\text{box}}(-1, 0, 1, 0) - a_2G_{1,\text{box}}(0, -1, 1, 0) - sa_2G_{1,\text{box}}(0, 0, 1, 0) \\ & + a_3G_{1,\text{box}}(-1, 0, 0, 1) - a_3G_{1,\text{box}}(0, -1, 0, 1), \end{aligned} \tag{A.2}$$

$$\begin{aligned} 0 = & a_0G_{1,\text{box}}(1, -1, 0, 0) - a_0G_{1,\text{box}}(1, 0, -1, 0) + sa_0G_{1,\text{box}}(1, 0, 0, 0) \\ & + (a_1 - a_2)G_{1,\text{box}}(0, 0, 0, 0) - a_1G_{1,\text{box}}(0, 1, -1, 0) + a_2G_{1,\text{box}}(0, -1, 1, 0) - a_3G_{1,\text{box}}(0, 0, 0, 1) \\ & + a_3G_{1,\text{box}}(0, -1, 0, 1) - a_3G_{1,\text{box}}(0, 0, -1, 1), \end{aligned} \tag{A.3}$$

$$\begin{aligned}
0 = & (a_3 - a_0)G_{1,\text{box}}(0, 0, 0, 0) + a_0G_{1,\text{box}}(1, 0, 0, -1) - a_1G_{1,\text{box}}(-1, 1, 0, 0) \\
& + a_1G_{1,\text{box}}(0, 1, 0, -1) - a_1G_{1,\text{box}}(0, 1, 0, 0) - a_2G_{1,\text{box}}(-1, 0, 1, 0) + a_2G_{1,\text{box}}(0, 0, 1, -1) \\
& + sa_2G_{1,\text{box}}(0, 0, 1, 0) - a_3G_{1,\text{box}}(-1, 0, 0, 1).
\end{aligned} \tag{A.4}$$

For the sake of simplicity, the coefficients a_i 's in the latter equations are calculated only for a selected set of master integrals. Here, we focus only on the relevant integral decomposition for our box example. We find

$$\begin{aligned}
G_{1,\text{box}}(0, 0, 2, 0) & \rightarrow 0, \\
G_{1,\text{box}}(0, 1, 2, 1) & \rightarrow \frac{(4d - 12)G_{1,\text{box}}(0, 1, 0, 1)}{(d - 6)t^2}, \\
G_{1,\text{box}}(1, 1, 2, 1) & \rightarrow \frac{(4d^2 - 32d + 60)G_{1,\text{box}}(0, 1, 0, 1)}{(d - 6)st^2} + \frac{(5 - d)G_{1,\text{box}}(1, 1, 1, 1)}{s}, \\
G_{1,\text{box}}(1, 0, 2, 1) & \rightarrow \frac{(2d - 6)G_{1,\text{box}}(1, 0, 1, 0)}{s^2}, \\
G_{1,\text{box}}(1, 1, 2, 0) & \rightarrow \frac{(2d - 6)G_{1,\text{box}}(1, 0, 1, 0)}{s^2}, \\
G_{1,\text{box}}(1, 0, 2, -1) & \rightarrow \frac{1}{2}(d - 2)G_{1,\text{box}}(1, 0, 1, 0), \\
G_{1,\text{box}}(1, 0, 2, 0) & \rightarrow \frac{(3 - d)G_{1,\text{box}}(1, 0, 1, 0)}{s}, \\
G_{1,\text{box}}(1, -1, 2, 0) & \rightarrow \frac{1}{2}(d - 2)G_{1,\text{box}}(1, 0, 1, 0).
\end{aligned} \tag{A.5}$$

Appendix B

Computation of M_2 and M_3

WE SAW EARLIER that Feynman parameterization for $G_{1,\mathcal{T}}$ yields

$$G_{1,\mathcal{T}}(a_1, \dots, a_P) = \frac{\Gamma(a) e^{\varepsilon\gamma_E} (\mu^2)^\varepsilon}{i\pi^{d/2} \prod_{i=1}^P \Gamma(a_i)} \int d^d\ell \int_{[0,1]} \bigwedge_{i=1}^P X_i^{a_i-1} dX_i \frac{\delta\left(1 - \sum_{i=1}^P X_i\right)}{\left(\sum_{i=1}^P \left(\left(\ell + \sum_{j=1}^i p_j\right)^2 - m_i^2\right) X_i\right)^a}.$$

If we shift the loop momenta such that

$$\ell^\mu \rightarrow \tilde{\ell}^\mu := \ell^\mu - \sum_{i=1}^P X_{i+1} \left(\sum_{j=1}^i p_j^\mu \right),$$

we find

$$G_{1,\mathcal{T}}(a_1, \dots, a_P) = \frac{\Gamma(a) e^{\varepsilon\gamma_E} (\mu^2)^\varepsilon}{i\pi^{d/2} \prod_{i=1}^P \Gamma(a_i)} \int d^d\ell \int_{[0,1]} \bigwedge_{i=1}^P X_i^{a_i-1} dX_i \frac{\left(\sum_{i=1}^P X_i\right)^{a-d} \delta\left(1 - \sum_{i=1}^P X_i\right)}{\left(\tilde{\ell}^2 - \Delta\right)^a},$$

where

$$\begin{aligned} \Delta &= \sum_{i < j} X_i X_j (m_i^2 + m_j^2 - (p_{i-1} - p_{j-1})^2) \\ &= \sum_{i < j} X_i X_j S_{ij}. \end{aligned}$$

If we Wick rotate $\tilde{\ell}^0 \rightarrow i\tilde{\ell}^0$ to Euclidean space, we can perform the loop integration

$$\int \frac{d^d L}{i\pi^{d/2}} \frac{1}{(\tilde{\ell}^2 - \Delta)^a} = \frac{(-1)^a \Gamma(a - d/2)}{\Gamma(a)} \Delta^{d/2-a}.$$

Therefore,

$$G_{1,\mathcal{T}}(a_1, \dots, a_P) = \frac{(-1)^a \Gamma(a - d/2) e^{\varepsilon \gamma_E} (\mu^2)^\varepsilon}{i \pi^{d/2} \prod_{i=1}^P \Gamma(a_i)} \int_{[0,1]} \bigwedge_{i=1}^P X_i^{a_i-1} dX_i \frac{\left(\sum_{i=1}^P X_i \right)^{a-d} \delta \left(1 - \sum_{i=1}^P X_i \right)}{\left(\sum_{i < j} X_i X_j S_{ij} \right)^{a-d/2}},$$

with $S_{ij} := m_i^2 + m_j^2 - (p_{i-1} - p_{j-1})^2$. A L -loop generalization of this can be found in [75, 109].

This form of the FI makes it trivial to compute $G_{1,\text{box}}(a_1, 0, a_3, 0)$. Given $s_{ij} = s_{13} = -(p_1 - p_2)^2 = s$, we have

$$\begin{aligned} G_{1,\text{box}}(a_1, 0, a_3, 0) &= \frac{(-1)^{a_1+a_3} \Gamma(a_1 + a_3 - d/2)}{\Gamma(a_1) \Gamma(a_3)} \int_{[0,1]} dx_1 x_1^{a_1-1} \int_{[0,1]} dx_3 x_3^{a_3-1} \frac{(x_1 + x_3)^{a_1+a_3-d} \delta(1 - x_1 - x_3)}{(s x_1 x_3)^{a_1+a_3-d/2}} \\ &= (-s)^{d/2-a_1-a_3} \frac{\Gamma(a_1 + a_3 - d/2)}{\Gamma(a_1) \Gamma(a_3)} \int_{[0,1]} dx_1 x_1^{d/2-a_3-1} (1 - x_1)^{d/2-a_1-1} \\ &= (-s)^{d/2-a_1-a_3} \frac{\Gamma(a_1 + a_3 - d/2)}{\Gamma(a_1) \Gamma(a_3)} \beta(d/2 - a_3, d/2 - a_1) \\ &= (-s)^{d/2-a_1-a_3} \frac{\Gamma(a_1 + a_3 - d/2)}{\Gamma(a_1) \Gamma(a_3)} \frac{\Gamma(d/2 - a_3) \Gamma(d/2 - a_1)}{\Gamma(d - a_1 - a_3)}. \end{aligned}$$

Therefore, by setting $d \rightarrow 4 - 2\varepsilon$, expanding to leading order in ε and `FunctionExpand`-ing in MATHEMATICA, we find

$$\begin{aligned} \mathbf{M}_2 &= -\varepsilon (e^{\varepsilon \gamma_E} (-s)^{\varepsilon+1}) G(1, 0, 2, 0) \\ &\xrightarrow{\varepsilon \rightarrow 0} -1 + \frac{\pi^2}{12} \varepsilon^2 + \frac{7}{3} \zeta_3 \varepsilon^3 + \frac{47}{1440} \pi^4 \varepsilon^4 + \mathcal{O}(\varepsilon^5). \end{aligned}$$

By definition of our basis and from the above computation we see, in $D = 4 - 2\varepsilon$,

$$\frac{\mathbf{M}_2}{\mathbf{M}_3} = \frac{s(-s)^{-1-\varepsilon}}{t(-t)^{-1-\varepsilon}} = x^\varepsilon \Rightarrow G_{1,\text{box}}(0, 1, 0, 2) = x^\varepsilon G_{1,\text{box}}(1, 0, 2, 0).$$

Appendix C

Kinematic Limits and Their Geometries

IT IS WORTHWHILE TO HIGHLIGHT the fact that multi-Regge kinematics has an insightful geometric interpretation. To see that, we compute the (momentum) dual variables y_i defined by

$$p_i = y_i - y_{i-1}. \quad (\text{C.1})$$

To enforce momentum conservation, we fix $y_n = 0$. Thus, the dual variables can be written in terms of the momenta as

$$y_i = \sum_{k=1}^i p_k. \quad (\text{C.2})$$

Using the momenta above, we have¹

$$y_n = \begin{pmatrix} 0 & 0 \\ 0 & 0 \end{pmatrix}, \quad y_1 = \begin{pmatrix} 0 & 0 \\ 0 & -\epsilon^{-(n-3)/2} \sum_{j=3}^n p_j^- \epsilon^{n-j} \end{pmatrix}, \quad (\text{C.3})$$

$$y_j = \begin{pmatrix} -\epsilon^{-(n-3)/2} \sum_{k=j+1}^n p_k^+ \epsilon^{k-3} & \sum_{k=3}^j \mathbf{p}_k^\perp \\ \sum_{k=3}^j (\mathbf{p}_k^\perp)^\star & -\epsilon^{-(n-3)/2} \sum_{k=j+1}^n p_k^- \epsilon^{n-k} \end{pmatrix}, \quad 3 \leq j \leq n. \quad (\text{C.4})$$

¹It may be tempting at this point to again keep in each individual entry only the leading term in the limit $\epsilon \rightarrow 0$. This, however, would make certain momentum twistor invariants vanish identically. Since we need to keep track of the leading behavior of every independent invariant, it is *essential* not to truncate these expansions prematurely, but rather to keep all orders of ϵ in the computation of the y 's. The same will be true for the \mathcal{Z} 's.

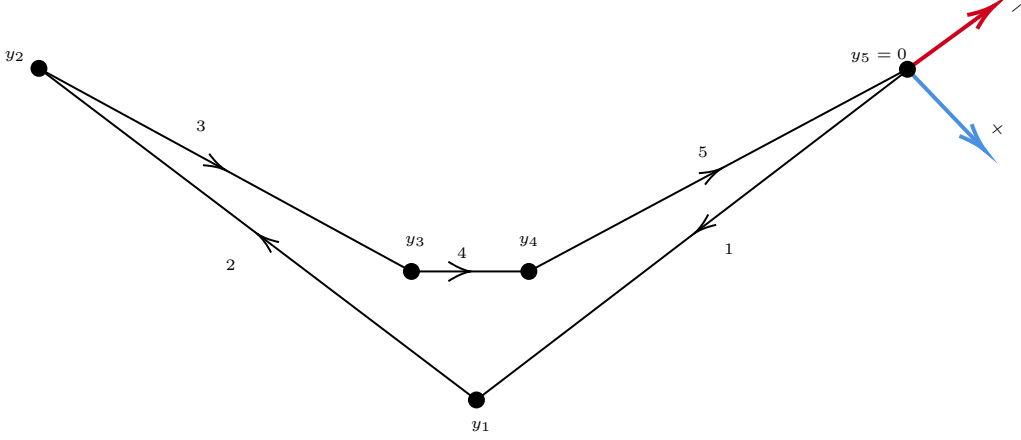


Figure C.1: The geometry: The i^{th} edge vector is the momentum p_i^μ of particle i .

In the MRK limit, the dual variables give a “geometry”. For instance, let’s consider the $n = 5$ case, where

$$y_1 = \begin{pmatrix} 0 & 0 \\ 0 & -\epsilon p_3^- - \frac{p_5^-}{\epsilon} - p_4^- \end{pmatrix}, \quad (\text{C.5})$$

$$y_2 = \begin{pmatrix} -\frac{p_3^+}{\epsilon} - p_5^+ \epsilon - p_4^+ & 0 \\ 0 & -\epsilon p_3^- - \frac{p_5^-}{\epsilon} - p_4^- \end{pmatrix}, \quad (\text{C.6})$$

$$y_3 = \begin{pmatrix} -p_5^+ \epsilon - p_4^+ & \sqrt{|p_3^-|} \sqrt{|p_3^+|} e^{i\phi_3} \\ \sqrt{|p_3^-|} \sqrt{|p_3^+|} e^{-i\phi_3} & -\frac{p_5^-}{\epsilon} - p_4^- \end{pmatrix}, \quad (\text{C.7})$$

$$y_4 = \begin{pmatrix} -\epsilon p_5^+ & \sqrt{|p_3^-|} \sqrt{|p_3^+|} e^{i\phi_3} + \sqrt{|p_4^-|} \sqrt{|p_4^+|} e^{i\phi_4} \\ \sqrt{|p_3^-|} \sqrt{|p_3^+|} e^{-i\phi_3} + \sqrt{|p_4^-|} \sqrt{|p_4^+|} e^{-i\phi_4} & -\frac{p_5^-}{\epsilon} \end{pmatrix}, \quad (\text{C.8})$$

$$y_5 = \begin{pmatrix} 0 & 0 \\ 0 & 0 \end{pmatrix}. \quad (\text{C.9})$$

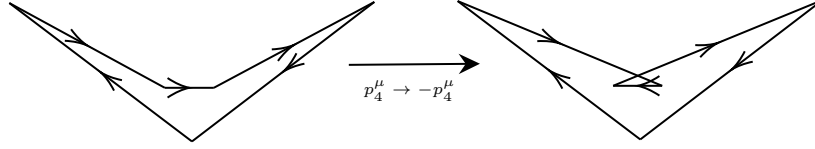
Keep in mind that momentum conservation in the \perp -direction implies that

$$\sqrt{|p_3^-|} \sqrt{|p_3^+|} e^{\pm i\phi_3} + \sqrt{|p_4^-|} \sqrt{|p_4^+|} e^{\pm i\phi_4} = -\sqrt{|p_5^-|} \sqrt{|p_5^+|} e^{\pm i\phi_5}. \quad (\text{C.10})$$

The geometry is given in Fig.C.1. We can use it to guide us in how to pullback a gluon from the future to the past and vice versa – i.e., on how to take the possibly correct multiple scaling limits. Note that the geodesic distance between the y_i ’s to the bottom light-cone

measure, in some sense, the strength of the off-diagonal components (\perp -components). For example, since $y_{1,2,5}$ lie on the bottom light-cone, their off-diagonal components vanish, while this is not the case for $y_{3,4}$.

For example, we can pullback particle 4 in the past, $p_4^\mu \rightarrow -p_4^\mu$. According to the dual coordinates above for $n = 5$, this transformation makes y_3 a little closer to $y_5 = 0$ than y_4 is. So we effectively flip y_3 with y_4



Because gluon 5 is way more energetic than gluon 4, it is not as straightforward than it is for particle 4 to interpret what happens geometrically as $p_5^\mu \rightarrow -p_5^\mu$, but the underlying idea is the same.

We can get similar pictures from the corresponding momentum twistors. See [33] for a comprehensive introduction. We start by computing the μ components of the twistors, which are defined by the incidence relation

$$\mu_{i,\dot{\alpha}} = -\lambda_i^\alpha y_{i,\alpha\dot{\alpha}} = \lambda_{i,\alpha} \varepsilon^{\alpha\beta} y_{i,\beta\dot{\alpha}} = (\lambda_i^\top \cdot \varepsilon \cdot y_i)_{\dot{\alpha}}. \quad (\text{C.11})$$

The momentum twistors are then simply defined by

$$\mathcal{Z}_i = (\lambda_{i,\alpha}, \mu_{i,\dot{\alpha}}). \quad (\text{C.12})$$

Note that the \mathcal{Z} 's are projectively invariant ($\mathcal{Z} \in \mathbb{CP}^3$), that is, for every $t \neq 0$, $t\mathcal{Z} \sim \mathcal{Z}$. We can use this projective invariance to set the first non-vanishing component of each \mathcal{Z}_i twistor to one. In this manner we finally obtain the following momentum twistor parameterization of the MRK

$$\mathcal{Z}_n = \begin{pmatrix} 1 & \epsilon^{-(n-3)/2} \sqrt{\frac{p_n^- p_n^\perp}{p_n^+ (p_n^\perp)^*}} & 0 & 0 \end{pmatrix}^\top, \quad (\text{C.13})$$

$$\mathcal{Z}_1 = \begin{pmatrix} 0 & 1 & 0 & 0 \end{pmatrix}^\top, \quad (\text{C.14})$$

$$\mathcal{Z}_2 = \begin{pmatrix} 1 & 0 & 0 & -\sum_{k=3}^n \sqrt{\frac{p_k^- p_k^\perp}{p_k^+ (p_k^\perp)^*}} (p_k^\perp)^* \epsilon^{(n+3)/2-k} \end{pmatrix}^\top, \quad (\text{C.15})$$

$$\mathcal{Z}_j = \begin{pmatrix} 1 \\ \epsilon^{(n+3)/2-j} \sqrt{\frac{p_j^- \mathbf{p}_j^\perp}{p_j^+ (\mathbf{p}_j^\perp)^\star}} \\ \sum_{k=3}^j \mathbf{p}_k^\perp + \sqrt{\frac{p_j^- \mathbf{p}_j^\perp}{p_j^+ (\mathbf{p}_j^\perp)^\star}} \sum_{k=j+1}^n \epsilon^{k-2} \mathbf{p}_k^\perp \left(\sqrt{\frac{p_k^- \mathbf{p}_k^\perp}{p_k^+ (\mathbf{p}_k^\perp)^\star}} \right)^{-1} \\ -\epsilon^{(n+3)/2-j} \sqrt{\frac{p_j^- \mathbf{p}_j^\perp}{p_j^+ (\mathbf{p}_j^\perp)^\star}} \sum_{k=3}^j (\mathbf{p}_k^\perp)^\star - \sum_{k=j+1}^n \epsilon^{(n+3)/2-k} \sqrt{\frac{p_k^- \mathbf{p}_k^\perp}{p_k^+ (\mathbf{p}_k^\perp)^\star}} (\mathbf{p}_k^\perp)^\star \end{pmatrix}, \quad 3 \leq j \leq n-1. \quad (\text{C.16})$$

Broadly speaking, twistor diagrams are conformal compactifications of the dual diagrams [146]. Thus, to understand geometrically what happens when parameters gets bigger and bigger, they are more useful than the dual ones, for which points can be pushed at infinity.

These geometric tools do not guarantee the transport in the kinematic space they depict is easy to do in practice. They simply seem to be insightful on how limits may overlap with each other. What is really giving this information are the symbols present in each scaling limit.

References

- [1] M. Czakon, P. Fiedler, A. Mitov and J. Rojo, *Further exploration of top pair hadroproduction at NNLO*, in *27th Rencontres de Physique de La Vallée d'Aoste*, May, 2013 [1305.3892].
- [2] C. Itzykson and J.-B. Zuber, *Quantum field theory*, International series in pure and applied physics, McGraw-Hill, New York, NY (1980).
- [3] I. Newton, *Philosophiae naturalis principia mathematica*, vol. 2, typis A. et JM Duncan (1833).
- [4] G.T. Jones, *The uncertainty principle, virtual particles and real forces*, *Physics Education* **37** (2002) 223.
- [5] S.L. Glashow, *Partial Symmetries of Weak Interactions*, *Nucl. Phys.* **22** (1961) 579.
- [6] S. Weinberg, *A Model of Leptons*, *Phys. Rev. Lett.* **19** (1967) 1264.
- [7] A. Salam and J.C. Ward, *Weak and electromagnetic interactions*, *Nuovo Cim.* **11** (1959) 568.
- [8] P.W. Higgs, *Broken symmetries, massless particles and gauge fields*, *Phys. Lett.* **12** (1964) 132.
- [9] P.W. Higgs, *Broken Symmetries and the Masses of Gauge Bosons*, *Phys. Rev. Lett.* **13** (1964) 508.
- [10] F. Englert and R. Brout, *Broken Symmetry and the Mass of Gauge Vector Mesons*, *Phys. Rev. Lett.* **13** (1964) 321.
- [11] P.W. Higgs, *Spontaneous Symmetry Breakdown without Massless Bosons*, *Phys. Rev.* **145** (1966) 1156.
- [12] ATLAS collaboration, *Observation of a new particle in the search for the Standard Model Higgs boson with the ATLAS detector at the LHC*, *Phys. Lett. B* **716** (2012) 1 [1207.7214].
- [13] CMS collaboration, *Observation of a New Boson at a Mass of 125 GeV with the CMS Experiment at the LHC*, *Phys. Lett. B* **716** (2012) 30 [1207.7235].

- [14] R.K. Ellis, W.J. Stirling and B.R. Webber, *QCD and collider physics*, Cambridge monographs on particle physics, nuclear physics, and cosmology, Cambridge University Press, Cambridge (2003), 10.1017/CBO9780511628788.
- [15] CTEQ COLLABORATION collaboration, *Handbook of perturbative QCD; Version 1.1, September 1994*, Tech. Rep. FERMILAB-PUB-94-316, FERMILAB, Batavia, IL (1994).
- [16] P.D. Group, P.A. Zyla, R.M. Barnett, J. Beringer, O. Dahl, D.A. Dwyer et al., *Review of Particle Physics, Progress of Theoretical and Experimental Physics* **2020** (2020) [<https://academic.oup.com/ptep/article-pdf/2020/8/083C01/34673722/ptaa104.pdf>].
- [17] H. Frellesvig, F. Gasparotto, M.K. Mandal, P. Mastrolia, L. Mattiazzi and S. Mizera, *Vector Space of Feynman Integrals and Multivariate Intersection Numbers, Physical Review Letters* **123** (2019) .
- [18] S. Laporta, *High precision calculation of multiloop Feynman integrals by difference equations, Int. J. Mod. Phys. A* **15** (2000) 5087 [[hep-ph/0102033](#)].
- [19] F.V. Tkachov, *An algorithm for calculating multiloop integrals, Theor. Math. Phys.* **56** (1983) 866.
- [20] V.A. Smirnov, *Analytic Tools for Feynman Integrals*, Springer tracts in modern physics, Springer, Berlin (2012), 10.1007/978-3-642-34886-0.
- [21] E. Remiddi, *Differential equations for Feynman graph amplitudes, Nuovo Cim. A* **110** (1997) 1435 [[hep-th/9711188](#)].
- [22] M. Argeri and P. Mastrolia, *Feynman Diagrams and Differential Equations, International Journal of Modern Physics A* **22** (2007) 4375–4436.
- [23] J. Broedel, C. Duhr, F. Dulat, R. Marzucca, B. Penante and L. Tancredi, *An analytic solution for the equal-mass banana graph, JHEP* **09** (2019) 112 [[1907.03787](#)].
- [24] M. Hidding, *DiffExp, a Mathematica package for computing Feynman integrals in terms of one-dimensional series expansions, 2006.05510*.
- [25] A. Primo and L. Tancredi, *Maximal cuts and differential equations for feynman integrals. an application to the three-loop massive banana graph, Nuclear Physics B* **921** (2017) 316–356.
- [26] P. Vanhove, *Feynman integrals, toric geometry and mirror symmetry*, in *KMPB Conference: Elliptic Integrals, Elliptic Functions and Modular Forms in Quantum Field Theory*, 7, 2018, DOI [[1807.11466](#)].
- [27] K. Bönisch, F. Fischbach, A. Klemm, C. Nega and R. Safari, *Analytic Structure of all Loop Banana Amplitudes, 2008.10574*.
- [28] J.L. Bourjaily, A.J. McLeod, M. von Hippel and M. Wilhelm, *Bounded Collection of Feynman Integral Calabi-Yau Geometries, Physical Review Letters* **122** (2019) .

- [29] J.M. Henn, *Multiloop Integrals in Dimensional Regularization Made Simple*, *Physical Review Letters* **110** (2013) .
- [30] A.B. Goncharov, *Multiple polylogarithms and mixed Tate motives*, [[math/0103059](#)].
- [31] C. Duhr and F. Dulat, *PolyLogTools — polylogs for the masses*, *Journal of High Energy Physics* **2019** (2019) .
- [32] E. Remiddi and J.A.M. Vermaseren, *Harmonic Polylogarithms*, *International Journal of Modern Physics A* **15** (2000) 725–754.
- [33] H. Elvang and Y.-t. Huang, *Scattering amplitudes in gauge theory and gravity*, Cambridge University Press, Cambridge (Feb, 2015), 1107069254.
- [34] L.J. Dixon, *A brief introduction to modern amplitude methods*, in *Theoretical Advanced Study Institute in Elementary Particle Physics: Particle Physics: The Higgs Boson and Beyond*, pp. 31–67, 2014, DOI [[1310.5353](#)].
- [35] M. Srednicki, *Quantum Field Theory*, Cambridge Univ. Press, Cambridge (2007).
- [36] S. Coleman, *Aspects of Symmetry: Selected Erice Lectures*, Cambridge University Press, Cambridge, U.K. (1985), 10.1017/CBO9780511565045.
- [37] A. Zee, *Group Theory in a Nutshell for Physicists*, Princeton University Press, USA (2016).
- [38] H. Osborn, *PART I: Symmetries and particles, Lecture notes* .
- [39] F. Halzen and A.D. Martin, *Quark & Leptons: An Introductory Course In Modern Particle Physics*, John Wiley & Sons (2008).
- [40] R.F. Streater and A.S. Wightman, *PCT, Spin and Statistics, and All That*, Princeton University Press (1989).
- [41] M.E. Peskin and D.V. Schroeder, *An introduction to quantum field theory*, Westview, Boulder, CO (1995).
- [42] M.D. Schwartz, *Quantum field theory and the standard model*, Cambridge Univ. Press, Cambridge (2014), 1107034736.
- [43] L.D. Faddeev and V.N. Popov, *Feynman diagrams for the Yang-Mills field*, *Physics Letters B* **25** (1967) 29.
- [44] I.V. Tyutin, *Gauge Invariance in Field Theory and Statistical Physics in Operator Formalism*, 0812.0580.
- [45] S. Sapeta, *QCD and jets, Lecture 1: Foundations*, in *Ecole Internationale de Physique Subatomique, Lyon, 20-25 October, 2014*, 2014.
- [46] R.P. Feynman, *Very high-energy collisions of hadrons*, *Phys. Rev. Lett.* **23** (1969) 1415.

- [47] W.-K. Tung, *Parton Distribution Functions and the QCD Improved Parton Model: An Overview*, *Int. J. Mod. Phys. A* **2** (1987) 1369.
- [48] J. Chyla, *Quarks, partons and Quantum Chromodynamics*, *Lecture notes* (2004) .
- [49] J. Rafelski, *Melting Hadrons, Boiling Quarks*, in *Melting Hadrons, Boiling Quarks - From Hagedorn Temperature to Ultra-Relativistic Heavy-Ion Collisions at CERN: With a Tribute to Rolf Hagedorn*, J. Rafelski, ed., pp. 417–439 (2016), DOI.
- [50] B. Andersson, *The Lund model*, vol. 7, Cambridge University Press (7, 2005).
- [51] D0 collaboration, *Evidence for production of single top quarks*, *Phys. Rev. D* **78** (2008) 012005 [0803.0739].
- [52] A.V. Manohar, *Large N QCD*, in *Les Houches Summer School in Theoretical Physics, Session 68: Probing the Standard Model of Particle Interactions*, pp. 1091–1169, 2, 1998 [hep-ph/9802419].
- [53] D. Tong, *Lectures on gauge theory*, *Lecture notes* (2018) .
- [54] J. Bartels, L.N. Lipatov and A. Sabio Vera, *BFKL Pomeron, Reggeized gluons and Bern-Dixon-Smirnov amplitudes*, *Phys. Rev. D* **80** (2009) 045002 [0802.2065].
- [55] T. Schuster, *Color ordering in QCD*, *Phys. Rev. D* **89** (2014) 105022 [1311.6296].
- [56] C. Schwinn, *Modern Methods of Quantum Chromodynamics*, *Universität Freiburg* (2015) .
- [57] R. Kleiss and H. Kuijf, *Multi-Gluon Cross-sections and Five Jet Production at Hadron Colliders*, *Nucl. Phys. B* **312** (1989) 616.
- [58] Z. Bern, J.J.M. Carrasco and H. Johansson, *New relations for gauge-theory amplitudes*, *Physical Review D* **78** (2008) .
- [59] E. Casali, S. Mizera and P. Tourkine, *Monodromy relations from twisted homology*, *JHEP* **12** (2019) 087 [1910.08514].
- [60] S.G. Naculich, *All-loop group-theory constraints for color-ordered $SU(N)$ gauge-theory amplitudes*, *Physics Letters B* **707** (2012) 191–197.
- [61] A.C. Edison and S.G. Naculich, *$SU(N)$ group-theory constraints on color-ordered five-point amplitudes at all loop orders*, *Nuclear Physics B* **858** (2012) 488–501.
- [62] R. Britto, *Introduction to Scattering Amplitudes Lecture 1: QCD and the Spinor-Helicity Formalism*, *Lecture notes* (2011) .
- [63] S. Abreu, L.J. Dixon, E. Herrmann, B. Page and M. Zeng, *Two-Loop Five-Point Amplitude in $\mathcal{N} = 4$ Super-Yang-Mills Theory*, *Physical Review Letters* **122** (2019) .
- [64] S.J. Parke and T.R. Taylor, *An Amplitude for N -Gluon Scattering*, *Phys. Rev. Lett.* **56** (1986) 2459.

- [65] R. Boels, *Covariant representation theory of the Poincaré algebra and some of its extensions*, *Journal of High Energy Physics* **2010** (2010) .
- [66] J.L. Diaz-Cruz, B.O. Larios and O. Meza-Aldama, *An Introduction to the Massive Helicity Formalism with applications to the Electroweak SM*, *J. Phys. Conf. Ser.* **761** (2016) 012012 [[1608.04129](#)].
- [67] N. Arkani-Hamed, J. Bourjaily, F. Cachazo and J. Trnka, *Local integrals for planar scattering amplitudes*, *Journal of High Energy Physics* **2012** (2012) .
- [68] V.I. Smirnov and R.A. Silverman, *Linear algebra and group theory*, Courier Corporation (2011).
- [69] G. Passarino and M.J.G. Veltman, *One Loop Corrections for e^+, e^- Annihilation Into $\mu^+ \nu^-$ in the Weinberg Model*, *Nucl. Phys. B* **160** (1979) 151.
- [70] O.V. Tarasov, *Reduction of Feynman graph amplitudes to a minimal set of basic integrals*, *Acta Phys. Polon. B* **29** (1998) 2655 [[hep-ph/9812250](#)].
- [71] P. Mastrolia and S. Mizera, *Feynman integrals and intersection theory*, *Journal of High Energy Physics* **2019** (2019) .
- [72] S. Mizera, *Towards the Geometric Color-Kinematics Duality*, in *Zoomplitudes 2020*, May, 2020.
- [73] A.G. Grozin, *Integration by Parts: an introduction*, *International Journal of Modern Physics A* **26** (2011) 2807–2854.
- [74] K. Osterwalder and R. Schrader, *Axioms for Euclidean Green’s functions*, *Communications in mathematical physics* **31** (1973) 83.
- [75] S. Mizera and A. Pokraka, *From infinity to four dimensions: higher residue pairings and Feynman integrals*, *Journal of High Energy Physics* **2020** (2020) .
- [76] R.C. Hwa and V.L. Teplitz, *Homology and Feynman integrals*, Mathematical physics monograph series, Benjamin, New York, NY (1966).
- [77] S. Mizera, *Status of Intersection Theory and Feynman Integrals*, [2002.10476](#).
- [78] S. Caron-Huot and A. Pokraka, *On the Poincaré dual of Feynman integrals*, to appear .
- [79] N. Kalyanapuram, *Stokes polytopes and intersection theory*, *Physical Review D* **101** (2020) .
- [80] J.M. Henn and J.C. Plefka, *Scattering amplitudes in gauge theories*, Lecture notes in physics, Springer, Berlin (2014), [10.1007/978-3-642-54022-6](#).
- [81] Z. Bern, L. Dixon and D.A. Kosower, *Dimensionally-regulated pentagon integrals*, *Nuclear Physics B* **412** (1994) 751–816.

- [82] R.J. Eden, P.V. Landshoff, D.I. Olive and J.C. Polkinghorne, *The analytic S-matrix*, Cambridge Univ. Press, Cambridge (1966).
- [83] R. Zwicky, *A brief Introduction to Dispersion Relations and Analyticity*, in *Quantum Field Theory at the Limits: from Strong Fields to Heavy Quarks*, pp. 93–120, 2017, DOI [1610.06090].
- [84] Y. Dokshitzer, *Demystifying Strong Interactions: I.1 crossing, unitarity and Feynman diagrams*, in *Graduate Lectures for Cambridge HEP Group Graduate Students*, Jan., 2016.
- [85] T. Gehrmann and E. Remiddi, *Differential equations for two-loop four-point functions*, *Nuclear Physics B* **580** (2000) 485–518.
- [86] R. Lee, *Group structure of the integration-by-part identities and its application to the reduction of multiloop integrals*, *Journal of High Energy Physics* **2008** (2008) 031–031.
- [87] A.V. Smirnov and A.V. Petukhov, *The Number of Master Integrals is Finite*, *Lett. Math. Phys.* **97** (2011) 37 [1004.4199].
- [88] A.V. Smirnov and F.S. Chuharev, **FIRE6: Feynman Integral REduction with Modular Arithmetic**, *Comput. Phys. Commun.* **247** (2020) 106877 [1901.07808].
- [89] P. Maierhöfer, J. Usovitsch and P. Uwer, **KIRA — A Feynman integral reduction program**, *Comput. Phys. Commun.* **230** (2018) 99 [1705.05610].
- [90] C. Studerus, **Reduze — Feynman Integral Reduction in C++**, *Comput. Phys. Commun.* **181** (2010) 1293 [0912.2546].
- [91] R.N. Lee, **LiteRed 1.4: a powerful tool for reduction of multiloop integrals**, *J. Phys. Conf. Ser.* **523** (2014) 012059 [1310.1145].
- [92] A. Georgoudis, K.J. Larsen and Y. Zhang, **Azurite: An algebraic geometry based package for finding bases of loop integrals**, *Comput. Phys. Commun.* **221** (2017) 203 [1612.04252].
- [93] J. Boehm, M. Wittmann, Z. Wu, Y. Xu and Y. Zhang, *IBP reduction coefficients made simple*, *JHEP* **12** (2020) 054 [2008.13194].
- [94] J. Gluza, K. Kajda and D.A. Kosower, *Towards a basis for planar two-loop integrals*, *Physical Review D* **83** (2011) .
- [95] J.D. Hauenstein, R. Huang, D. Mehta and Y. Zhang, *Global structure of curves from generalized unitarity cut of three-loop diagrams*, *Journal of High Energy Physics* **2015** (2015) .
- [96] Z. Bern and Y.-t. Huang, *Basics of generalized unitarity*, *Journal of Physics A: Mathematical and Theoretical* **44** (2011) 454003.

- [97] R. Britto, *Loop amplitudes in gauge theories: Modern analytic approaches*, *Journal of Physics A: Mathematical and Theoretical* **44** (2011) 454006.
- [98] J.J.M. Carrasco and H. Johansson, *Generic multiloop methods and application to $\mathcal{N} = 4$ super-Yang-Mills*, *Journal of Physics A: Mathematical and Theoretical* **44** (2011) 454004.
- [99] J. Henn, B. Mistlberger, V.A. Smirnov and P. Wasser, *Constructing d -log integrands and computing master integrals for three-loop four-particle scattering*, *Journal of High Energy Physics* **2020** (2020) .
- [100] Z. Bern, E. Herrmann, S. Litsey, J. Stankowicz and J. Trnka, *Logarithmic Singularities and Maximally Supersymmetric Amplitudes*, *JHEP* **06** (2015) 202 [1412.8584].
- [101] A. Bilal, *Introduction to supersymmetry*, hep-th/0101055.
- [102] J. Wess and J.A. Bagger, *Supersymmetry and supergravity; 2nd ed.*, Princeton series in physics, Princeton Univ. Press, Princeton, NJ (1992).
- [103] J.M. Henn, *What can we learn about QCD and collider physics from $N=4$ super Yang-Mills?*, 2006.00361.
- [104] N. Arkani-Hamed, J.L. Bourjaily, F. Cachazo and J. Trnka, *Singularity Structure of Maximally Supersymmetric Scattering Amplitudes*, *Phys. Rev. Lett.* **113** (2014) 261603 [1410.0354].
- [105] N. Arkani-Hamed, J.L. Bourjaily, F. Cachazo, A.B. Goncharov, A. Postnikov and J. Trnka, *Grassmannian Geometry of Scattering Amplitudes*, Cambridge University Press (4, 2016), 10.1017/CBO9781316091548, [1212.5605].
- [106] Z. Bern, E. Herrmann, S. Litsey, J. Stankowicz and J. Trnka, *Evidence for a Nonplanar Amplituhedron*, *JHEP* **06** (2016) 098 [1512.08591].
- [107] C. Dlapa, X. Li and Y. Zhang, *Leading singularities in Baikov representation and Feynman integrals with uniform transcendental weight*, 2103.04638.
- [108] T. Gehrmann, J.M. Henn and T. Huber, *The three-loop form factor in $\mathcal{N} = 4$ super Yang-Mills*, *Journal of High Energy Physics* **2012** (2012) .
- [109] J.M. Henn, *Lectures on differential equations for Feynman integrals*, *Journal of Physics A: Mathematical and Theoretical* **48** (2015) 153001.
- [110] C. Dlapa, J. Henn and K. Yan, *Deriving canonical differential equations for Feynman integrals from a single uniform weight integral*, *JHEP* **05** (2020) 025 [2002.02340].
- [111] P. Mastrolia, *Scattering Amplitudes at LHC*, *Nucl. Part. Phys. Proc.* **267-269** (2015) 131.

- [112] S. Weinzierl, *Iterated integrals related to Feynman integrals associated to elliptic curves*, in *Antidifferentiation and the Calculation of Feynman Amplitudes*, 12, 2020 [2012.08429].
- [113] S. Weinzierl, *Introduction to Feynman Integrals*, in *6th Summer School on Geometric and Topological Methods for Quantum Field Theory*, pp. 144–187, 2013, DOI [1005.1855].
- [114] J. Tavares, *Chen Integrals, Generalized Loops and Loop Calculus*, *International Journal of Modern Physics A* **09** (1994) 4511–4548.
- [115] F. Moriello, *Feynman integrals beyond multiple polylogarithms: recent developments and perspectives*, in *DESY Zeuthen*, 2016.
- [116] J.L. Bourjaily, A.J. McLeod, C. Vergu, M. Volk, M. von Hippel and M. Wilhelm, *Embedding Feynman integral (Calabi-Yau) geometries in weighted projective space*, *Journal of High Energy Physics* **2020** (2020) .
- [117] R. Brüser, S. Caron-Huot and J.M. Henn, *Subleading Regge limit from a soft anomalous dimension*, *JHEP* **04** (2018) 047 [1802.02524].
- [118] N.A. Lo Presti, T. Gehrmann and J. Henn, *Two-loop five-point integrals in massless QCD*, *PoS* **LL2016** (2016) 051.
- [119] A.L. Presti, “Five-point two-loop master integrals in QCD.”
https://www.physik.uzh.ch/dam/jcr:f107f559-a00b-4965-bc1e-4d3aa223e549/adriano_lo_presti.pdf.
- [120] V. Shtabovenko, R. Mertig and F. Orellana, *New Developments in FeynCalc 9.0*, *Comput. Phys. Commun.* **207** (2016) 432 [1601.01167].
- [121] J. Vollinga, *GiNaC: Symbolic computation with C++*, *Nucl. Instrum. Meth. A* **559** (2006) 282 [hep-ph/0510057].
- [122] M. Aaboud, G. Aad, B. Abbott, J. Abdallah, O. Abdinov, B. Abeloos et al., *Determination of the strong coupling constant α_s from transverse energy–energy correlations in multijet events at $\sqrt{s} = 8$ TeV using the ATLAS detector*, *The European Physical Journal C* **77** (2017) .
- [123] M. Aaboud, G. Aad, B. Abbott, O. Abdinov, B. Abeloos, S. Abidi et al., *Measurement of the production cross section of three isolated photons in pp collisions at $s=8$ TeV using the ATLAS detector*, *Physics Letters B* **781** (2018) 55–76.
- [124] A.M. Sirunyan, A. Tumasyan, W. Adam, F. Ambroggi, E. Asilar, T. Bergauer et al., *Event shape variables measured using multijet final states in proton-proton collisions at $\sqrt{s} = 13$ TeV*, *Journal of High Energy Physics* **2018** (2018) .
- [125] D. Chicherin, J. Henn and V. Mitev, *Bootstrapping pentagon functions*, *Journal of High Energy Physics* **2018** (2018) .

- [126] S. Caron-Huot, D. Chicherin, J. Henn, Y. Zhang and S. Zoia, *Multi-Regge Limit of the Two-Loop Five-Point Amplitudes in $\mathcal{N} = 4$ Super Yang-Mills and $\mathcal{N} = 8$ Supergravity*, *JHEP* **10** (2020) 188 [2003.03120].
- [127] T. Gehrmann, J. Henn and N. Lo Presti, *Analytic Form of the Two-Loop Planar Five-Gluon All-Plus-Helicity Amplitude in QCD*, *Physical Review Letters* **116** (2016) .
- [128] S. Badger, C. Brønnum-Hansen, H.B. Hartanto and T. Peraro, *Analytic helicity amplitudes for two-loop five-gluon scattering: the single-minus case*, *Journal of High Energy Physics* **2019** (2019) .
- [129] D. Chicherin, “PentagonFunctions Project.”
<https://pentagonfunctions.hepforge.org>.
- [130] S. Abreu, L.J. Dixon, E. Herrmann, B. Page and M. Zeng, *Two-Loop Five-Point Amplitude in $\mathcal{N} = 4$ Super-Yang-Mills Theory*, *Physical Review Letters* **122** (2019) .
- [131] D. Chicherin, T. Gehrmann, J. Henn, P. Wasser, Y. Zhang and S. Zoia, *All Master Integrals for Three-Jet Production at Next-to-Next-to-Leading Order*, *Physical Review Letters* **123** (2019) .
- [132] J. Böhm, A. Georgoudis, K.J. Larsen, H. Schönemann and Y. Zhang, *Complete integration-by-parts reductions of the non-planar hexagon-box via module intersections*, *Journal of High Energy Physics* **2018** (2018) .
- [133] S. Abreu, B. Page and M. Zeng, *Differential equations from unitarity cuts: nonplanar hexa-box integrals*, *Journal of High Energy Physics* **2019** (2019) .
- [134] D. Chicherin, T. Gehrmann, J.M. Henn, N.A. Lo Presti, V. Mitev and P. Wasser, *Analytic result for the nonplanar hexa-box integrals*, *Journal of High Energy Physics* **2019** (2019) .
- [135] C.G. Papadopoulos, D. Tommasini and C. Wever, *The pentabox Master Integrals with the Simplified Differential Equations approach*, *Journal of High Energy Physics* **2016** (2016) 1–18.
- [136] S. Abreu, H. Ita, F. Moriello, B. Page, W. Tschernow and M. Zeng, *Two-Loop Integrals for Planar Five-Point One-Mass Processes*, *JHEP* **11** (2020) 117 [2005.04195].
- [137] T. Gehrmann, J.M. Henn and N.A. Lo Presti, *Pentagon functions for massless planar scattering amplitudes*, *Journal of High Energy Physics* **2018** (2018) .
- [138] C. Duhr, H. Gangl and J.R. Rhodes, *From polygons and symbols to polylogarithmic functions*, *Journal of High Energy Physics* **2012** (2012) .
- [139] J. Henn, E. Herrmann and J. Parra-Martinez, *Bootstrapping two-loop Feynman integrals for planar $\mathcal{N} = 4$ sYM*, *Journal of High Energy Physics* **2018** (2018) .

- [140] V. Del Duca, S. Druc, J. Drummond, C. Duhr, F. Dulat, R. Marzucca et al., *Multi-Regge kinematics and the moduli space of Riemann spheres with marked points*, *Journal of High Energy Physics* **2016** (2016) .
- [141] B. Basso, A. Sever and P. Vieira, *Collinear Limit of Scattering Amplitudes at Strong Coupling*, *Phys. Rev. Lett.* **113** (2014) 261604 [[1405.6350](#)].
- [142] M. Hidding, *Computational and mathematical aspects of Feynman integrals*, Ph.D. thesis, Trinity Coll., Dublin, 2021.
- [143] D. Chicherin and V. Sotnikov, *Pentagon functions for scattering of five massless particles*, *Journal of High Energy Physics* **2020** (2020) .
- [144] S. Caron-Huot, L.J. Dixon, A. McLeod and M. von Hippel, *Bootstrapping a Five-Loop Amplitude Using Steinmann Relations*, *Physical Review Letters* **117** (2016) .
- [145] S. Abreu, J. Dormans, F. Febres Cordero, H. Ita, B. Page and V. Sotnikov, *Analytic form of the planar two-loop five-parton scattering amplitudes in QCD*, *Journal of High Energy Physics* **2019** (2019) .
- [146] A. Hodges, *Twistors and amplitudes*, *Phil. Trans. Roy. Soc. Lond. A* **373** (2015) 20140248.